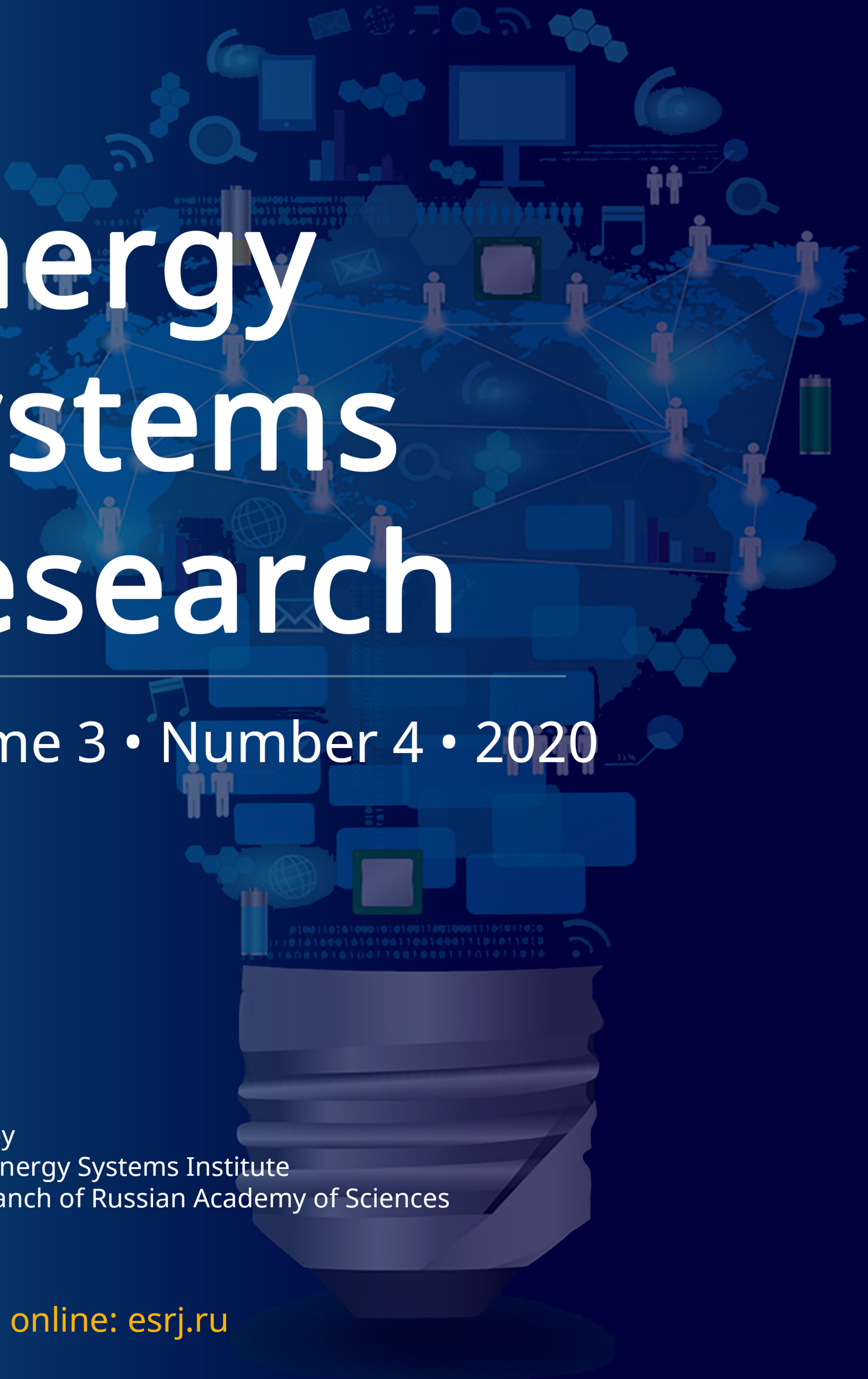

Energy Systems Research

Volume 3 • Number 4 • 2020

Published by
Melentiev Energy Systems Institute
Siberian Branch of Russian Academy of Sciences

Available online: esrj.ru

ISSN 2618-9992

Energy Systems Research

Volume 3 • Number 4 • 2020
International scientific peer-reviewed journal
Available online: http://esrj.ru

About the journal

Energy Systems Research is an international peer-reviewed journal addressing all the aspects of energy systems, including their sustainable development and effective use, smart and reliable operation, control and management, integration and interaction in a complex physical, technical, economic and social environment.

Energy systems research methodology is based on a systems approach considering energy objects as systems with complicated structure and external ties, and includes the methods and technologies of systems analysis.

Within this broad multi-disciplinary scope, topics of particular interest include strategic energy systems development at the international, regional, national and local levels; energy supply reliability and security; energy markets, regulations and policy; technological innovations with their impacts and future-oriented transformations of energy systems.

The journal welcomes papers on advances in heat and electric power industries, energy efficiency and energy saving, renewable energy and clean fossil fuel generation, and other energy technologies.

Energy Systems Research is also concerned with energy systems challenges related to the applications of information and communication technologies, including intelligent control and cyber security, modern approaches of systems analysis, modeling, forecasting, numerical computations and optimization.

The journal is published by Melentiev Energy Systems Institute of Siberian Branch of Russian Academy of Sciences. The journal's ISSN is 2618-9992. There are 4 issues per year (special issues are available). All articles are available online on English as Open access articles.

Topics

- Energy production, conversion, transport and distribution systems
- Integrated energy systems
- Energy technologies
- International, regional, local energy systems
- Energy system protection, control and management
- Smart energy systems, smart grids
- Energy systems reliability and energy security
- Electricity, heating, cooling, gas and oil systems
- Energy system development and operation
- Demand-side management
- Energy economics and policy
- Renewable energy and clean fossil fuel based systems
- Distributed energy systems
- Sustainable energy transitions
- System problems of power and thermal engineering
- Artificial intelligence in energy systems
- Information and communication technologies in energy systems
- Energy systems analysis and modelling
- Computational methods and optimization in energy systems

Contacts

Scientific secretary:	Alexey Mikheev, Dr. of Eng.
E-mail:	info@esrj.ru
Tel:	+7 (3952) 950980 (English, Russian)
Fax:	+7 (3952) 426796
Address:	130, Lermontov str., Irkutsk, 664033, Russia

Contents

Specifics of Emergency Operation in Distribution Grid and their Effect on Integration and Functioning of Distributed Generation Facilities

P. V. Ilyushin[1,*], A. L. Kulikov[2]

[1] Energy Research Institute of the Russian Academy of Sciences, Moscow, Russia
[2] R.E. Alekseev Nizhny Novgorod State Technical University, Russia

Abstract **— This paper focuses on the characteristic features of distribution grids, which have the greatest impact on the stability of generators and motor loads. It shows that severe accidents in distribution and transmission grids differ in nature, starting with an overload leading to line disconnections and further evolving into a voltage collapse. It appears that where generator capacity is commensurate with the total power of motors in a grid, the motor load has a significant impact on transients. The paper discusses how asynchronous operation is triggered, progresses, and can be addressed in a grid with distributed generation (DG) facilities. It further analyzes the consequences of deep grid sectionalization and proves why grid structure needs to be optimized for further development. The paper also shows how to take into account the specifics of emergency processes (i.e., accident-associated processes) in distribution grids when integrating and operating DG facilities.**

Index Terms: **Distribution grid, emergency operation, distributed generation facilities, gas-turbine unit, steam-turbine unit, asynchronous operation, resynchronization, self-start, sectionalization.**

I. Introduction

Over the past decade, the power industries in many countries (including Russia) have focused on measures lying in three key dimensions of development: decentralization, decarbonization, and digitalization.

This 3D approach stems from society's need for reasonably priced energy in required amounts, which is complicated by the necessity of delivering electricity reliably and safely.

Decentralization manifests itself through the adoption of an increasing number of distributed generation (DG) facilities, including renewable energy facilities (REF) that can be integrated into the power system or in islanded areas. Adding such facilities to the generator set alters substantially the transients [1-3].

Commissioning a DG facility enables its owner to deliver electricity to their power equipment reliably and independently; it also cuts energy costs, helping manufacture a cheaper-to-make and, therefore, more competitive product.

In the capacity range under consideration (several MW to several dozens MW), distributed generation is dominated by:

- gas-turbine power plants (GTPP) for the whole capacity range;
- gas-reciprocating power plants (GRPP) and diesel-fired power plants (DPP) at the lower end of the range;
- combined cycle gas-turbine plants (CCGTP), with gas-turbine units (GTUs) providing most power [4].

Balanced use of conventional power plants and DG facilities in power systems makes such systems more durable and easier to control, intensifies regional economic development, and creates demand for innovation in power engineering [5, 6].

Integration of DG facilities is an efficient tool for optimizing the investment in upgrading the generating equipment employed at conventional power plants. In some cases, it is more cost-effective to commission DG facilities rather than to construct grid facilities to connect new customers. It is also recommendable to construct DG facilities instead of reconstructing grid facilities as long as the capacity of power transmission lines (PTL) and power transformers increases.

Notably, emergency operation is different in medium- and high-voltage distribution grids, and this needs to be borne in mind when integrating DG facilities. Let us analyze the specifics of such an operation and the limitations it imposes.

* Corresponding author.
E-mail: ilyushin.pv@mail.ru

http://dx.doi.org/10.38028/esr.2020.04.0001
Received November 06, 2020. Revised November 19, 2020.
Accepted December 13, 2020. Available online February 01, 2021.

II. Specifics of Distribution Grids

There are several common factors descriptive of distribution grids. These are the factors that determine how transients progress in light of the significant variability of these parameters. The factors are:

- equivalent resistance values x_{ext} of interplant connections given in per-unit reduced to the baselines of the generators tested for stability ($S_{bas} = S_{g.nom}$, $U_{bas} = U_{g.nom}$). Lower x_{ext}, all other things being equal, stands for a more stable generator;
- the intensity of the load transient effect on generator transients. The load has the most profound impact when the motor slip considerably exceeds the critical value. The lower the resistance between the generator outputs and the busbars of electricity users, the greater the load-on-generator impact.

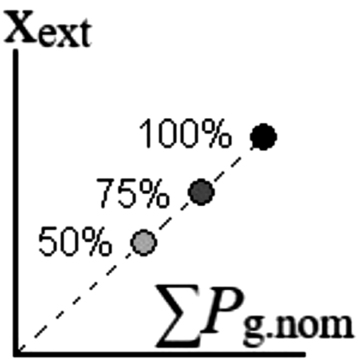

Fig. 1. ***x_{ext} as affected by reducing the number of generators online.***

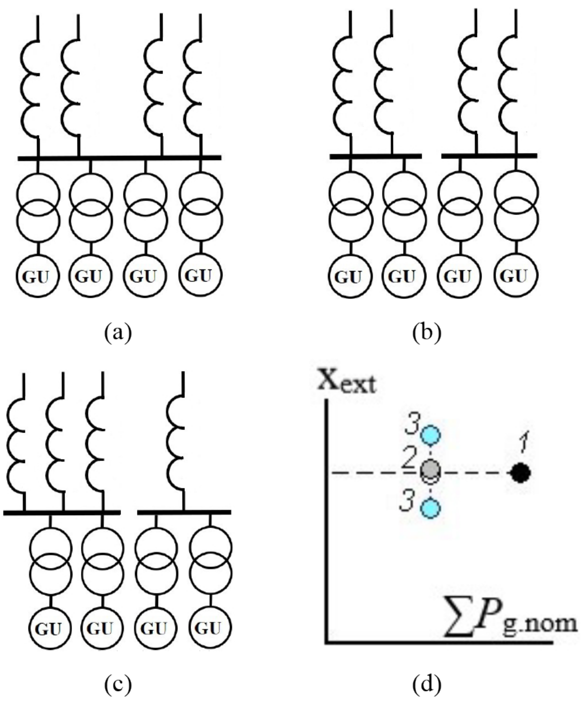

Fig. 2. ***x_{ext} as affected by sectionalizing power plant busbars: (a)-(c) are the busbar sectionalization alternatives; (d) is the curve of x_{ext}.***

For the first factor, it is important that reactance values xext follow a statistical pattern that shows: the higher is the capacity of the power plant, for which xext has been calculated, the higher are the reactance values. This is because the corresponding Ohm resistance values (X_{ext}) depend on the grid density. The baseline resistance values are inversely proportional to the power plant capacity values

$$Z_{bas} = U^2{}_{nom} / \sum S_{g.nom}.$$

Therefore, the relative resistance values $x_{ext} = X_{ext} / Z_{bas}$ are on average proportional to $\sum S_{g.nom}$. Given that in addition to normal operation, the grid may be switched to one of several repair circuitries, and that the equipment currently online may vary in composition, it is the values $x_{ext} = f(\sum P_{g.nom})$ that will correspond to the actual operating situations. Reducing the number of generators online will decrease $\sum P_{g.nom}$ and x_{ext} (increasing Z_{bas}), see Fig. 1

When sectionalizing a distribution grid, each part of a power plant (a DG facility) needs to be analyzed individually. Switching from complete circuitry 2*a* to sectionalized circuitry 2*b* will not affect the value x_{ext}, as it increases X_{ext} and Z_{bas}; in the case of the asymmetrical circuitry 2*c* one of the values x_{ext} will drop, and the other one will rise, see Fig. 2*d*.

In transmission grids, xext values vary to a far greater extent compared to distribution grids, as the latter cover only small areas, where "weak cutsets" are usually not found. Since stability problems are mostly associated with such "weak cutsets", ensuring the dynamic stability of a distribution grid is less of an issue. Analysis of system-wide accidents and emergencies in distribution grids shows that they differ in nature from those in transmission grids [7-11].

As for the second factor, load transients are known to affect the dynamic stability of generators in distribution grids. If the generator capacity is commensurate with the total motor power at an industrial facility, or with the total power of another equipment cluster where the load is homogeneous, such a load will have an immense impact.

Consider the calculated transients in a 220-kV distribution grid as caused by simultaneously disconnecting two power transmission lines that share the passage for over half the length of a shorter line, where the disconnection has been caused by a single-phase short circuit (SC) near a gas-turbine power plant (GTPP) under commissioning. This causes a desynchronization (a pole slip), see Fig. 3*a*, which will be interrupted by the pole slip protection system (PSP).

Given that an SC-associated voltage sag will cause a substantial load-shedding (due to under-voltage protection, etc.), which will reduce the current drawn by the decelerating motors from the grid, the grid voltage will rise to prevent the GTPP generators from losing their dynamic stability, see Fig. 3*b* [12, 13].

Load transients affect generator stability in distribution grids to a greater extent compared to transmission grids for two reasons:

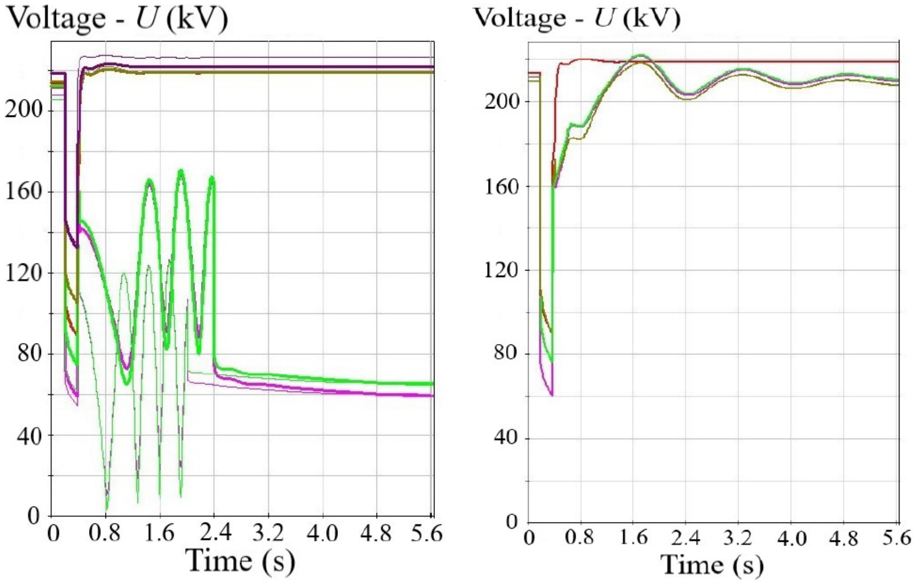

(a) (b)

Fig. 3. Transient voltages in the case of a near-GTPP SC:
(a) the entire load is self-starting (thin lines mean the GTPP is offline, thick lines show the GTPP is online);
(b) 30% of the load is disconnected at U < 0.7Unom (the GTPP is online).

- a transmission grid disturbance will involve multiple customers' loads in the transient, thus leveling the effects of, and on, each of them;
- a transmission grid SC will tend to cause a far lesser voltage sag on the customers' busbars compared to a distribution grid SC due to the resistance of power transformers.

Therefore, when seeking to ensure the stability of generators at power plants in a distribution grid having DG facilities, one needs to take into account the properties of loads at the adjacent grid nodes. In practice, the use of calculation flowcharts that neither include nor are adjusted to the equations of induction motors at load nodes in most cases will produce wrong results [14, 15].

Let us analyze what consequences the above-mentioned specific features of distribution grids might have.

III. Ensuring the Dynamic Stability of Generators

In the case of a failure to retain the dynamic stability of generators in a distribution grid, the voltage drop in the grid has a greater impact than the increase in the rotor angle against other generators (Δδ).

Excess in power transmitted through a weak cutset of the power system will violate the aperiodic static stability when such power P(Δδ) peaks. Dynamic stability is similarly upset when the slip angle (Δδ) increases to such an extent that re-syncing becomes impossible.

In a transmission grid, when static stability is lost and generators switch to asynchronous operation, they may or may not cause a significant voltage drop on the power plant busbars, as the weak (or overloaded) cutset will

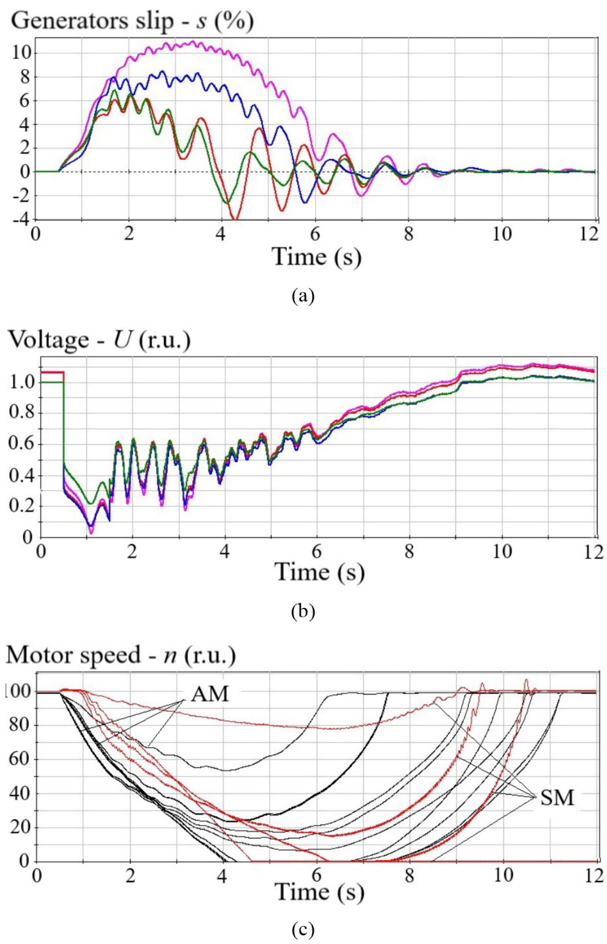

Fig. 4. Transient response to the de-syncing and re-syncing of CHP-1 and CHP-2 generators.

carry the bulk of the equivalent resistance between the EMFs of the generators whose mutual stability has been disrupted.

In a distribution grid, where inter-generator equivalent resistances are low, loss of static stability by generators due to excessive power transmission through a cutset will only be possible if the grid overloads considerably exceed the permissible limits. For this reason, distribution grid destabilization first manifests itself as the overload of grid components.

In Phase I, the current load on the grid is growing while the node voltages are within the acceptable range. Power transmission lines are disconnected due to loads, whether the effects of the latter are direct or indirect. The grid is weakened, which leads to further growth in current loads and more disconnections.

In Phase II, the voltage on the customer side drops so much that the customer needs to consume more reactive power, which leads to a further voltage sag and triggers a voltage collapse at the load nodes.

In this situation, the emergency is not caused by but results in generator destabilization, and the key factor here is the voltage sag on the customer side, which reduces their equivalent resistance to ground and increases the equivalent mutual inter-generator resistance, further increasing the angles $\Delta\delta$. Fig. 4 shows an example of such a process for a 110-kV distribution grid.

In the transient shown in Fig. 4, a 1-second voltage sag in a 110-kV grid cutset adjacent to CHP-1 and CHP-2 causes the loss of synchronism in CHP generators. Early in the transient, generator slips (Fig. 4*a*) develop at a relatively low rate, then such development accelerates due to a voltage sag, which, in turn, is caused by the deceleration of motors at the major industrial facilities nearby. Asynchronous operation ends when most of the motors self-start (some of the synchronous motors fail to do so).

Therefore, voltage closely links the transients (which determine the stability of generators in a distribution grid, including DG facilities) and the motor stability (self-starting).

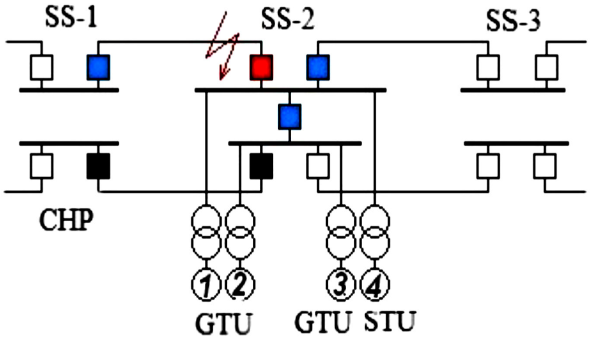

***Fig. 5.** Simplified single-line circuit diagram of a 110-kV distribution grid fragment with CCGTP: red is for SC-induced circuit breaker failure; blue is for circuit breakers disconnected by the CBFP; black is for circuit breakers disconnected for PTL repair.*

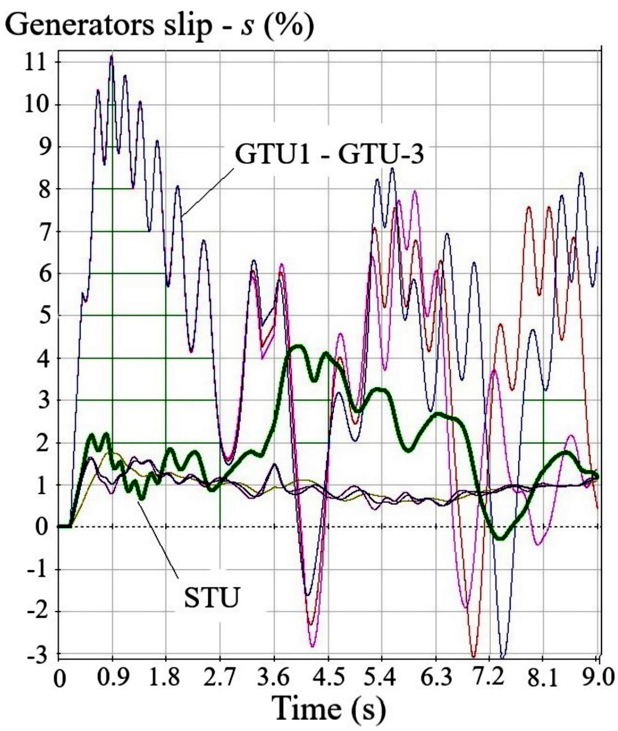

***Fig. 6.** Transient: short-term asynchronous operation due to a three-phase SC near the CCGTP.*

IV. Specifics of Asynchronous Operation in Distribution Grids

Distribution grids contain multiple closely located medium- and low-capacity power plants, including DG facilities. As a result, SC-induced dynamic instability is usually localized and only affects a small segment of the grid.

Consider the asynchronous operating conditions at a combined cycle gas-turbine plant (CCGTP) comprised of three gas-turbine units (GTU) and a single steam-turbine unit (STU); let a three-phase SC on a 110-kV PTL running from the substation SS-2 cause a circuit breaker fault and trigger the circuit breaker failure protection (CBFP). Fig. 5 shows a simplified single-line diagram of a fragment of this 110-kV distribution grid with the CCGTP.

Fig. 6 shows a short-term multi-machine asynchronous operation: transients in the GTUs and STU of the CCGTP are nearly independent due to the low x_{ext} values for this facility as compared to other power plants in the grid, as well as due to the high mutual resistance between the units.

The following segments can be seen in Fig. 6:

- at 0 s < t < 3.5 s, there is two-machine asynchronous operation as it involves the GTU cluster (GTUs 1 to 3) and the STU;
- at 4 s < t < 4.5 s, there is two-machine asynchronous operation as it involves the STU and the GTU cluster, although GTUs 1 to 3 are temporarily resynchronized within the cluster;

- at 4.5 s < t < 5 s, there is two-machine asynchronous operation as it involves the GTU cluster and the STU;
- at 5 s < t < 6.5 s, there is multi-machine asynchronous operation, $f_{GTU\text{-}1\ to\ GTU\text{-}3} > f_{STU} > f_{grid}$;
- at t > 7 s, GTU-1 and the STU are resynchronized to each other, GTU-2 and GTU-3 are resynchronized as well, albeit only for a short time;
- at $t \approx 8$ s, three different frequencies can be observed simultaneously for a short time: $f_{GTU\text{-}2} > f_{GTU\text{-}3} > f_{grid}$.

In distribution grids, swing centers are rarely outside a power plant; in some cases, the swing center is near the generator outputs but more often within the step-up transformer. This is an immediate consequence of having many connections in a distribution grid at low relative resistances x_{ext}. The chances that the generators will resynchronize themselves spontaneously are high, but so is the probability of the asynchronous operation evolving to affect multiple machines, which will prevent resynchronization (Fig.6) [16-18].

This is due to two factors:

- if there are multiple synchronous motors (SM) at a grid node, a generator slip at a nearby power plant will likely cause a loss of their synchronism as well (a vise-a-versa sequence is also possible);
- a multi-machine asynchronous operation may start if the same grid segment has STUs and GTUs with a free gas turbine. The mechanical constant of inertia is two to three times lower for the latter than for STUs or single-shaft GTUs. Loss of stability in a group of such generators will likely result in a multi-machine slip.

In transmission grids, slips are handled by separating the de-synced parts of the system; this happens so fast that secondary loss of stability does not occur.

The method is ineffective in the case of a distribution grid, as it quickly develops a multi-machine slip. Given that the swing center is near the generator, the PSPs will successfully disconnect it, even in the case of a multi-machine asynchronous operation. In the event that the asynchronous operation involves desynchronized SMs, they must be disconnected to facilitate the self-resynchronization of generators.

V. Consequences of Sectionalizing a Distribution Grid

As loads increase in major cities and megacities, while opportunities for further grid development are limited, SC currents often tend to exceed the capacity of circuit breakers. For instance, SC currents would exceed 120 kA in Moscow in the case of retaining a normal grid circuitry, which is twice the switching capacity of circuit breakers (63 kA). Today and in the near future, the most practical SC-limiting solutions for 110- to 220-kV grids are:

A. Uncontrolled current-limiting reactors (CLR)

This is the easiest method; however, the voltage regulation and stability requirements, especially for substations at the end of a dead-end feeder, mean that it is unacceptable to have a significant CLR resistance. On the other hand, too many CLRs would be needed if their resistance were low (1 to 4 Ohm).

B. Controlled current limiters (CL)

These devices are capable of an inertia-free first-approximation increase in their inductance by a factor of dozens to hundreds, with the restoration to normal operation, once the SC has been cleared. Whether it is a CL or a CLR, such units are difficult to install at an existing substation.

C. Grid Sectionalization

SC currents are the highest at substations where the SC current is contributed to by multiple sources: power plants or transmission grid coupling transformers. As some circuit breakers are disconnected, this contribution will be less and the total SC current will be reduced.

Bus-section circuit breakers are the most effective and safest to disconnect from the standpoint of grid reliability.

As of today, sectionalizing 110- to 220-kV distribution grids is a necessary and common measure. Sectionalizing weakens the grid and makes electricity delivery less reliable. The practice has shown that a sufficiently extensive

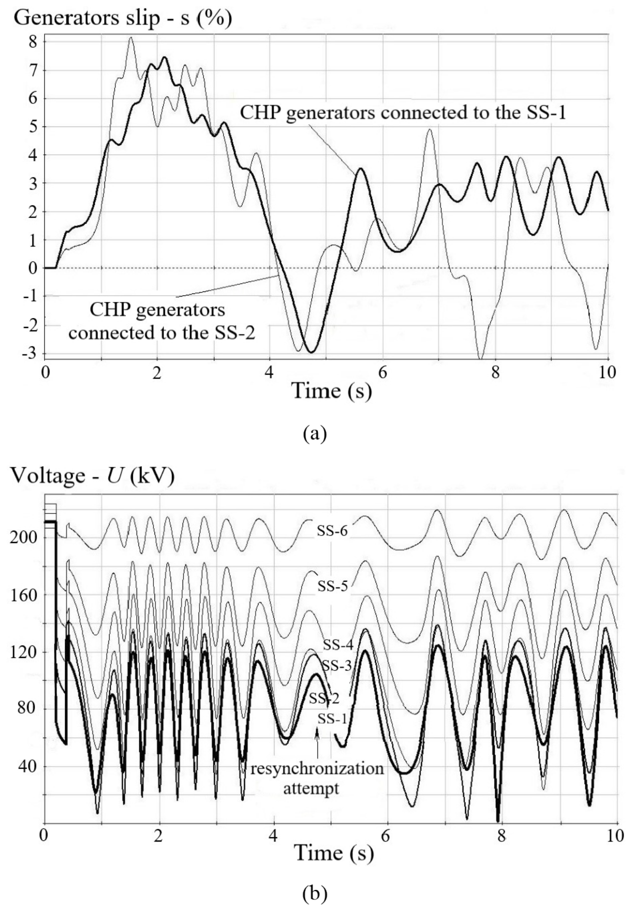

Fig. 7. Transient response to a two-phase ground fault in an extensively sectionalized grid: (a) generator slips at SS-1 and SS-2; (b) busbar voltages at the adjacent SSs.

sectionalization prevents immediate severe consequences. Sectionalization opportunities are limited by grid controllability; besides, this effort needs to be continued whenever more power plants and customers are connected.

Consider a 220-kV distribution grid, the extensive sectionalization of which has had a negative impact on the dynamic stability of power plant generators. Fig. 7 shows a transient caused by a two-phase ground fault in a 220-kV PTL, causing an SS-1 circuit breaker failure and triggering the CBFP.

Fig. 7 shows a transient, where at $t \approx 4.3$ s the system attempts to re-sync the generators of the CHP; however, the attempt fails, as motors at the adjacent nodes decelerate due to low voltage.

A series of transient calculations shows that the severity of the SC consequences depends not on the initial generator power shedding, which would depend on the SC type, but on the post-emergency condition of the grid, which in the case of three-phase rather than phase-by-phase circuit breaker control does not depend on the SC type.

A CL installed at SS-1 in series with the bus section circuit breaker would enable switching the circuit breakers on in the adjacent 220-kV grid, and the transient would develop absolutely differently (Fig.8).

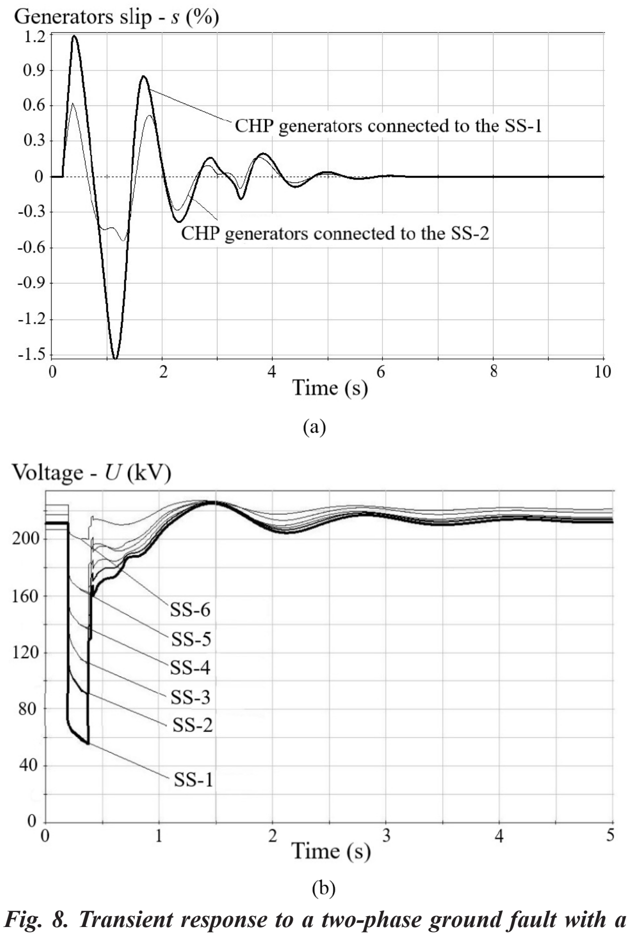

Fig. 8. Transient response to a two-phase ground fault with a CL at SS-1: (a) generator slips at SS-1 and SS-2; (b) busbar voltages at the adjacent SSs.

The transient shown in Fig. 8 does not cause secondary destabilization; motors at the load nodes restart quickly and without difficulty.

Therefore, if an emergency in a weakened (extensively sectionalized) grid develops slowly, the corresponding segment must be de-sectionalized to reduce the load to be disconnected, thus mitigating the negative impact of sectionalization.

However, if the emergency develops quickly as shown in Fig. 7, load shedding becomes necessary to avoid a voltage collapse; in that case, the amount of load to be shed by the relay protection and emergency control system will proportionately depend on the extent to which the grid is sectionalized [19-22].

As of today, opportunities for sectionalization that reduces SC currents but also weakens the grid have been nearly depleted, which calls for research of urban grid development to optimize the structure of such grids so that they could function reliably while reducing the SC currents.

VI. Specifics of Distributed Generation Facilities

Loads to be carried by the grids in major cities and megacities are rising, as many more customers are being newly connected, especially at the locations of comprehensive and infill development. The overloads occur in the PTLs, whether overhead or cable, as well as in power transformers at substations.

To address this issue, distributed generation facilities need to be constructed and connected to the existing distribution grids. They should be configured to concentrate the installed capacity in a small area so as to avoid overloading the distribution grid with transit power flows.

With respect to the reliability of electricity supply, the connection of DG facilities featuring low- and medium-capacity generator sets is an effort that requires due attention to its specifics, and here is why:

- generator-to-grid connection resistance varies broadly;
- in the case of a power system accident, islanding DG facilities to deliver electricity to the nearest customers might be problematic.

The DG operation practice shows that using non-selectively protected generator sets, i.e., the manufacturer's default protection settings, makes sense if the DG facility is connected to a "rigid" grid with the sole purpose of minimizing energy costs, where reliability is not a concern.

If the purpose of constructing a DG facility is to normalize the operating parameters of a weak or overloaded grid segment, the use of non-selectively protected generator sets to provide backup power to a variety of customers is not an acceptable solution.

Therefore, when designing a DG facility connection, one needs to determine whether the selected generator sets are well-compatible with the electricity delivery and consumption parameters, and the operating parameters of the distribution grid under consideration; and take into account the costs of commissioning/upgrading power equipment and secondary equipment (relay protection, emergency control systems, process protections, and automatic devices).

VII. Conclusion

Distribution grids contain multiple closely located medium- and low-capacity power plants. As a result, SC-induced losses of dynamic stability are usually localized and only affect a small grid segment.

Unlike the most severe emergencies in transmission grids, those in distribution grids usually begin when PTLs are overloaded and disconnected sequentially, followed by a voltage collapse and loss of stability in generator/motor.

Distribution grids are at risk of loss of synchronism when exposed to an accident-associated (emergency) disturbance, especially if some generator sets have low mechanical constants of inertia; these asynchronous operating conditions might involve multiple machines, although generators may resynchronize spontaneously as well.

At low- and medium-capacity power plants, the swing center is usually near the generator outputs or in the step-up transformer.

Opportunities have been nearly depleted for sectionalization that reduces SC currents but also weakens the grid, which calls for research of urban grid development to optimize the structure of such grids so that they could function reliably while reducing the SC currents.

When designing a DG facility connection, one needs to determine whether the selected generator sets are well-compatible with the electricity delivery and consumption parameters, and the operating parameters of the distribution grid under consideration. The costs of commissioning (upgrading) power equipment and secondary equipment (relay protection, emergency control systems, process protections, and automatic devices) must also be taken into account.

References

[1] N. I. Voropai, “Multi-criteria problems in electric power system expansion planning,” *Energy Systems Research*, vol. 1, is. 2, pp. 27–34, 2018.

[2] Z. Li, G. Yao, G. Geng, and Q. Jiang, “An efficient optimal control method for open-loop transient stability emergency control,” *IEEE Transactions on Power Systems*, vol. 32, is. 4, pp. 2704–2713, 2017.

[3] A. Wen, M. Y. Zhao, W. F. Huang, and C. Z. Wei, "Design and development of wide-area protection and emergency control for application in distribution networks of embedded generation," *Proceedings of the IEEE Power & Energy Society General Meeting*, pp. 1–5, 2015.

[4] G. M. Tina, S. Licciardello, and D. Stefanelli, “Conventional techniques for improving emergency control of transient stability in renewable-based power systems,” *Proceedings of the 9th Int. Renewable Energy Congress*, 2018.

[5] Th. L. Vu and K. Turitsyn, “Options for emergency control of power grids with high penetration of renewables,” *Proceedings of the IEEE Int. Conf. on Sustainable Energy Technologies*, 2016.

[6] R. Zhang, X. Lin, P. Yang, and Z. Li, "The emergency control strategies of a short-run isolated island wind farm," *Proceedings of the Int. Conf. on Renewable Energy Research and Application,* pp. 203–211, 2014.

[7] P. V. Ilyushin, A. L. Kulikov, “Adaptive algorithm for automated undervoltage protection of industrial power districts with distributed generation facilities,” *Proceedings of International Russian Automation Conference*, 2019.

[8] Sk. R. Islam, D. Sutanto, and K. M. Muttaqi, “Coordinated decentralized emergency voltage and reactive power control to prevent long-term voltage instability in a power system,” *IEEE Transactions on Power Systems*, vol. 30, is. 5, pp. 2591–2603, 2015.

[9] N. I. Voropai, V. A. Stennikov, B. Zhou, E. A. Barakhtenko, D. N. Karamov, O. N. Voitov, D. V. Sokolov, “An approach to the modeling of decentralized integrated energy systems with renewable energy sources,” *Energy Systems Research*, vol. 2, is. 1, pp. 5–12, 2019.

[10] N. I. Voropai, “General methodological approaches to hierarchical modeling of complex systems,” *Energy Systems Research*, vol. 2, is. 4, pp. 17–21, 2019.

[11] S. I. Budi, A. Nurdiansyah, and A. Lomi, “Impact of load shedding on frequency and voltage system,” *Proceedings of the Int. Sem. on Intelligent Technology and Its Applications*, 2017.

[12] K. B. Kilani, M. Elleuch, and A. H. Hamida, “Dynamic under frequency load shedding in power systems,” *Proceedings of the 14th Int. Multi-Conf. on Systems, Signals, and Devices*, 2017.

[13] Ya. L. Artsishevskiy and B. M. Gieev, "Adaptation of UFLS to a variable level of responsibility of 0.4 kV electric receivers," *Power engineer*, vol. 5, pp. 18–21, 2017.

[14] A. L. Kulikov, M. V. Sharygin, P. V. Ilyushin, “Principles of organization of relay protection in microgrids with distributed power generation sources,” *Power Technology and Engineering*, vol. 53, is. 5, pp. 611–617, 2020.

[15] A. L. Kulikov, D. I. Bezdushniy, M. V. Sharygin, and V. Yu. Osokin, "Analysis of the support vector machine implementation in the multi-dimensional relay protection," *Izvestia RAN. Energetika*, no. 2, pp. 123–132, 2020. (in Russian)

[16] P. V. Ilyushin, “Emergency and post-emergency control in the formation of micro-grids,” *Proceedings of Methodological Problems in Reliability Study of Large Energy Systems*, vol. 25, 2017.

[17] P. V. Ilyushin, O. A. Sukhanov, “The structure of emergency-management systems of distribution networks in large cities,” *Russian Electrical Engineering*, vol. 85, is. 3, pp. 133–137, 2014.

Pavel V. Ilyushin is chief researcher, head of the center "Intelligent Power Systems and Distributed Generation" of the Energy Research Institute of the Russian Academy of Sciences. P.V. Ilyushin graduated from Novosibirsk State Technical University in 1997. In 2020, he received his D.Sc. degree from the Scientific and Technical Center of the Federal Grid Company of the Unified Energy System. He is a chairman of SC C6 in the CIGRE Russian national committee. His research interests include distributed generation and distribution grids, power system automation.

Alexander L. Kulikov is a professor at the Department of Power Engineering, Power Supply and Power Electronics of Nizhny Novgorod State Technical University named after R.E. Alekseev. A.L. Kulikov graduated from the Military Radio Engineering Academy of Air Defense named after Govorov L.A. in 1992. In 2007, he received his D.Sc. degree from V.I.Lenin Ivanovo State Power Engineering University. His research interests are relay protection, fault location, and digital signal processing.

The Influence of Fuel and Steam Consumption on Characteristics of Fixed Bed Process of Woody Biomass Steam Gasification with Intensive Heat Supply

I. G. Donskoy*

Melentiev Energy Systems Institute of Siberian Branch of Russian Academy of Sciences, Irkutsk, Russia

***Abstract* — Plant biomass is one of the most widespread renewable energy sources. Energy utilization of biomass allows solving some problems associated with the development of off-grid energy systems and the processing of combustible waste (primarily agricultural and forestry waste). This paper is devoted to the study of an allothermal gasification process of plant biomass materials using a kinetic-thermodynamic model developed by the author. The gasification process is considered stationary, and steam is used as a gasification agent. The power of the supplied heat is considered constant (10 kW). One of the significant tasks related to allothermal gasification is to choose flowrate parameters so that the heat supplied is efficiently used in chemical reactions without the threat of reactor overheating. The determination of the boundaries of the safe gasifier operation involved variant calculations with a view to optimizing the gasification conditions. The calculation results show that the allothermal gasification process can proceed with a thermochemical efficiency of about 70%. For each fixed fuel consumption level, there is an optimal fuel-steam ratio. The complete conversion of biomass requires sufficiently high temperatures. The produced gas contains a significant steam fraction (>50** vol%**) even under optimal conditions. The calculated fraction of hydrogen in dry gas is up to 60**vol%**. The data obtained can be used to assess the efficiency of energy units with biomass gasification using high-temperature sources, for example, in systems that use and store solar thermal energy.**

***Index Terms*: bioenergy, allothermal gasification, mathematical modeling, hydrogen, solar energy.**

I. Introduction

Thermochemical biomass conversion technologies have prospects for being used in distributed generation systems, not only in agricultural regions, where a large quantity of cheap reserves of combustible waste is available [1, 2] but also in developed countries, where renewable energy sources are attractive due to their environmental characteristics [3, 4]. The significant energy potential of biomass (primarily forestry and agriculture waste) is currently used to an extremely small extent, although it can be technically and economically beneficial for a wide range of energy systems [5, 6]. Biomass is used both as an addition to fossil fuels to reduce hazardous emissions produced [7, 8] and as the primary fuel [9]. The involvement of biomass in energy production requires new methods and modification of the known methods of its thermochemical processing. The reliable technologies based on these methods can only be created through an in-depth scientific study of all stages of the process, from the selection of suitable raw materials to the control of processes in the reactor and design of cleaning systems [10, 11].

Biomass is characterized by a high moisture content, high reactivity (compared to fossil fuel), the variability of mechanical properties (biomass particles may agglomerate [12], or, vice versa, disintegrate during thermal conversion [13]), production of significant amounts of tarry products during heating and oxidation [14], and a low content of ash (which, however, often has increased corrosive properties and a tendency to form fine particulate matter [10, 15]). Combustion (including co-combustion) is the most widely

* Corresponding author.
E-mail: donskoy.chem@mail.ru

http://dx.doi.org/10.38028/esr.2020.04.0002
Received October 09, 2020. Revised October 21, 2020.
Accepted November 03, 2020. Available online February 01, 2021.

used biomass conversion technology [16]. Many processes of low-temperature thermochemical processing of biomass with the production of high-calorific gas through pyrolysis and gasification have been proposed [17, 18], but their efficiency is very sensitive to the conditions of their implementation. There are more specific conversion processes, for example, plasma processing [19], and the use of supercritical fluids [20]. However, they are technologically more complicated and have high energy demands.

Pyrolysis and gasification of biomass have the potential to be applied in the areas with low energy consumption, in decentralized power supply systems. Researchers tend to consider low-capacity power units [21, 22], working with internal combustion engines [23, 24], microturbines [25], fuel cells [26], or gas burners [27]. Analysis of the life cycle of bioenergy units, even for small capacities, shows their high environmental efficiency compared to the units using fossil fuels [28, 29]. Gasification efficiency in typical small-scale processes (fixed bed and fluidized bed) is about 50-70%. Given the thermal efficiency of the gas engine at the level of 20-30%, one can obtain fuel utilization efficiency of 10-20%. One of the ways to improve the efficiency of gasification-based energy units is to use external heat sources to enhance conditions in the reactor.

Solar radiation is usually concentrated using collectors [30–32], which allow reaching a peak thermal power of up to 100 MW with a radiation collection efficiency of the order of several tens of W/m^2. The use of biomass makes it possible to smooth stochastic generation as part of hybrid power plants [33, 34]. The processes of thermochemical conversion of biomass can be used to store the energy of solar radiation (along with electric batteries [35, 36], carbonate and oxide cycles [37, 38], and others). To this end, fixed or fluidized bed reactors and vortex devices were developed [39-41]. The gasification agent is usually steam or vapor-air mixtures [42, 43]. The produced combustible gas with high hydrogen content can be used for direct oxidation or stored in a gasholder [44, 45]. Concentrated solar radiation can also be used at thermal power plants with solid fuel processing, for example, for heating of working fluid [46] or air when burning low-calorific fuels [47].

Experimentally, biomass and coal gasification and combustion under the intense radiation were investigated in [48-50]. The conversion factor of radiant energy in the biomass gasification process is usually low (10-20%). Kinetics of gasification of carbonaceous materials at high temperatures was studied in [51, 52]. Mathematical models of gasification processes under the influence of solar radiation are proposed in [53-58]. Allothermal processes of biomass pyrolysis and gasification were investigated in [59–67], including those in a staged gasification unit [68, 69]. Schemes with the heat recirculation of the produced gas were proposed in [70]. Mathematical models of allothermal reactors were proposed in [71–75]. This study considers a version of the model [74] with fuel and steam heating by a constant heat flow. The gasification process is optimized by direct calculation of an output parameters on a grid of input parameters and selection of the best parameters according to efficiency criteria (completeness of fuel conversion, hydrogen yield) under some constraints (for example, on the maximum temperature). The computational efficiency of the mathematical model allows making such calculations in a reasonable time.

II. Mathematical model description and initial data

The equations describing stationary heat transfer in the fuel bed can be written as follows:

$$\lambda^g \frac{d^2T^g}{dz^2} - C_p^g J^g \frac{dT^g}{dz} - \alpha_1 S_1 \left(T^g - T^f\right) - \\ - \alpha_2 S_2 \left(T^g - T^w\right) + q^g\left(z\right) = 0,$$

$$\lambda^f \frac{d^2T^f}{dz^2} - C_p^f J^f \frac{dT^f}{dz} + \alpha_1 S_1 \left(T^g - T^f\right) - \\ - \alpha_3 S_2 \left(T^f - T^w\right) + q^f\left(z\right) = 0,$$

$$\frac{d^2T^2}{dz^2} + \alpha_2 S_2 \left(T^g - T^w\right) + \alpha_3 S_2 \left(T^f - T^w\right) + q^w(z) = 0.$$

Here T is temperature, K; C_p is heat capacity, J/kg/K, λ is effective thermal conductivity, W/m/K; α is heat transfer coefficient, W/m^2/K; J is flowrate, kg/m^2/s; S_1 is gas-fuel heat transfer surface, m^2/m^3; S_2 is gas-wall heat transfer surface, m^2/m^3; q is a heat source, W/m^3; z is spatial coordinate (reaction zone length), m; indexes f, g, and w correspond to fuel, gas and wall.

When solving the problem numerically, the reactor is divided along the axis into some small-volume elements. Knowing the residence time of the gas in each of these elements, one can write the function of the heat source for the selected i-th element in the form:

$$q = Q_{dry} r_{dry} + Q_{pyr} r_{pyr} + Q_{gas} r_{gas}.$$

Here Q is a thermal effect, J/kg; r is process rate, kg/m^3/s; indexes dry, pyr, and gas correspond to drying, pyrolysis, and char gasification processes, respectively. Values of q could be calculated using enthalpies of individual components and mass balance for every spatial element of length Δz:

$$q_i = \frac{J_{i-1}}{\Delta z} \sum_j h_{i-1}^j \left(T_{i-1}\right) y_{i-1}^j - \frac{J_i}{\Delta z} \sum_j h_i^j \left(T_i\right) y_i^j.$$

Here index i corresponds to spatial element number; h^j is specific enthalpy of j-th component, J/kg; y^j is the mass fraction of j-th component.

The change in the chemical composition is calculated in two steps. The first step suggests considering heterogeneous processes: drying, pyrolysis, and the charcoal reactions with CO_2 and H_2O (oxidation by O_2 is not taken into account):

$$\frac{dy_{H_2O}}{dz}=\frac{\rho^g}{J^g}\beta S_1\left(\frac{C^{eq}_{H_2O}}{\rho^g}-y_{H_2O}\right),$$

$$\frac{dm_V}{dz}=-\frac{\rho^f}{J^f}k_{pyr}m_V,$$

$$\frac{dm_C}{dz}=\frac{1-V_{daf}}{V_{daf}}\frac{dm_V}{dz}+\frac{\rho^f}{J^f}\left(-k^{eff}_{CO_2}S_1\rho_g y_{CO_2}-k^{eff}_{H_2O}S_1\rho_g y_{H_2O}\right).$$

Here ρ is the density, kg/m^3; β is coefficient of mass transfer, m/s; C^{eq} is the equilibrium concentration of water vapors, kg/m^3; k_{pyr} is pyrolysis rate constant, s^{-1}; m_V is the quantity of volatiles in the fuel, kg; m_C is the amount of carbon in the fuel, kg; y_{CO_2}, y_{H_2O} are mass fractions of gasification agents in the porous volume; k^{eff} is the effective rate constant of a heterogeneous reaction, m/s. The effective rate constant of the heterogeneous reaction k^{eff} is determined in the quasi-stationary approximation [76]:

$$k^{eff}=\frac{1}{\frac{1}{\beta}+\frac{1}{k_0e^{-\frac{E}{RT}}}}.$$

Here k_0 is the pre-exponential factor, m/s; E is the activation energy, J/mol; R is the universal gas constant. Chemical kinetics of reactions in the gas phase is not considered: it is assumed that the gas phase quickly reaches a state of equilibrium. Thus, at the second step of the calculation, chemical transformations are described using a thermodynamic model with macrokinetic constraints on the rate of heterogeneous transformations. This approach is applicable to high-temperature processes, in which the rate of gas-phase processes is quite high, compared to that of heterophase processes. In the iterations, the local temperature can be considered a constant parameter, and the heat balance is taken into account when solving the heat transfer equations [77]. Kinetic coefficients are presented in Table 1.

Table 1. Kinetic coefficients

Reaction	k_0, s^{-1}	E_a, kJ/mol
Pyrolysis	5×10^4	96
C + CO_2	1.32×10^7	250
C + H_2O	9.3×10^5	175

The presented model of a fixed bed conversion was used earlier in the study on low-grade fuels gasification processes in [78, 79]. This research assumes that the reaction zone of the reactor is uniformly heated through the wall with a constant heat flux of 10 kW. The reaction zone dimensions taken for calculations are - length is 0.25 m and diameter is 0.2 m. The fuel is woody biomass with the following composition: W^r = 12%, A^d = 0.67%, V^{daf} = 80% C^{daf} = 46.96%, H^{daf} = 5.92%; O^{daf} = 45.23%; N^{daf} = 1.08%; S^{daf} = 0.08%; average particle size is 2.5 cm. Variable parameters are fuel flowrate (4-10 kg/h) and steam flowrate (2-10 kg/h). The fuel inlet temperature is 300 K, the steam inlet temperature is 600 K. The characteristics of interest are the outlet gas composition, the degree of fuel conversion, and the thermochemical efficiency of the process (η). Efficiency is defined as the ratio of the output flow of chemical energy (calorific value of the generator gas Q^gJ^g) to the input flow of energy (calorific value of the fuel Q^fJ^f and supplied heat q^{ex}):

$$\eta=\frac{Q^gJ^g_{out}}{Q^fJ^f_{in}+q^{ex}}.$$

The calorific value of the generator gas is calculated as the weighted sum of the calorific values of its constituent components. With a higher calorific value of the feedstock of about 15 MJ/kg, the supplied heat is equivalent to 25-60% of the calorific value of the biomass entering the reactor.

III. Results and discussion

At low biomass and steam flowrates, most of the supplied heat goes to temperature increase: as seen in

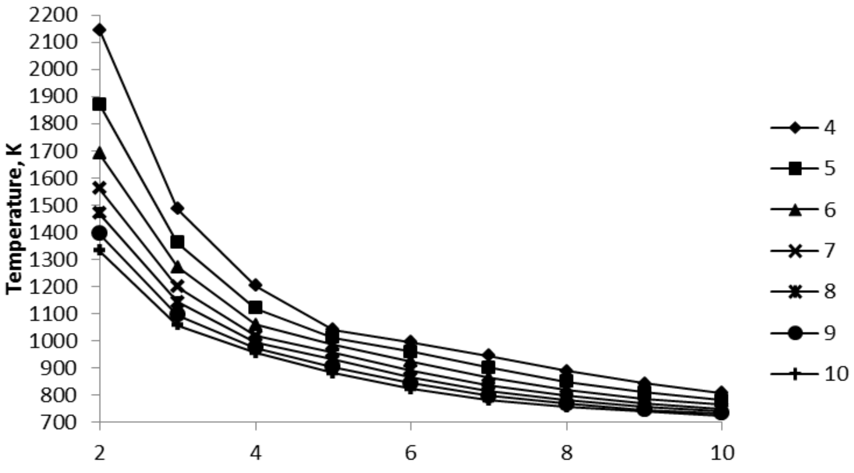

Fig. 1. Relationship between maximum temperature in gasifier and steam and fuel flow rates (numbers in the legend are fuel flowrates, kg/h).

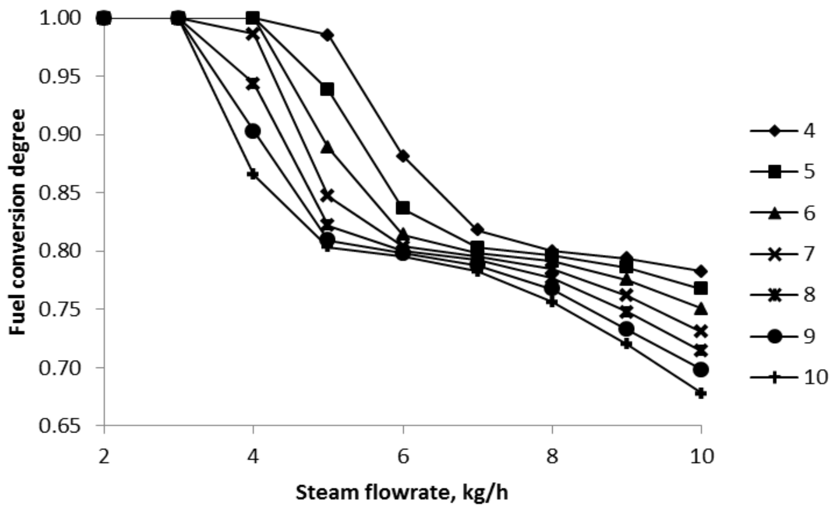

Fig. 2. Relationship between fuel conversion degree and steam and fuel flowrates (numbers in the legend are fuel flowrates, kg/h).

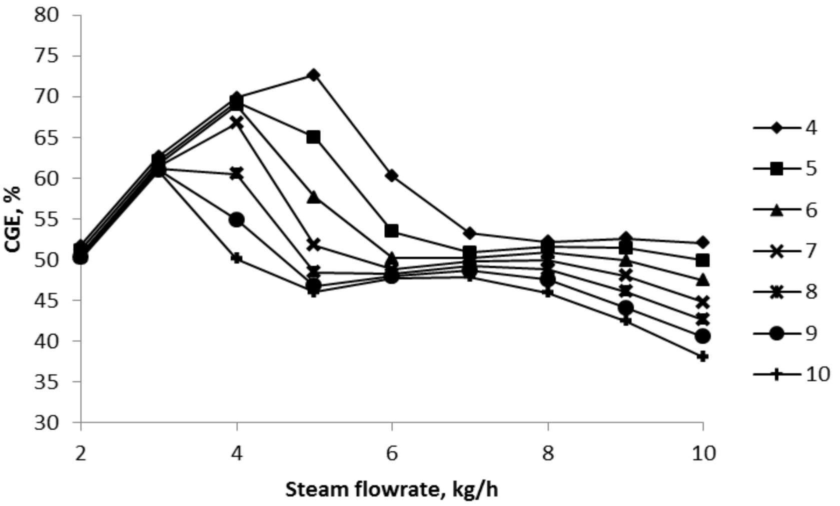

Fig. 3. Relationship between thermochemical efficiency of gasification process and steam and fuel flowrates (numbers in the legend are fuel flowrates, kg/h).

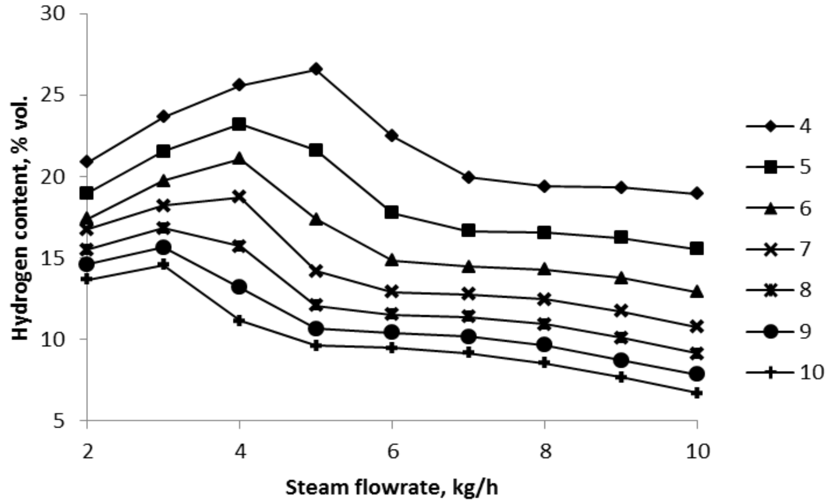

Fig. 4. Relationship between hydrogen concentration in raw produced gas and steam and fuel flowrates (numbers in the legend are fuel flowrates, kg/h).

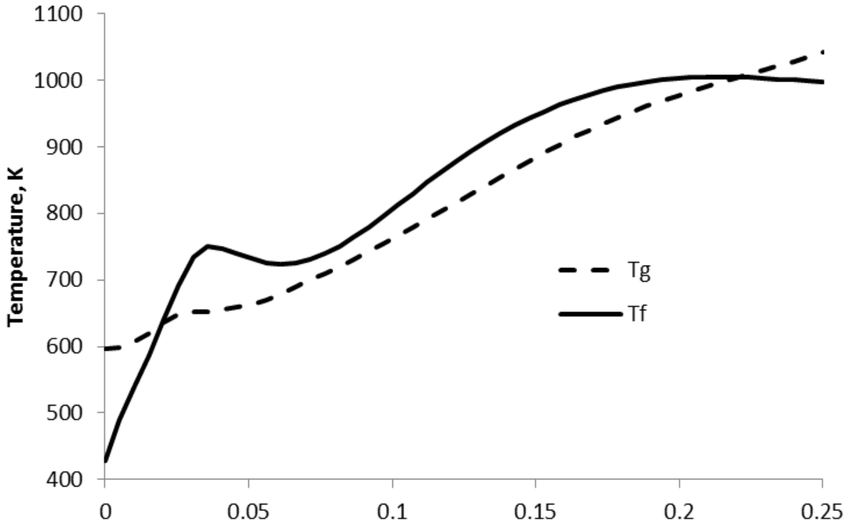

Fig. 5. Distribution of gas and fuel temperature along the reaction zone.

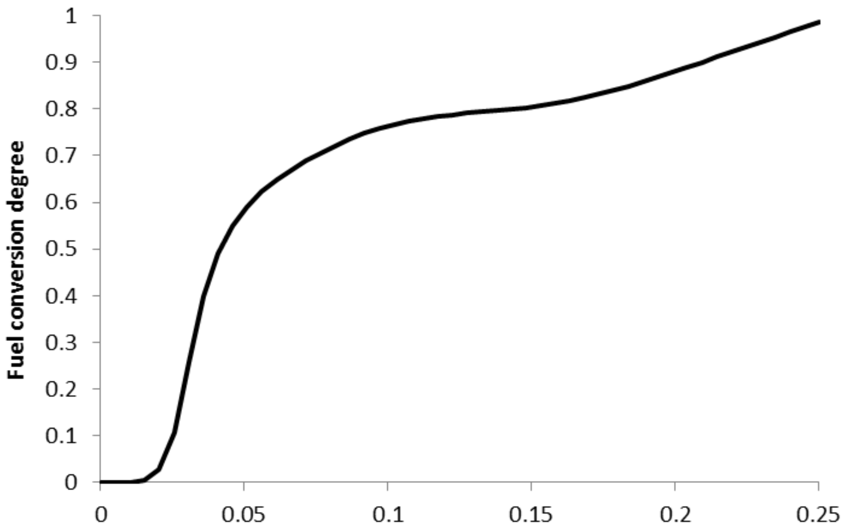

Fig. 6. Distribution of fuel conversion degree along the reaction zone.

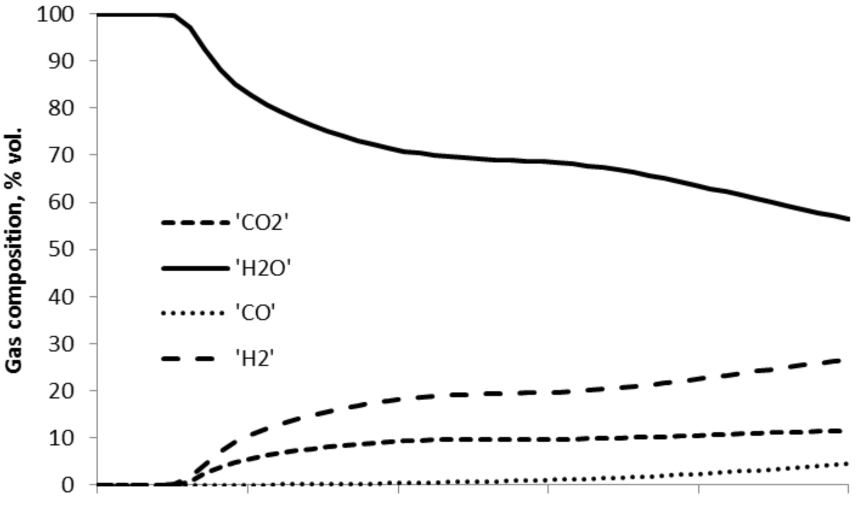

Fig. 7. Distribution of gas composition along the reaction zone.

Table 2. Comparison of modeling results with published data on dry gas composition (vol%.)

Source		H_2	CO	CO_2	CH_4
[82]		44.7	25.2	5.8	1.8
[83]	Pyrolysis	44.2	51.8	18.3	23.8
	Gasification	48.8	32.8	16.7	1.7
[49]		52.4	38.9	3.2	1.5
[67]		44.6	19.7	22.3	13.4
[40]		37.2	40.0	11.1	8.8
Present work	High steam-fuel ratio	54.5	26.7	15.5	2.5
	Optimal	61.0	10.3	26.4	1.5

Fig. 1, temperatures can reach very high values (up to 2000 K). These conditions are not suitable for real units due to constraints on material properties. Additionally, the kinetics of chemical reactions and transport processes at high temperatures may differ from that assumed in the model. Already in this stage of consideration, it is possible to exclude a range of inappropriate parameters.

With an increase in the fuel and steam flowrate, however, the conversion of fuel decreases (Fig. 2). The lower the temperature, the lower the gasification rate, which is why, at a steam flowrate of more than 3-4 kg/h, charcoal yield increases sharply. At a high fuel flowrate, the reactor can operate as a pyrolyzer (for example, for the production of activated carbon [80]). For complete gasification of biomass, it is necessary to select conditions with low fuel flowrates and high steam flowrates, most of which serves as ballast to prevent overheating. Fig. 3 shows the relationship between the efficiency and the process parameters: with a change in the steam flowrate and fixed fuel flowrate, the gasification process efficiency has an extremum corresponding to the complete conversion of fuel carbon. The maximum concentration of hydrogen in the produced gas is also observed (about 26 vol%).

Thus, with a fixed external heat supply, the optimal parameters of the allothermal gasification process are determined by the fuel-steam ratio and the total flowrate of reagents (at low flowrates, the temperature in the reactor becomes unacceptably high). The range of suitable temperatures, in which the gasification reactions proceed quite intensively, can be limited, but the reactor overheating is not observed in a range of 1000-1100 K. Then, according to Fig. 1, one can cut off the area of unsuitable conditions.

The temperature distribution over the reactor length for one set of parameters (fuel flowrate 4 kg/h and steam flowrate 5 kg/h) is shown in Fig. 5. The fuel is heated at an almost constant rate until intense devolatilization begins.

As seen in Fig. 6, with an increase in the degree of conversion, the devolatilization slows down. The gasification stage begins approximately in the middle of the bed but has enough time to complete. The gas composition is shown in Fig. 7: an excess of water vapor leads to a shift in the equilibrium in the water-gas reaction towards the formation of hydrogen and carbon dioxide, CO is formed only at the gasification region, and its fraction in gas is very low (4.5 vol%). If the produced gas is dried by cooling and complete condensation of water vapors, then hydrogen content in it can reach 60%. Some of the hydrogens, however, will be converted into a water shift reaction ($CO_2 + H_2 = H_2O + CO_2$).

Fuel gasification using concentrated solar radiation, in reality, occurs with significant fluctuations of heat flow even at short times, which is associated with the natural variability of atmospheric conditions. Therefore, for a more accurate assessment of the efficiency of such processes, it is necessary to take into account the variable nature of heat supply. Another disadvantage of the model is the absence of tar in the gasification products: according to experimental data on allothermal gasification, the tar yield can be up to 45% per organic mass [81]. These problems are to be solved in further works. A comparison of the obtained results with experimental data is presented in Table 2.

It is worth noting that the experimental data are very heterogeneous: some relate to continuous reactors (mainly, fluidized bed), while others are obtained by averaging unsteady conditions. Nevertheless, the experimental data can be ranked according to their proximity to pyrolytic conditions. During biomass pyrolysis, methane content is quite high (up to 10-20 vol%). During gasification, methane content is up to 2 vol%. Thus, the presented simulation results are in good qualitative agreement with data on solar-driven steam gasification of biomass. The pyrolysis region is described with lower accuracy: the equilibrium model predicts an increase in the hydrogen yield with a decrease in the specific steam flowrate (due to high temperature and water vapor concentration), but experiments show an increase in the methane yield.

IV. Conclusion

The present study considers a mathematical model of the biomass gasification process with steam under intensive external heat supply. It focuses on the influence of fuel and steam mass flowrates on the efficiency of the gasification process. The findings suggest that to maintain the process at a suitable temperature (i.e., to prevent overheating and provide sufficient fuel conversion), it is necessary to accurately estimate mass flowrates and a fuel-stream ratio. The results show that under 10 kW of external heat supply, suitable parameters are fuel flowrate is of 4-10 kg/h and the steam flowrate is of 3-6 kg/h. The maximum thermochemical efficiency of the allothermal gasification process (given the heat consumption for heating the reactor) is about 70%; the maximum hydrogen content in the dry produced gas is about 60%. The suitable parameters for biomass gasification are in the area where the complete conversion of fuel carbon is not achieved.

Acknowledgments

This work is financially supported by an international collaborative project (BRICS2019-040) under the BRICS STI Framework Programme with government funding organizations of Brazil CNPq (402849/2019-1), Russia RFBR (19-58-80016), India DST (CRG/2018/004610, DST/TDT/ TDP-011/2017), China MOST (2018YFE0183600), and South Africa NRF (BRIC190321424123). Equipment of multi-access center "High-Temperature Circuit" (ESI SB RAS) was used in this study.

References

[1] A. S. Bisht and N. S. Thakur, "Small scale biomass gasification plants for electricity generation in India: Resources, installation, technical aspects, sustainability criteria & policy," Renewable Energy Focus, vol. 28, pp. 112-126, 2019. DOI: 10.1016/j.ref.2018.12.004

[2] H. Li, X. Min, M. Dai, and X. Dong, "The Biomass Potential and GHG (Greenhouse Gas) Emissions Mitigation of Straw-Based Biomass Power Plant: A Case Study in Anhui Province, China," Processes, vol. 7, p. 608, 2019. DOI: 10.3390/pr7090608

[3] M. Castaldi, J. van Deventer, J. M. Lavoie, J. Legrand, A. Nzihou, Y. Pontikes, X. Py, C. Vandecasteele and P. T. Vasuedevan, "Progress and Prospects in the Field of Biomass and Waste to Energy and Added-Value Materials," Waste and Biomass Valorization, vol. 8, no. 6, pp. 1875-1884, 2017. DOI: 10.1007/s12649-017-0049-0

[4] S. Jablonski, A. Pantaleo, A. Bauen, P. Pearson, C. Panoutsou and R. Slade, "The potential demand for bioenergy in residential heating applications (bio-heat) in the UK based on a market segment analysis," Biomass and Bioenergy, vol. 32, no. 7, pp. 635-653, 2008. DOI: 10.1016/j.biombioe.2007.12.013

[5] A. Kozlov, O. Marchenko, and S. Solomin, "The modern state of wood biomass gasification technologies and their economic efficiency," Energy Procedia, vol. 158, pp. 1004-1008, 2019. https://doi.org/10.1016/j.egypro.2019.01.244

[6] A. Molino, S. Chianese, and D. Musmarra, "Biomass gasification technology: The state of the art overview," Journal of Energy Chemistry, vol. 25, no. 1, pp. 10-25, 2016. DOI: 10.1016/j.jechem.2015.11.005

[7] A. A. Bhuiyan, A. S. Blicblau, A. K. M. Sadrul Islam and J. Naser, "A review on thermo-chemical characteristics of coal/biomass co-firing in industrial furnace," Journal of the Energy Institute, vol. 91, no. 1, pp. 1-18, 2018. DOI: 10.1016/j.joei.2016.10.006

[8] A. D. Kamble, V. K. Saxena, P. D. Chavan, and V. A. Mendhe, "Co-gasification of coal and biomass an emerging clean energy technology: Status and prospects of development in the Indian context," International Journal of Mining Science and Technology, vol. 29, no. 2, pp. 171-186, 2019. DOI: 10.1016/j.ijmst.2018.03.011

[9] P. R. Bhoi, R. L. Huhnke, A. Kumar, N. Indrawan and S. Thapa, "Co-gasification of Municipal Solid Waste and Biomass in a Commercial Scale Downdraft Gasifier," Energy, vol. 163, pp. 513-518, 2018. DOI: 10.1016/j.energy.2018.08.151

[10] M. Hupa, O. Karlstrom and E. Vainio, "Biomass combustion technology development – It is all about chemical details," Proceedings of the Combustion Institute, vol. 36, no. 1, pp. 113-134, 2017. DOI: 10.1016/j.proci.2016.06.152

[11] Coal and biomass gasification. Recent advances and future challenges, S. De, A.K. Agarwal, V.S. Moholkar and B. Thallada, eds. Singapore: Springer, 2018. DOI: 10.1007/978-981-10-7335-9

[12] E. Madadian, "Experimental Observation on Downdraft Gasification for Different Biomass Feedstocks" in Gasification for Low-Grade Feedstock, Rjieka: InTech, 2018, pp. 79-93. DOI: 10.5772/intechopen.77119

[13] H. Tolvanen, T. Keipi, and R. Raiko, "A study on raw, torrefied, and steam-exploded wood: Fine grinding, drop-tube reactor combustion tests in N2/O2 and CO2/O2 atmospheres, particle geometry analysis, and numerical kinetics modeling," Fuel, vol. 176, pp. 153-164, 2016. DOI: 10.1016/j.fuel.2016.02.071

[14] T. Kan, V. Strezov and T.J. Evans, "Lignocellulosic biomass pyrolysis: A review of product properties and effects of pyrolysis parameters," Renewable and Sustainable Energy Reviews, vol. 57, pp. 1126-1140, 2016. DOI: 10.1016/j.rser.2015.12.185

[15] A. Akhtar, V. Krepl and T. Ivanova, "A Combined Overview of Combustion, Pyrolysis, and Gasification of Biomass," Energy Fuels, vol. 32, no. 7, pp. 7294-7318, 2018. DOI: 10.1021/acs.energyfuels.8b01678

[16] M. Kortelainen, J. Jokiniemi, P. Tiltta, J. Tissari, H. Lamberg, J. Leskinen, J.G.-L. Rodriguez, H. Koponen, S. Antikanen, I. Nuutinen, R. Zimmermann and O. Sippula, "Time-resolved chemical composition of small-scale batch combustion emissions from various wood species," Fuel, vol. 233, pp. 224-236, 2018. DOI: 10.1016/j.fuel.2018.06.056

[17] S. Heidenreich and P.U. Foscolo,"New concepts in biomass gasification," Progress in Energy and Combustion Science, vol. 46, pp. 72-95, 2015. DOI: 10.1016/j.pecs.2014.06.002

[18] S. K. Sansaniwal, M. A. Rosen and S. K. Tyagi, "Global challenges in the sustainable development of biomass gasification: An overview," Renewable and Sustainable Energy Reviews, vol. 80, pp. 23-43, 2017.

[19] I. Hirka, O. Zivny, and M. Hrabovsky, "Numerical Modelling of Wood Gasification in Thermal Plasma Reactor," Plasma Chemistry and Plasma Processing, vol. 34, pp. 947-965, 2017. DOI: 10.1007/s11090-017-9812-z

[20] O. Yakaboylu, I. Albrecht, J. Harinck, K.G. Smit, G.-A. Tsalidis, M. Di Marcello, K. Anastasakis and W. de Jong, "Supercritical water gasification of biomass in fluidized bed: First results and experiences obtained from TU Delft/Gensos semi-pilot scale setup," Biomass and Bioenergy, vol. 111, pp. 330-342, 2018. DOI: 10.1016/j.biombioe.2016.12.007

[21] K. B. Sutar, S. Kohli, M. R. Ravi, "Design, development, and testing of small downdraft gasifiers for domestic cookstoves," Energy, vol. 124, pp. 447-460, 2017. DOI: 10.1016/j.energy.2017.02.076

[22] A. A. P. Susastriawan, H. Saptoadi, and Purnomo, "Small-scale downdraft gasifiers for biomass gasification: A review," Renewable and Sustainable Energy Reviews, vol. 76, pp. 989-1003, 2017. DOI: 10.1016/j.rser.2017.03.112

[23] E. Elsner, M. Wysocki, P. Niegodajew and R. Borecki, "Experimental and economic study of small-scale CHP installation equipped with downdraft gasifier and internal combustion engine," Applied Energy, vol. 202, pp. 213-227, 2017. DOI: 10.1016/j.apenergy.2017.05.148

[24] N. Indrawan, S. Thapa, P. R. Bhoi, R. L. Huhnke, and A. Kumar, "Engine power generation and emission performance of syngas generated from low-density biomass," Energy Conversion and Management, vol. 148, pp. 593-603, 2017. DOI: 10.1016/j.enconman.2017.05.066

[25] M. Renzi, C. Riolfi and M. Baratieri, "Influence of the syngas feed on the combustion process and performance of a micro gas turbine with steam injection," Energy Procedia, vol. 105, pp. 1665-1670, 2017. DOI: 10.1016/j.egypro.2017.03.543

[26] R. O. Gadsboll, A. V. Garcia, J. Ahrenfeldt and U. B. Henriksen, "Solid oxide fuel cell stack coupled with an oxygen-blown TwoStage gasifier using minimal gas cleaning," Renewable Energy, vol. 139, pp. 1255-1262, 2019. DOI: 10.1016/j.renene.2019.03.038

[27] I. Obernberger, T. Brunner, C. Mandl, M. Kerschbaum and T. Svetik, "Strategies and technologies towards zero-emission biomass combustion by primary measures," Energy Procedia, vol. 120, pp. 681-688, 2017. DOI: 10.1016/j.egypro.2017.07.184

[28] C. Y. Li, J. Y. Wu, C. Chavasint, S. Sampattagul, T. Kiatsiriroat, and R. Z. Wang, "Multi-criteria optimization for a biomass gasification-integrated combined cooling, heating, and power system based on life-cycle assessment," Energy Conversion and Management, vol. 178, pp. 383-399, 2018. DOI: 10.1016/j.enconman.2018.10.043

[29] F. Ardolino, C. Lodato, T. F. Astrup, U. Arena, "Energy recovery from plastic and biomass waste by means of fluidized bed gasification: A life cycle inventory model," Energy, vol. 165B, pp. 299-314, 2018.

[30] S. A. Kalogirou, "Solar thermal collectors and applications," Progress in Energy and Combustion Science, vol. 30, no. 3, pp. 231-295, 2004. DOI: 10.1016/j.pecs.2004.02.001

[31] Y. Tian and C. Y. Zhao, "A review of solar collectors and thermal energy storage in solar thermal applications," Applied Energy, vol. 104, pp. 538-553, 2013. DOI: 10.1016/j.apenergy.2012.11.051

[32] E. Gonzalez-Roubaud, D. Perez-Osorio, and C. Prieto, "Review of commercial thermal energy storage in concentrated solar power plants: Steam vs. molten salts," Renewable and Sustainable Energy Reviews, vol. 80, pp. 133-148, 2017. DOI: 10.1016/j.rser.2017.05.084

[33] A. Gonzalez, J.-R. Riba and A. Rius, "Optimal sizing of a hybrid grid-connected photovoltaic-wind-biomass power system," Sustainability, vol. 7, pp. 12787-12806, 2015. DOI: 10.3390/su70912787

[34] M. Suarez-Almeida, A. Gomez-Barea, A. F. Ghoniem, and C. Pfeifer, "Solar gasification of biomass in a dual fluidized bed," Chemical Engineering Journal, vol. 406, paper no. 126665, 2020. DOI: 10.1016/j.cej.2020.126665

[35] D. N. Karamov, "Integration of the storage battery categorization process into the task of optimizing the equipment of stand-alone energy systems with renewable energy sources," Bulletin of the Tomsk Polytechnic University. Geo Assets Engineering, vol. 330, no 5, pp. 113-130, 2019. DOI: 10.18799/24131830/2019/5/262

[36] D. Sidorov, D. Panasetsky, N. Tomin, D. Karamov, A. Zhukov, I. Muftahov, A. Dreglea, F. Liu and Y. Li, "Toward Zero-Emission Hybrid AC/DC Power Systems with Renewable Energy Sources and Storages: A Case Study from Lake Baikal Region," Energies, vol. 13, paper no. 1226, 2020. DOI: 10.3390/en13051226

[37] T. Kodama, "High-temperature solar chemistry for converting solar heat to chemical fuels," Progress in Energy and Combustion Science, vol. 29, no. 6, pp. 567-597, 2003. DOI: 10.1016/S0360-1285(03)00059-5

[38] R. Bader and W. Lipinski, "Solar thermal processing," in Advances in Concentrating Solar Thermal Research and Technology, Elsevier, 2017, pp. 403-459. DOI: 10.1016/B978-0-08-100516-3.00018-6

[39] M. Puig-Arnavat, E. A. Tora, J.C. Bruno, and A. Coronas, "State of the art on reactor designs for solar gasification of carbonaceous feedstock," Solar Energy, vol. 97, pp. 67-84, 2013. DOI: 10.1016/j.solener.2013.08.001

[40] M. Kruesi, Z. R. Jovanovic and A. Steinfeld, "A two-zone solar-driven gasifier concept: Reactor design and experimental evaluation with bagasse particles," Fuel, vol. 117, pp. 680-687, 2014. DOI: 10.1016/j.fuel.2013.09.011

[41] H. Boujjat, S. Rodat, S. Chuayboon, and S. Abanades, "Numerical simulation of reactive gas-particle flow in a solar jet spouted bed reactor for continuous biomass

gasification," International Journal of Heat and Mass Transfer, vol. 144, paper no. 118572, 2019. DOI: 10.1016/j.ijheatmasstransfer.2019.118572

[42] P. von Zedtwitz and A. Steinfeld, "The solar thermal gasification of coal - energy conversion efficiency and CO2 mitigation," Energy, vol. 28, pp. 441-456, 2003. DOI: 10.1016/S0360-5442(02)00139-1

[43] A. P. Muroyama, I. Guscetti, G. L. Schieber, S. Haussener and P. G. Loutzenhiser, "Design and demonstration of a prototype 1.5 kWth hybrid solar/autothermal steam gasifier," Fuel, vol. 211, pp. 331-340, 2018. DOI: 10.1016/j.fuel.2017.09.059

[44] O. V. Marchenko and S. V. Solomin, "Matematicheskoe modelirovanie avtonomnoi sistemy elektrosnabzheniya s gazogeneratornoi elektrostantsiei [Mathematical modelling of autonomous power supply system with gasifier power station]" Information and Mathematical Technologies in Science and Control. Proceedings of the 13th Baykal Conference, Irkutsk: MESI SB RAS, vol. 1, pp. 14-19, 2008.

[45] M. Rokni, "Biomass gasification integrated with a solid oxide fuel cell and Stirling engine," Energy, vol. 77, pp. 6-18, 2014. DOI: 10.1016/j.energy.2014.01.078

[46] D. Popov, "An option for solar thermal repowering of fossil fuel-fired power plants," Solar Energy, vol. 85, no. 2, pp. 344-349. 2011. DOI: 10.1016/j.solener.2010.11.017

[47] J. H. Lim, A. Chinnici, B. B. Dally, and G. J. Nathan, "Assessment of the potential benefits and constraints of a hybrid solar receiver and combustor operated in the MILD combustion regime," Energy, vol. 116(1), pp. 735-745, 2016. DOI: 10.1016/j.energy.2016.10.017

[48] V. Pozzobon, S. Salvador, and J.J. Bezian, "Biomass gasification under high solar heat flux: Experiments on thermally thick samples," Fuel, vol. 174, pp. 257-266, 2016. DOI: 10.1016/j.fuel.2016.02.003

[49] S. Chuayboon, S. Abanades and S. Rodat, "Comprehensive performance assessment of a continuous solar-driven biomass gasifier," Fuel Processing Technology, vol. 182, pp. 1-14. 2018. DOI: 10.1016/j.fuproc.2018.10.016

[50] A. S. Zaitsev, R. I. Egorov, and P. A. Strizhak, "Light-induced gasification of the coal-processing waste: Possible products and regimes," Fuel, vol. 212, pp. 347-352, 2018. DOI: 10.1016/j.fuel.2017.10.058

[51] S. Sobek and S. Werle, "Kinetic modeling of waste wood devolatilization during pyrolysis based on thermogravimetric data and solar pyrolysis reactor performance," Fuel, vol. 261, paper no. 116459, 2020. DOI: 10.1016/j.fuel.2019.116459

[52] P. G. Loutzenhiser and A. P. Muroyama, "A review of the state-of-the-art in solar-driven gasification processes with carbonaceous materials," Solar Energy, vol. 156, pp. 93-100, 2017. DOI: 10.1016/j.solener.2017.05.008

[53] W. Lipinski and A. Steinfeld, "Transient radiative heat transfer within a suspension of coal particles undergoing steam gasification," Heat and Mass Transfer, vol. 41, no. 11, pp. 1021-1032, 2005. DOI: 10.1007/s00231-005-0654-5

[54] N. Piatkowski and A. Steinfeld, "Solar gasification of carbonaceous waste feedstocks in a packed-bed reactor - Dynamic modeling and experimental validation," American Institute of Chemical Engineers Journal, vol. 57, no. 12, pp. 3522-3533, 2011. https://doi.org/10.1002/aic.12545

[55] V. M. Wheeler, R. Bader, P. B. Kreider, M. Hangi, S. Haussener and W. Lipinski, "Modelling of solar thermochemical reaction systems," Solar Energy, vol. 156, pp. 149-168, 2017. DOI: 10.1016/j.solener.2017.07.069

[56] J. Soria, K. Zheng, D. Asensio, D. Gauthier, G. Flamant and G. Mazza, "Comprehensive CFD modeling of solar fast pyrolysis of beech wood pellets," Fuel Processing Technology, vol. 158, pp. 226-237, 2017. DOI: 10.1016/j.fuproc.2017.01.006

[57] S. Bellan, N. Gokon, K. Matsubara, H.S. Cho, and T. Kodama, "Heat transfer analysis of 5kWth circulating fluidized bed reactor for solar gasification using concentrated Xe light radiation," Energy, vol. 160, pp. 245-256, 2018. DOI: 10.1016/j.energy.2018.06.212

[58] M. R. Gomaa, R. J. Mustafa and N. Al-Dmour, "Solar thermochemical conversion of carbonaceous materials into syngas by Co-Gasification," Journal of Cleaner Production, vol. 248, paper no. 119185, 2020. DOI: 10.1016/j.jclepro.2019.119185

[59] K. Umeki, K. Yamamoto, T. Namioka and K. Yoshikawa, "High-temperature steam-only gasification of woody biomass," Applied Energy, vol. 87, pp. 791-798, 2010. DOI: 10.1016/j.apenergy.2009.09.035

[60] P. Lamarche, M. Tazerout, F. Gelix, S. Kohler, K. Mati, and F. Paviet, "Modelling of an indirectly heated fixed bed pyrolysis reactor of wood: Transition from batch to continuous staged gasification," Fuel, vol. 106, pp. 118-128, 2013. DOI: 10.1016/j.fuel.2012.12.005

[61] M. Mayerhofer, P. Mitsakis, X. Meng, W. de Jong, H. Spliethoff and M. Gaderer, "Influence of pressure, temperature and steam on tar and gas in allothermal fluidized bed gasification," Fuel, vol. 99, pp. 204-209, 2012. DOI: 10.1016/j.fuel.2012.04.022

[62] A. N. Brattsev, V. A. Kuznetsov, V. E. Popov, and A. A. Ufimtsev, "Arc gasification of biomass: example of wood residue," High Temperature, vol. 49, no. 2, pp. 244-248, 2011. DOI: 10.1134/S0018151X11010020

[63] K. Qin, W. Lin, P. A. Jensen, and A. D. Jensen, "High-temperature entrained flow gasification of biomass," Fuel, vol. 93, pp. 589-600, 2012. DOI: 10.1016/j.fuel.2011.10.063

[64] J. Stasiek, M. Jewartowski and W. Yang, "Small Scale Gasification of Biomass and Municipal Wastes for Heat and Electricity Production using HTAG Technology," E3S Web of Conference, vol. 13, paper no. 03005, 2017. DOI: 10.1051/e3sconf/20171303005

[65] C. Freda, F. Nanna, A. Villone, D. Barisano, S. Brandani, and G. Cornacchia, "Air gasification of digestate and its co-gasification with residual biomass

in a pilot-scale rotary kiln," International Journal of Energy and Environmental Engineering, vol. 10, pp. 335-346, 2019. DOI: 10.1007/s40095-019-0310-3

[66] F. Campuzano, R. C. Brown and J. D. Martinez, "Auger reactors for pyrolysis of biomass and wastes," Renewable and Sustainable Energy Reviews, vol. 102, pp. 372-409, 2019. DOI: 10.1016/j.rser.2018.12.014

[67] J. Chojnacki, J. Najser, K. Rokosz, V. Peer, J. Kielar, and B. Berner, "Syngas composition: gasification of wood pellet with water steam through a reactor with continuous biomass feed system," Energies, vol. 13, paper no. 4376, 2020. DOI: 10.3390/en13174376

[68] W. F. Fassinou, L. Van de Steene, S. Toure, G. Volle, and P. Girard, "Pyrolysis of Pinus pinaster in a two-staged gasifier: Influence of processing parameters and thermal cracking of tar," Fuel Processing Technology, vol. 90, pp. 75-90, 2009. DOI: 10.1016/j.fuproc.2008.07.016

[69] R. O. Gadsboll, L. R. Clausen, T. P. Thomsen, J. Ahrenfeldt and U. B. Henriksen, "Flexible TwoStage biomass gasifier designs for polygeneration operation," Energy, vol. 166, pp. 939-950, 2019. DOI: 10.1016/j.energy.2018.10.144

[70] J. Ran and C. Li, "High-temperature gasification of woody biomass using regenerative gasifier," Fuel Processing Technology, vol. 99, pp. 90-96, 2012. DOI: 10.1016/j.fuproc.2012.01.002

[71] K. Umeki, T. Namioka and K. Yoshikawa, "Analysis of an updraft biomass gasifier with high-temperature steam using a numerical model," Applied Energy, vol. 90, no. 1, pp. 38-45, 2012. DOI: 10.1016/j.apenergy.2010.12.058

[72] P. Lamarche, M. Tazerout, F. Gelix, S. Kohler, K. Mati, and F. Paviet, "Modelling of an indirectly heated fixed bed pyrolysis reactor of wood: Transition from batch to continuous staged gasification," Fuel, vol. 106, pp. 118-128, 2013. DOI: 10.1016/j.fuel.2012.12.005

[73] T. M. Ismail and M. A. El-Salam, "Parametric studies on biomass gasification process on updraft gasifier high-temperature air gasification," Applied Thermal Engineering, vol. 112, pp. 1460-1473, 2017. DOI: 10.1016/j.applthermaleng.2016.10.026

[74] I. G. Donskoi, A. N. Kozlov, D. A. Svishchev and V. A. Shamanskii, "Numerical investigation of the staged gasification of wet wood," Thermal Engineering, vol. 64, no. 4, pp. 258-264, 2017. DOI: 10.1134/S0040601517040024

[75] A. Levin, A. Kozlov, D. Svishchev and M. Penzik, "Verification of the heat transfer model for screw reactor," MATEC Web of Conferences, vol. 240, paper no. 05017, 2018. DOI: 10.1051/matecconf/201824005017

[76] D. A. Frank-Kamenetskii, Diffusion and Heat Exchange in Chemical Kinetics, Princeton Univ. Press, 2015.

[77] V. I. Kovenskii, "Method of calculating the bed combustion of a solid fuel coke residue," Theoretical Foundations of Chemical Engineering, vol. 46, no. 2, pp. 180-192, 2012.

[78] I. G. Donskoy, "Process simulation of the co-gasification of wood and polymeric materials in a fixed," Solid Fuel Chemistry, vol. 52, no 2, pp. 121-127, 2018. DOI: 10.3103/S0361521918020027

[79] I. G. Donskoy, "Mathematical modeling of coal and sewage sludge co-conversion using downdraft gasifier," Bulletin of the Tomsk Polytechnic University. Geo Assets Engineering, vol. 330, no. 2, pp. 7-18, 2019. DOI: 10.18799/24131830/2019/2/89

[80] A. D. Nikitin, G. I. Nikitina, S. V. Buinachev, and A. F. Ryzhkov, "Effect of steam conversion parameters on the activated coal characteristics," AIP Conference Proceedings, vol. 2015, paper no. 020064, 2018. DOI: 10.1063/1.5055137

[81] A. V. Keiko, D. A. Svishchev and A. N. Kozlov, Gasification of low-grade fuels: state of the art and perspectives of technologies, Irkutsk: MESI SB RAS, 2007.

[82] H. Boujjat, S. Rodat and S. Abanades, "Solar-hybrid Thermochemical Gasification of Wood Particles and Solid Recovered Fuel in a Continuously-Fed Prototype Reactor," Energies, vol. 13, paper no. 5217, 2020. DOI: 10.3390/en13195217

[83] L. Arribas, N. Arconada, C. Gonzalez-Fernandez, C. Lohrl, J. Gonzalez-Aguilar, M. Kaltschmitt, and M. Romero, "Solar-driven pyrolysis and gasification of low-grade carbonaceous materials," International Journal of Hydrogen Energy, vol. 42, no. 19, pp. 13598-13606, 2017. DOI: 10.1016/j.ijhydene.2017.02.026

Igor Donskoy received the Ph.D. degree in energy systems in 2014. He is currently a senior researcher in the Laboratory of Thermodynamics at Melentiev Energy Systems Institute SB RAS (Irkutsk). His main research interests include mathematical modeling, fuel processing, and thermal engineering.

Trends in and Prospects for the Coal Industry Development in Russia's Eastern Regions

L.N. Takaishvili*, A.D. Sokolov

Melentiev Energy Systems Institute of Siberian Branch of Russian Academy of Sciences, Irkutsk, Russia

***Abstract* — The paper presents an analysis of trends in coal industry development in Russia's eastern regions and its significance for the national coal industry. The study focuses on the prospects for the coal industry development in Russia's east and the potential directions of coal use there. The coal production and supplies for export are projected for the period up to 2035.**

***Index Terms*: coal, production, supplies, export, balance reserves, eastern regions of Russia, projects, trends.**

I. Introduction

The coal industry of Russia's eastern regions plays a significant part in providing Russia's regions with resources and exporting them. The eastern regions are East Siberia and the Far East. Coal plays a leading role in the energy balance of these regions and is the primary fuel for thermal power plants. The coal industry is of high social significance as a mainstay of the coal-producing entities of the federation.

The coal share in the fuel consumption structure of the federation entities of the eastern regions ranges between 5% and 95% and averages 50%. It accounts for 50-60% in West Siberia and 0-8% in European Russia. In the retrospective, coal consumption decreased both in the country and in the eastern regions. Coal is consumed in the coal-mining regions of the country. It is supplied to other Russia's regions and for export. The coal share in exports in the eastern direction is growing steadily. For the reasons of the high social and economic significance of the coal industry in Russia's east, the study of its development appears to be of great importance.

* Corresponding author.
E-mail: luci@isem.irk.ru

http://dx.doi.org/10.38028/esr.2020.04.0003
Received November 10, 2020. Revised November 30, 2020. Accepted December 13, 2020. Available online February 01, 2021.

II. Current state

Russia is one of the world leaders in the volumes of coal reserves, production, consumption, and export [1]. The coal industry share of the eastern regions increases and at present is sufficiently high (Table 1). The analysis of the dynamics of coal supplies from the eastern regions revealed a considerable growth of coal supplies for export with the relative stability of supplies to the internal market (Table 2). In the structure of export supplies, in 2011-2018, the European regions of Russia increased the coal supplies by 28%, West and East Siberia approximately twice, and the Far East almost by four times. During this period, coal supplies in the eastern direction increased almost nine times and in the western direction only by 28% [2]. The growing coal supplies for export in the eastern direction were provided by the enterprises of the eastern regions and West Siberia.

The tendency toward coal production growth was observed primarily in the regions supplying coal for export. Starting in 2010, most of them increased coal production and export almost twice, excluding the Sakhalin region, where coal export increased more than 14 times. In 2019, the share of coal supplied for export made up from 35 to 90% of production volumes for different regions. Of great significance for the coal industry in the eastern regions is closeness to the trade markets and shorter transportation distances compared to West Siberia. China, Japan, and other APR countries are major coal importers from Russia's eastern regions.

In the internal coal market, coal consumers in the eastern regions are situated basically in the coal production areas and those close to them. Power plants are the major coal consumers in Russia's east. In the considered period, coal supplies for coking purposes in the eastern regions increased against the decrease in coal supplies for coking in the country as a whole.

III. Coal reserves

The eastern regions of Russia possess considerable balance and non-commercial reserves of steaming and coking coals, including those of deficient ranks (Table 3). The share of the eastern regions in the structure of coal reserves accounts for 45%, that of West Siberia is 46%, and of the European part of Russia - 9% [3]. The available

Table 1. Coal industry of Russia and its eastern regions (as of 2019)

Indicator	Russia	Eastern regions
Balance reserves (A+B+C1), billion t	196.2	88.0 (44.7%)
The number of enterprises:	187	65 (34.8%)
including		
- mines	57	5 (8.8%)
- open-pits	130	60 (46.2%)
Production capacity, million tons	541.1	218.1 (40.3%)
Number of dressing works	64	7 (1.9%)
Coal production, million tons	441.4	161.4 (36.5%)
-underground mining, million tons	107.3	6.8 (6.3%)
-surface mining, million tons	334.1	154.6 (46.3%)
Coal processing, million tons	206.0	49.0 (23.8%)
Coal import, million tons	21.1	3/4
Coal supply by coal producers, million tons	373.6	141.7 (37.9%)
including export, million tons	206.3* 192.3**	47.1 (24.5%)
Consumption, million tons (2018)	233.0	91.6 (39.3%)
including internal, million tons	211.9	88.2

Source: [2]

* JSC Russian Railways

** CDU TEK

Table 2. Characteristic of the coal industry of Russia's eastern regions, million t

Indicator	Year				
	2010	2015	2017	2018	2019
Production	111.2	131.2	142.8	152.8	156.2
Processing	20.4	39.7	47.4	47.4	49.0
Supplies, including:	109.3	119.8	128.8	137.9	141.7
-export	16.3	34.2	38.4	42.0	47.3
-Russia's regions, of which	93.0	89.1	90.4	95.9	94.4
- Coking demand	0.1	1.9	2.6	2.6	2.7
- Power plants	64.5	64.3	63.1	63.1	67.5
-Population and residential consumers	13.7	11.5	12.2	12.2	13.1
-Other consumers	14.7	11.4	12.6	12.6	12.6

Source: [2]

Table 3. Coal reserves of the eastern regions of Russia by category of reserves as of January 1, 2019, billion t

Type of coal	Balance reserves by category			Non-commercial reserves
	A+B+C1	C2	A+B+C1+C2	
Total, including	88.0	39.9	127.8	29.2
- brown (lignite)	61.2	25.4	86.6	12.0
- hard	26.7	14.4	41.2	17.1
of which coking	8.9	4.5	13.4	1.4
including highly valuable ranks	4.3	2.7	7.1	0.1
Anthracite	0.03	0.03	0.07	0.07
Surface mining, including	71.7	28.5	100.1	16.0
- brown (lignite)	57.8	22.5	80.3	10.4
- hard	13.9	6.0	19.8	5.6
of which coking	2.1	0.4	2.5	0.1
including highly valuable ranks	1.4	0.3	1.8	0.0
Anthracite	0.02	0.01	0.03	0.02

Source: [3]

Table 4. Projection of coal production in the eastern regions of Russia, million t /year.

Federation entity	Year		
	2019	2030	2035
	actual	projection	
Total, including	160.5	185-227	195-271
Krasnoyarsk Territory	42.7	43-50	39-50
Republic of Khakassia	27.1	35-41	37-45
Trans-Baikal Territory	23.9	27-30	27-36
Republic of Sakha (Yakutia)	18.6	24-31	29-35
Irkutsk Region	13.1	11-12	11-13
Sakhalin Region	12.9	14-15	14-19
Primorye Territory	7.9	9-10	9-11
Khabarovsk Territory	6.3	10-13	12-16
Amur Region	1.7	2-8	6-15
Republic of Tyva	3.4	4-4	4-8
Kamchatka Territory	0.0	1-3	1-8
Chukotka Autonomous Area	0.0	1-4	2-8
Other	2.9	4-6	4-7

Source: Authors' estimates

Table 5. Projection of coal export from the eastern regions of Russia, million t /year

Federation entity	Year		
	2019	2030	2035
	actual	forecast	
Total, including	47.13	64-95	74-129
Republic of Khakassia	11.27	17-22	17-25
Sakhalin Region	11.78	12-13	12-13
Trans-Baikal Territory	8.51	10-13	12-15
Republic of Sakha (Yakutia)	8.64	12-17	16-22
Khabarovsk Territory	3.28	6-9	6-11
Krasnoyarsk Territory	1.1	2-4	2-8
Republic of Tyva	0.1	1-6	2-11
Amur Region	0	0-2	2-6
Kamchatka Territory	0	1-2	1-6
Chukotka Autonomous Area	0	1-3	1-6
Other	2.45	2-4	3-6

Source: Authors' estimates

considerable coal resources and production capacities in the eastern regions allow us to consider coal as a reliable resource to meet the demand of domestic consumers and to supply it for export.

IV. Potential for coal production growth

The new and existing program documents of different levels include projects for the exploitation of new deposits, reconstruction, and expansion of the capacity of operating enterprises. At the same time, some existing enterprises use 50-90% of their production capacity. The projects address different coal utilization areas, first of all, its export, then the construction of coal-fired power plants, and the development of coal chemistry in the future. In recent years, the projects have been worked out for mining the deposits in the northern and north-eastern areas that are the most vulnerable from the environmental viewpoint but possess the reserves of coal demanded in the world market. Foreign companies are much interested in developing some of the deposits.

As for the international coal market, a coal demand projection made by international organizations is favorable for the intensive development of coal export from Russia's eastern regions to the potential coal importers [4]. The main coal competitors of Russia are Australia, Indonesia, and Mongolia in the future.

Construction of large coal-fired power plants in East Siberia and the Far East to meet the internal demand and to export electric power was considered in different Governmental [5-7], federal and regional strategies and programs. According to the documents, the plans were to construct coal-fired power plants on the run-of-mine coal and low-grade products of processing the coking and steaming coal.

Practically all brown and low-grade hard coals can be used in coal chemistry. The existing projects for the development of the coal chemical industry are at different stages of progress: from tentative estimation to specific steps of implementation. In the nearest future, coal supplies for coal chemistry will not essentially influence the coal production volumes.

According to the new projects, the production volumes for different deposits amount from 0.4 to 45 m t/year, and to 355 m t for the eastern regions as a whole. With the reconstruction and increase in the capacity of operating enterprises, coal production can reach up to 75 m t/year.

The dates of project implementation depend on various factors, the most important of which are the state (often absence) of the transport infrastructure, availability of investment, demand for products, distance from the trade markets, and competition with other energy carriers. The run-of-mine coal is produced basically for the internal market, its processing products (concentrates of steaming and coking coal) are intended for the world market, and the low-grade processing products should be used to satisfy the needs of the energy sector.

The coals of the eastern regions contain some valuable associated components [8-10]. Owing to the high sorption properties of coal, a considerable amount of different metals and rare-earth elements remained in it in the process of deposit formation. This is how the complex deposits (uranium-coal, germanium-coal, rare-earth-coal ones) appeared, which creates the preconditions for complex utilization of coal deposits.

V. Factors influencing the trends in coal industry development of the eastern regions of Russia

The analysis of trends in the coal industry development of the eastern regions of Russia revealed the following main favorable factors for coal production increase:

- availability of considerable coal reserves, including the coal highly-demanded in the world market, which is suitable for different uses: export, energy sector, by-product coke industry, coal chemistry;
- measures included in the program of coal industry development and other documents, such as the arrangement of interaction between science and industry, strengthening of the science-and-technology framework of coal companies and branch scientific centers; improvement in the transport infrastructure, including the port infrastructure, for development of coal export; development of coal-based energy sector using the advanced technologies of coal combustion; and others;
- location of coal deposits of the eastern regions promising for export development close to the world's key coal importers, namely the APR countries;
- the mid-term and long-term forecasts show the dynamics of the world coal consumption growth, mainly owing to the APR countries

The coal industry development of the eastern regions is hampered by the following factors:

- economic consequences of coronavirus pandemic in the world;
- deceleration of activity in the world coal markets;
- the fluctuation of the demand for and prices of coal in the world coal market;
- a lag between the development of the railway transport capacities and required shipping capabilities;
- environmental constraints on the development of the coal-based energy sector.

VI. Prospects for the development of coal production and supply

The coal industry development in the eastern regions of Russia and potential coal supply for export were projected for the entities of the eastern regions of Russia according to the economy and energy development scenarios, which were developed at MESI SB RAS [11,12], and the authors' estimates based on the existing trends in coal consumption and the analysis of program documents (Tables 4 and 5). The rise in the coal supply for export also depends on the increase in coal processing. The study relies on the software developed with the authors' participation [13, 14].

Table 4. Projection of coal production in the eastern regions of Russia, million t /year.

Source: Authors' estimates

Table 5. Projection of coal export from the eastern regions of Russia, million t /year

Source: Authors' estimates

VII. Conclusion

The main trends in coal industry development are related to the growing export component in coal production. Therefore, the coal industry in the regions depends on the demand for coal and the price fluctuations in the world coal market. Foreign companies are interested in the exploitation of some deposits. Coal production expansion at these deposits depends both on the extent to which these companies participate in the projects and on the stability of their interests.

The prospects for coal export development also depend on the potential expansion of the internal and external coal markets; geopolitical conditions that limit coal consumption, and opportunities to increase the geological exploration. Despite the existing demand for coal, the growth of its export can be limited by the capabilities of transport infrastructure, the tariffs of coal shipping, and the absence of demand for low-grade products of coal processing in the internal market.

The creation of industrial clusters based on coal deposits (which will combine production enterprises for processing coal and technology-related waste; energy facilities; coal chemical enterprises and enterprises providing reclamation and other measures aimed at decreasing the environmental damage) appears to be the most effective alternative for the economy and environment. The run-of-mine coal, low-grade beneficiation products, and gas from the coal seams can be used as fuel for energy facilities. The end products of coal chemical enterprises are the products with a high value-added, which are produced in coal processing, degassing of coal seams, mine water, slag, and emissions into the air after coal combustion at power plants. Associated valuable elements in coal can be extracted by effective technologies and the introduction of clean combustion technologies. Since coal deposits are unique in their quality and other characteristics and conditions of deposit exploitation, such projects should be implemented approaching each deposit individually.

References

[1] BP Statistical Review of World Energy June 2019 [Online]. Available: http://www.bp.com/statisticalreview. (Accessed: December 23, 2020)

[2] Statistical data of FSBI "CDU TEK" [Online]. Available: https://www.cdu.ru/catalog/statistic/?arrFilter_46_4252452532. (in Russian)

[3] The state balance of reserves of mineral resources of the Russian Federation as of January 1, 2019. Issue 91, Coal, I, Summary data. – M.: Ministry of Natural Resources and Environment of the Russian Federation, Federal Agency on Mineral Management, the Russian Federal Geological Foundation, 302 p. (2019). (in Russian)

[4] BP Energy Outlook. 125 p. [Online]. Available: https://www.bp.com/content/dam/bp/en/corporate/pdf/energy-economics/energy-outlook/bp-energy-outlook-2018.pdf. (2018). (Accessed: December 23, 2020). (in Russian)

[5] Scenario conditions of electric power industry development of Russia for the period until 2030. M.: Ministry of Energy, APBE, – 202 p. (2011). (in Russian)

[6] The scheme of territorial planning of the RF applicable to the energy sector until 2030. [Online]. Available: http://docs.cntd.ru/document/420369441. Accessed: December 23, 2020). (in Russian)

[7] The strategy of socio-economic development of the Far East and the Baikal region until 2025. [Online]. Available: http://docs.cntd.ru/document/902195483. (Accessed: December 23, 2020). (in Russian)

[8] Arbuzov S.I., Mashenkin V.S., Rybalko V.I., Sudyko A.F. The rare-metal potential of coals of Northern Asia (Siberia, the Russian Far East, Kazakhstan, Mongolia). Geology and mineral re-sources of Siberia. No.3, p.41-44. (2014). (in Russian)

[9] Lavrik N. A. Some prerequisites for complex mining of coal deposits in the south of the Far East // Mountain information-analytical bulletin. Individual issue: «The Far East» P. 420–430. (2005). (in Russian)

[10] Golitsyn M.V., Vyalov V.I., Bogomolov A.H., Pronina N.V., Makarova E.Yu., Mitronov D.V., Kuzevanova E.V., Makarov D.V. Prospects for the development of technological coal use in Rus-sia. Georesources. No. 2(61). P. 41-53. (2015). (in Russian)

[11] Lagerev A.V., Khanaeva V.N. Priorities in the energy sector development in the Asian regions of Russia in the long-term future // Spatial economy. No. 3. P. 154–166. DOI: 10.14530/se.2017.3.154-166 (2017). (in Russian)

[12] Smirnov K.S. Complex estimation of implementing the projects on the Russian electric power ex-port from East Siberia to China // Bulletin of Irkutsk State Technical University. 2017. V. 21. No. 10. P. 131–137. DOI: 10.21285/1814-3520-2017-10-131-13. (in Russian)

[13] Sokolov A.D., Takaishvili L.N. Information and modeling software for planning the expansion of coal systems based on the hierarchical approach / in Hierarchical modeling of energy systems (Novosibirsk. Academic Publishing House "GEO," 2020. p. 209-212.). (in Russian)

[14] Sokolov A.D., Takaishvili L.N. Implementation of the software to forecast coal industry devel-opment in Russia's regions. State-of-the-art technologies. System analysis. Modeling. No. 1(41), pp. 126-133. (2014). (in Russian)

Alexander Sokolov received D. Sc. degree in engineering from the Melentiev Energy Systems Institute of the Siberian Branch of the Russian Academy of Sciences in 2006. Currently, he is a chief researcher and the head of the Laboratory of the Energy Sector of Siberia and the Far East at the Melentiev Energy Systems Institute SB RAS. His research interests include the studies and modeling of the development prospects of the energy sector industries.

Liudmila Takaishvili received a Ph.D. in engineering from the Melentiev Energy Systems Institute of the Siberian Branch of the Russian Academy of Sciences in 1991. Currently, she is a senior researcher at the Melentiev Energy Systems Institute SB RAS. Her research areas include the studies of the coal industry development prospects and the development of software and information support for these studies.

Estimation of Power Losses Caused by Supraharmonics

A. Novitskiy[*], S. Schlegel, D. Westermann

Ilmenau University of Technology, Ilmenau, Germany

Abstract **— Nowadays, the number of power electronic devices in electrical distribution networks rapidly increases. Modern generation and consumption units use high switching frequency power converters for the network connection and therefore cause voltage and current distortion at frequencies higher than 2 kHz (so-called supraharmonics) in addition to conventional harmonics. Supraharmonics cause additional power losses in electrical equipment. The objective of this paper is to estimate the power losses caused by supraharmonics. The focus is on the method of assessing the supraharmonic power losses, which combines the analytic determination of AC cable resistances at supraharmonic frequencies and the use of supraharmonic currents measured in a real MV/LV cable network. The paper shows that the supraharmonic power losses in an MV cable can reach the values of several percent of power losses at the fundamental frequency and can exceed ten percent of power losses caused by conventional current harmonics.**

Index Terms: **Power losses, power quality, supraharmonics.**

I. Introduction

The increase in the number of power electronic devices in electrical distribution networks has been a characteristic trend in the development of electric power supply for many years. Modern generation and consumption units use high switching frequency power converters for the network connection, which leads to voltage and current distortion at frequencies higher than 2 kHz (so-called supraharmonics) in addition to conventional harmonics.

[*] Corresponding author.
E-mail: Alexander.Novitskiy@TU-Ilmenau.de

http://dx.doi.org/10.38028/esr.2020.04.0004
Received September 15, 2020. Revised October 14, 2020. Accepted November 10, 2020. Available online February 01, 2021.

The harmonic and supraharmonic distortion in electrical networks directly influence the power and energy losses in the electrical equipment. The harmonic and supraharmonic currents cause additional Joule heating of conductors and therefore increase the total power losses in these conductors.

The conductor resistance grows with a rise in the frequency and, therefore, relatively small harmonic or supraharmonic currents can cause notable power losses.

The studies presented in [1-3] show that additional power losses in LV cables and HV transmission lines caused by conventional current harmonics can be up to thirty percent of power losses at the fundamental frequency. The influence of supraharmonics on the additional power losses can be illustrated using the simplified assumption that the values of the line conductor resistances are proportional to the root of the frequency [2-5]:

$$R_{sh} = R_1 \sqrt{h}\ , \qquad (1)$$

where R_{sh}, R_1 are resistance values at the supraharmonic frequency f_{sh} and at the fundamental frequency f_1 respectively, $h = f_{sh}/f_1$ is the harmonic order.

Using the calculation formula for the Joule heating and taking into account (1), one can calculate the relative values of additional power losses caused by supraharmonics as follows:

$$P_{Lsh} / P_{L1} = (I_{sh} / I_1)^2 \sqrt{h}\ , \qquad (2)$$

where P_{Lsh}, P_{L1} are power losses caused by the supraharmonic current I_{sh} at the frequency f_{sh} and by the current I_1 at the fundamental frequency f_1, respectively.

The dependences (2) are presented in Figure 1 for some ratios of I_{sh} / I_1.

As seen from Figure 1, additional power losses caused by a supraharmonic can be, for example, ten percent of the power losses at the fundamental frequency and higher, and consequently, they cannot be neglected in the calculation of total power losses in electrical networks. The exact values of additional power losses depend on the supraharmonic frequency and the ratio of I_{sh} / I_1.

It is worth noting that (1) and (2) are valid mainly for overhead transmission lines.

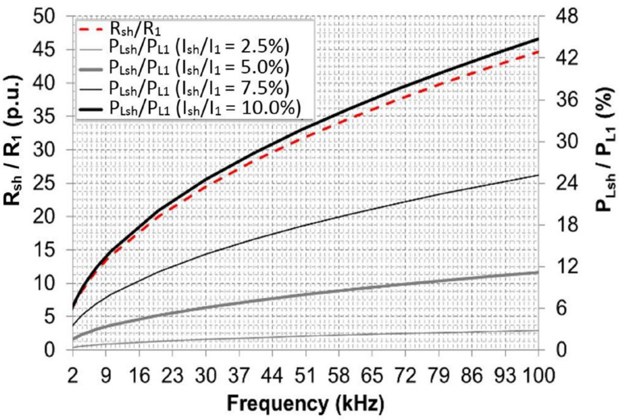

***Fig. 1. Relative supraharmonic power losses (2) and the corresponding ratio of** R_{sh}/R_1.*

The estimation of power losses caused by supraharmonics in a cable feeder under real operating conditions is presented below. The estimation is based on the measurement results obtained in a real MV/LV network in Germany [6].

II. Measurements of Supraharmonics

Results of the measurements carried out in the real MV / LV electrical network presented in Figure 2 were used to estimate the effect of supraharmonics on power losses in MV cable feeders.

The network supplies power to different settlements with mainly residential and commercial loads and contains a lot of decentralized renewable energy generating units. The network contains a MV wind plant and several MV

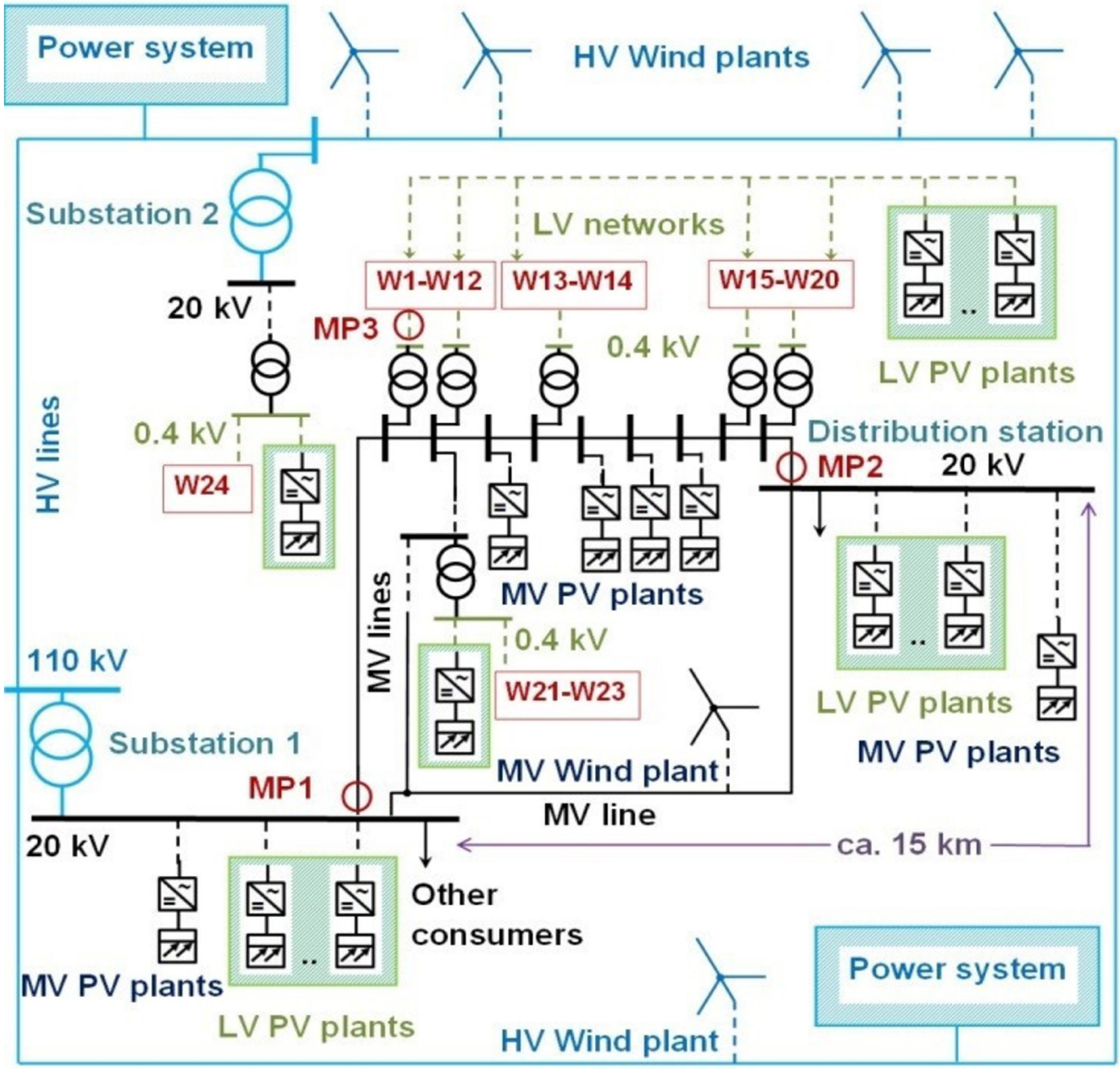

Fig. 2. MV/LV network under study and location of measuring devices.

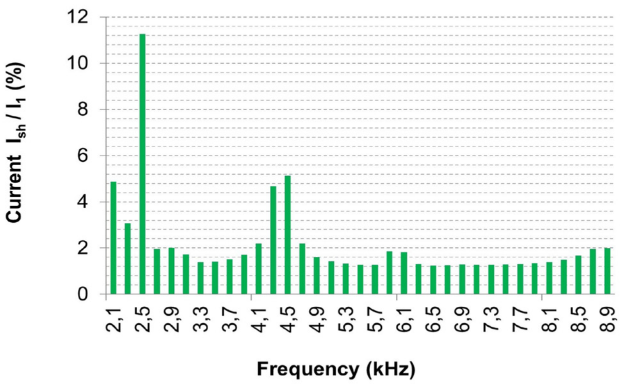

Fig. 3. Measured current spectrum, 95% quantiles of 1 min. average values, 200 Hz groups, measurement time 24 h, MP2

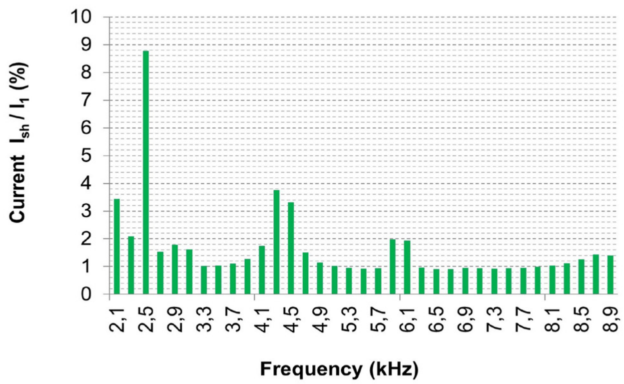

Fig. 4. Measured current spectrum, 95% quantiles of 1 min. average values, 200 Hz groups, measurement time is one week, MP2

PV plants distributed throughout the whole network and connected to the MV grid via dedicated transformers. Several powerful wind parks are located in the upstream HV network. Numerous LV PV power plants are connected to the downstream LV distribution networks together with other power electronic devices using high switching frequency power converters such as charging stations, consumer electronics, and others, via local area step-down MV / LV transformers.

Measurement devices SIRIUSi-HS [7] were located at the measurement points MP1 – MP3 and operated with a sampling rate of 100 kHz. Supraharmonic voltage and current 200 Hz groups (according to [8, 9]) were recorded as 1 min. average values over the measurement interval of 2 weeks.

Power quality (PQ) parameters were additionally measured at MP1 – MP3.

Instantaneous voltage values (a sampling rate of 10.240 kHz) and some PQ parameters as 1 sec average values were recorded at the measurement points W1-W24 (LV network) using measuring devices WeSense [10].

The effects of renewable energy sources on the supraharmonic distortion and the propagation of the supraharmonic distortion in the network under study were analyzed in [6, 11, and 12].

Power losses in the supraharmonic frequency range can be estimated using the supraharmonic currents measured in the MV feeder at the distribution station. This is the measurement point MP2 (Fig. 2).

Measuring device at MP2 was connected to the secondary winding of the current transformer via current clamps. Current clamps were certified for the measurements at a frequency up to 100 kHz.

The applicability of the standard MV current transformer to the measurements in the supraharmonic frequency range was assessed given the IEC Technical Report 61869-103 [13] and investigation results [14, 15].

Supraharmonic frequency range is divided into several subranges. The supraharmonics in the frequency subrange of 2 to 9 kHz are the subject of special consideration in the IEC standards for compatibility levels for conducted disturbances and signaling in public medium-voltage [16] and low-voltage [17] power supply systems. Technical requirements for the operation of customer installations and their connection to the MV network in Germany contain admissible values for the supraharmonic currents in a frequency range of 2 to 9 kHz [18]. Therefore, special attention should be paid to the transfer characteristics of MV current transformers in the frequency range of 2 to 9 kHz.

In [13], inductive current transformers are noted to be suitable for the use in the supraharmonic frequency range of 2 to 9 kHz. Given the measured frequency dependences

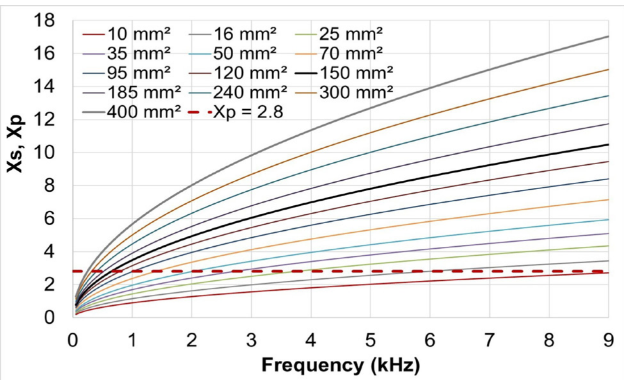

Fig. 5. Factors XS and Xp for cable solid aluminum conductors at the operating temperature of 20°C.

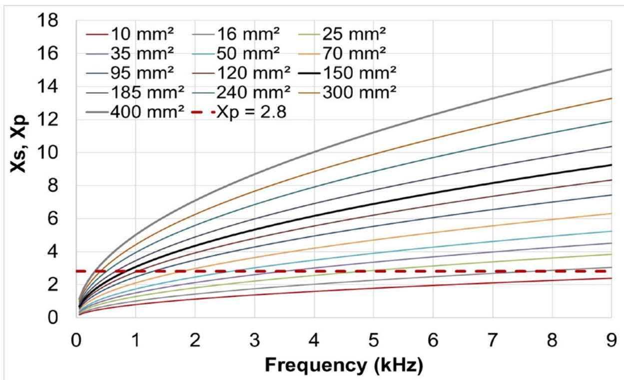

Fig. 6. Factors X_S and X_p for cable solid aluminum conductors at the operating temperature of 90°C

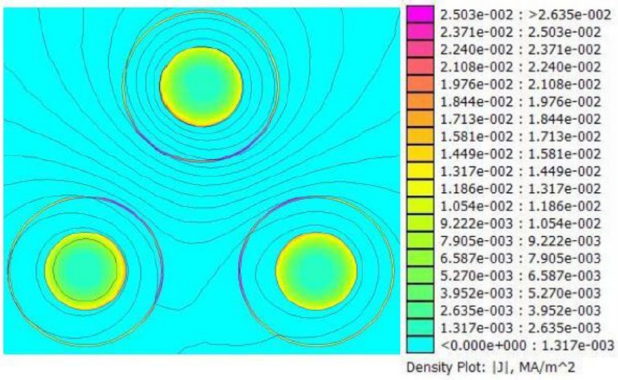

Fig. 7. Current density distribution in the aluminum conductors and copper screens of the MV cable 3x1x150/25 caused by the supraharmonic current 0.54 A (r.m.s. value) at the frequency of 2.5 kHz

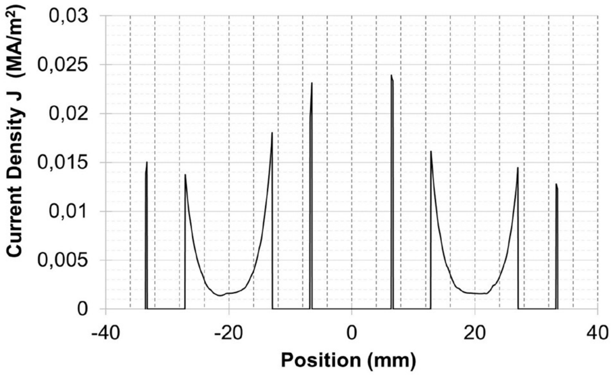

Fig. 8. Current density distribution J along the straight line crossing the centers of two neighboring conductors and screens of the MV 3x1x150/25 cable caused by the supraharmonic current 0.54 A (r.m.s. value) at the frequency 2.5 kHz

for ratio and phase errors of the MV current transformers presented in [14] and [15], one can conclude that the supraharmonic currents can be measured with the standard MV current transformers with sufficient accuracy (an error amplitude of up to several percent) for the simplified estimation of power losses in the frequency range of 2 to 9 kHz.

Examples of measured current spectra in the MV feeder (MV distribution station, measurement point MP2) are presented in Figs. 3 and 4.

As seen in Figures 3 and 4, the current spectra are characterized by the domination of the supraharmonic components of 2.5 kHz. In [6, 12], the authors show that these components in the considered network are mainly caused by the operation of the MV wind plant.

The components of 5.9 and 6.1 kHz are caused by the daily operation of solar plants, the components of 4.3 and 4.5 kHz result from the changes at the connection points of operating units.

The measurement point MP2 is the connection point of the MV 3x1x150/25 cable to the busbar of the distribution station. This MV cable connection contains three single-core cables with 150 mm^2 aluminum conductors and 25 mm^2 copper screens for each of them.

Determination of the frequency dependences for the cable resistances is considered below.

III. Determination of the frequency dependences for the cable resistances

A. Analytic calculation method

Calculation of AC resistance of a conductor is part of the IEC standard [19]. The standard states that the AC cable conductor resistance depends on the skin and the proximity effects. The following formula can be used:

$$R_{sh} = R'_{DC}\left(1+Y_S+Y_P\right), \tag{3}$$

where R_{sh} is a conductor resistance at the supraharmonic frequency f_{sh}, R'_{DC} is a DC resistance of conductor at the maximum operating temperature θ, Y_S is a skin effect factor, and Y_p is a proximity effect factor.

The values of Y_S and Y_p depend on the values of the factors X_S and X_p as follows:

$$X_S^2 = \left(1/R'_{DC}\right)8\pi f_{sh}10^{-7}k_S \tag{4}$$

and

$$X_P^2 = \left(1/R'_{DC}\right)8\pi f_{sh}10^{-7}k_P, \tag{5}$$

where k_S, k_p are coefficients, e.g. $k_S = 1$ and $k_p = 1$ for cables with solid copper or aluminum conductors [19].

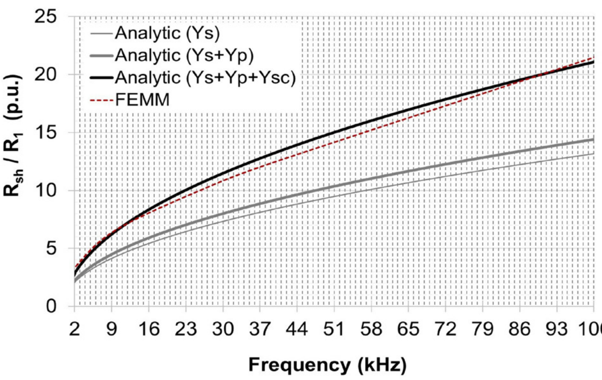

Fig. 9. Analytically and numerically (using the FEMM software) determined frequency dependences Rsh / R1 for the MV 3x1x150/25 cable in a supraharmonic frequency range

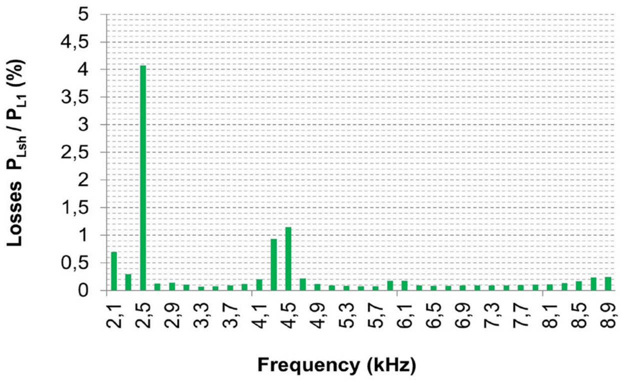

Fig. 10. Relative power losses in a 20 kV cable feeder, 95% quantiles of 1 min. values, 200 Hz groups, measurement time is 24 h, MP2

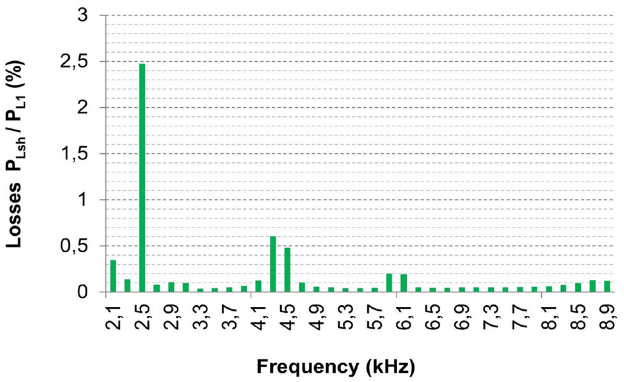

Fig. 11. Relative power losses in a 20 kV cable feeder, 95% quantiles of 1 min. values, 200 Hz groups, measurement time is one week, MP2

The skin effect factor Y_S is given by the following equations [19]:

for $0 < X_S \le 2.8$

$$Y_S = X_S^4 / \left(192 + 0.8 X_S^4\right), \tag{6}$$

for $2.8 < X_S \le 3.8$

$$Y_S = -0.136 - 0.0177 X_S + 0.056 X_S^2, \tag{7}$$

for $3.8 < X_S$

$$Y_S = 0.354 X_S - 0.733. \tag{8}$$

The proximity effect factor Y_p, according to [19], can be calculated only if factor X_p does not exceed 2.8.

As seen from (4) and (5), on the assumption that $k_S = k_p = 1$, for the cables with solid conductors $X_p = X_S$ [19].

The values of X_p and X_S calculated according to (4) and (5) for the cables with solid aluminum conductors are presented in Figures 5 and 6. The values R'_{DC} in (4) and (5) were determined for each cross-sectional area according to [20], based on the standard formula [19]:

$$R'_{DC} = R_{DC}\left(1 + \alpha_{20}\left(\theta - 20\right)\right), \tag{9}$$

where R_{DC} is a DC resistance of conductor at 20°C, R'_{DC} is a DC resistance of conductor at the maximum operating temperature θ, α_{20} is the constant mass temperature coefficient at 20°C per Kelvin.

The calculation results for the operating temperature of 20°C are presented in Figure 5, the calculation results for the maximum operating temperature of 90°C are presented in Figure 6.

It can be clearly seen from Figures 5 and 6 that the cable solid aluminum conductors with the standard cross-sectional areas starting with 16 mm^2 and larger are characterized by the values of X_p higher than 2.8 at least at some frequencies in the frequency range of 2 to 9 kHz.

Cable solid aluminum conductors with the standard cross-sections of 70 mm^2 and larger are characterized by the values of X_p higher than 2.8 in the entire frequency range of 2 to 9 kHz.

This means that the method for the analytic calculation of frequency-dependent cable resistances [19] is not applicable to the calculation of resistances at supraharmonic frequencies in many practical cases due to the constraints on the combination of parameters considered in [19].

A more common analytic method for the calculation of frequency-dependent cable resistances is presented in [21].

The analytic method for the calculation of the skin effect factor Y_S in [21] is identical with the method [19] described above.

The following formula is suggested in [21] for the calculation of the proximity effect factor Y_p for three single-core cables:

$$Y_P = m y^2 G_P / \left(2 - 5 y^2 H_P / 12\right), \tag{10}$$

where $m = 3$ for three single-core circular cables; y is a spacing ratio; G_p, H_p are coefficients.

The coefficients G_p, H_p are given by the following equations [21]:

for $0 < X_p \le 2.8$

$$G_P = 11 X_P^4 / \left(704 + 20 X_P^4\right), \tag{11}$$

for $2.8 < X_p \le 3.8$

$$G_P = -0.08 X_P^2 + 0.72 X_P - 1.04, \tag{12}$$

for $3.8 < X_p$

$$G_P = X_P / \left(4\sqrt{2}\right) - 1/8, \tag{13}$$

for $0 < X_p \le 2.8$

$$H_P = \left(1/3\right)\left(1 + 0.0283 X_P^4\right) / \left(1 + 0.0042 X_P^4\right), \tag{14}$$

for $2.8 < X_p \le 3.8$

$$H_P = 0.0384 X_P^2 + 0.119 X_P + 0.095, \tag{15}$$

for $3.8 < X_p$

$$H_P = \frac{2 X_P - 4.69}{X_P - 1.16}. \tag{16}$$

The spacing ratio $y = d_c/s$, where s is the spacing between conductor axes, d_c is the diameter of an equivalent circular conductor.

The construction of the MV 3x1x150/25 cable suggests that each cable conductor is surrounded by a cable screen.

The AC currents flowing in the cable conductors cause induced currents in the screens surrounding the cable and therefore cause some additional power losses in the screens. This means an increase in the equivalent cable resistances at the frequencies of the AC currents (fundamental frequency, harmonic and supraharmonic frequencies).

Therefore, formula (3) can be extended to consider the influence of power losses in cable screens on the conductor resistance as follows:

$$R_{sh} = R'_{DC}\left(1 + Y_S + Y_P + Y_{SC}\right), \tag{17}$$

where Y_{SC} is the screen losses factor.

It is worth noting that each cable containing axial conductor surrounded by a cable screen can be considered as a pipe-type cable. Taking into account the relation given in [22] to consider the increase in losses in the phase conductors due to the proximity of the pipe, we can use the following formula for the screen loss factor:

$$Y_{SC} = 0.5\left(Y_S + Y_P\right). \quad (18)$$

These considerations are in compliance with the recommendation [19] for the calculation of AC cable conductor resistances for pipe-type cables. The following formula can be used according to [19]:

$$R_{sh} = R'_{DC}\left(1 + 1.5\left(Y_S + Y_P\right)\right). \quad (19)$$

Using (4) – (16), (19), one can analyticly determine the values of the conductor resistances at the supraharmonic frequencies R_{sh} and the relations R_{sh} / R_1 for the MV 3x1x150/25 cable under study.

B. Numerical calculation method

The use of the finite element method (FEM) is a popular approach to the numerical calculation of frequency dependences for cable resistances.

The advantages of this method are the exact modeling of the cable geometry, the simulation of properties of the materials used in the cable construction, and the simultaneous consideration of all influencing effects named above: the skin effect, the proximity effect, the influence of cable screens and all other metallic elements (for example, cable armor, pipes, ducts, trays, and others), which can affect the AC resistances of the cable conductors.

The FEM approach makes it possible to calculate the current density distribution in all parts of the simulated cable construction. Taking into account the cable geometry and the electrical conductivities of simulated constructive materials, one can determine power losses in all elements of the cable construction.

The equivalent AC resistance of the cable conductor R_{sh} at the supraharmonic frequency f_{sh} can be calculated considering the following formula:

$$P_{Lsh} = I_{sh}^2 R_{sh}, \quad (20)$$

where P_{Lsh} is the average value of total power losses caused by the simulated supraharmonic conductor current I_{sh} at the frequency f_{sh} in each phase of the three-phase cable system.

In respect to the considered MV 3x1x150/25 cable construction:

$$P_{Lsh} = P_{Lsh\,cond} + P_{Lsh\,sc}, \quad (21)$$

where PLsh cond is an average value of power losses in each phase conductor and PLsh sc is an average value of power losses in each conductor screen. The frequency dependence for the equivalent AC cable resistance can be determined through a series of simulations at different frequencies. The frequency dependence can be determined from the following relations:

$$P_{Lsh} / P_{L1} = I_{sh}^2 R_{sh} / (I_1^2 R_1). \quad (22)$$

The values I_{sh} and I_1 can be taken, for example, from the measurement results.

Taking into account the FEM simulation of the heating processes, the cable operating temperature can be determined and the temperature effect on the electrical conductivity can be considered additionally [23-25].
To simplify the calculations, it is sufficient to assume that $I_{sh} = I_1$. In this case, it is enough to calculate the power losses (21) for each frequency under consideration. Formula (22) will be simplified as follows:

$$P_{Lsh} / P_{L1} = R_{sh} / R_1. \quad (23)$$

The frequency dependence for the equivalent AC cable resistance can be determined using (23).

It is noteworthy that the electrical conductivity of the cable insulation is very small in comparison with the conductivities of cable conductors and metallic screens. Therefore, it is sufficient to simulate only metallic parts of the cable configuration to simplify the estimation of power losses (20) and to calculate the equivalent AC resistance of the cable conductor.

Figure 7 presents a simulation example for the MV 3x1x150/25 cable. The trefoil formation with a spacing between conductor axes of 40 mm was simulated. Both aluminum conductors and copper screens were simplified and represented as solid objects.

The simulation was carried out using the FEMM software package [26].

The calculated current density distribution J in the aluminum cable conductors and in the copper cable screens is shown in Figure 7. The supraharmonic phase conductor currents of I_{sh} = 0.54 A (r.m.s. value) at the frequency f_{sh} = 2.5 kHz were simulated as the origin of the magnetic field in the cable. This value of the conductor current was measured as a 1 min value during the measurement campaign at the measurement point MP2.

The conductor currents were simulated as a three-phase set of balanced phasors with a 120° difference in phase angles between two neighboring phasors.

Figure 8 presents the line plot of the current density for the straight-line contour crossing the centers of two neighboring conductors with screens. The coordinates of centers in the "position" axis are – 20 mm and + 20 mm, respectively. The Figure also indicates skin effect, proximity effect, and influence of cable screens. Calculated frequency dependences for the MV cable under study

The analyticly calculated frequency dependences R_{sh} / R_1 for the MV 3x1x150/25 cable are presented in Figure 9. These are the frequency dependence calculated taking into account only the skin effect (parameter Y_S), the frequency dependence calculated taking into account both the skin effect and the proximity effect (parameters Y_S and Y_p), the frequency dependence calculated taking into account the skin effect, the proximity effect, and the influence of power losses in the conductor screens (parameters Y_S, Y_p, Y_{SC}).

The frequency dependence R_{sh} / R_1 determined with the FEMM software package for numerical calculations is presented for comparison in Figure 9.

The corresponding reference values R_{sh} / R_1 = 1 were calculated for each presented dependence, in terms of the fundamental frequency of 50 Hz.

Figure 9 shows that the skin effect is the dominating factor in the increase in the equivalent AC resistance of the cable conductor R_{sh} with a rise in the frequency in the supraharmonic frequency range.

As seen in Figure 9, the influence of power losses in conductor screens on the increase in the equivalent AC resistance of the cable conductor R_{sh} with a rise in the frequency is much higher in comparison with the influence of the proximity effect for the MV cable under study.

Based on the comparison of the analyticly and numerically calculated frequency dependences presented in Figure 9, we can conclude that the analytic formula (17), parameterized according to (18), or the direct formula (19) are most suitable for the analytic characterization of the increase in the equivalent AC resistance of the cable conductor R_{sh} when the frequency for the MV cable under study goes up in the supraharmonic frequency range of 2 to 100 kHz.

Given the frequency dependence (1) presented graphically in Figure 1, it can be concluded that the frequency dependences calculated by (19) or using FEMM simulations for the MV cable under study are characterized by lower values of the relations R_{sh} / R_1 than the square root of the harmonic order $h = f_{sh} / f_1$.

For the supraharmonic frequency range of 2 to 9 kHz, the following formula can be suggested for a simplified representation of the frequency dependence of R_{sh} / R_1 for the MV cable under study:

$$R_{sh} / R_1 \approx 0.48\sqrt{h}\,. \tag{24}$$

Deviations of (24) from the FEMM calculation results do not exceed several percent points in the range of 2 to 9 kHz.

IV. Use of measurement results for the supraharmonic power loss estimation

The supraharmonic power losses in the MV cable under study can be determined using (22). For clarity, (22) can be represented similar to (2) and rewritten as follows:

$$P_{Lsh} / P_{L1} = (I_{sh}^2 / I_1^2) R_{sh} / R_1\,. \tag{25}$$

Taking into consideration the calculated frequency dependences R_{sh} / R_1 for the MV cable under study and the measurement results for the time series I_{sh} / I_1 obtained during the measurement campaign, we can determine the time series for the relative values of supraharmonic power losses P_{Lsh} / P_{L1}.

Figures 10 and 11 show the supraharmonic spectra of relative power losses in the frequency range of 2 to 9 kHz in the 20 kV cable feeder under study determined according to (25) for the measurement interval of 24 hours (Figure 10) and for the measurement interval of one week (Figure 11).

The spectra in Figures 10 and 11 are presented for the supraharmonic groups of 200 Hz in accordance with the obtained measurement results for the supraharmonic currents. For the centered frequencies of each group, the frequency dependences R_{sh} / R_1 calculated according to (19) were taken into consideration.

It is worth noting that the sum of average values of 1 min. relative harmonic power losses (harmonics 2 to 40) for this day of measurement considered in Figure 10 is 24.4%, the sum of average values of 1 min relative supraharmonic power losses in the range of 2 to 9 kHz presented in Figure 10 is 2.4%. The sum of average values of 1 min relative harmonic power losses for the whole measurement week considered in Figure 11 is 12.9%, the sum of average values of 1 min relative supraharmonic power losses in the range of 2 to 9 kHz presented in Figure 11 is 1.6%.

This means that there are supraharmonic power losses in modern distribution networks and they can reach the values of several percent of power losses at the fundamental frequency. The analysis shows that the supraharmonic power losses can exceed ten percent of power losses caused by conventional current harmonics in the MV cable under study. Therefore, it can be recommended to consider supraharmonic power losses to correctly estimate the total power losses in modern distribution networks.

Conclusion

The paper has considered a method of estimating the supraharmonic power losses, which combines the analytic determination of AC cable resistances at the supraharmonic frequencies and the use of measurements of supraharmonic currents in a real MV/LV cable network.

The results of the analytic calculations of the AC cable resistances at supraharmonic frequencies have been verified and made more precise using the FEMM simulations for a MV cable chosen for the investigation. We have proposed a simplified formula for the estimation of the increase in the AC cable resistances with respect to the cable resistance at the fundamental frequency of the MV cable under study for the frequency range of 2 to 9 kHz.

The findings indicate that the estimation of the supraharmonic power losses in MV networks in the frequency range of 2 to 9 kHz can be simplified using the measurement results obtained by conventional current measuring instruments.

The study has shown that supraharmonic power losses in the considered MV cable operating in a real network can reach the values of several percent of power losses at the fundamental frequency and can exceed ten percent of the power losses caused by conventional current harmonics.

It can be recommended to consider supraharmonic power losses to correctly estimate the total power losses in networks with high presence of power electronic devices.

References

[1] L. Topolski, J. Warecki, Z. Hanzelka, "Calculating Power Losses In LV Cables Loaded With Nonsinusoidal Currents," in *Proc. CPEE,* Banska Stiavnica, Slovakia, 2018, pp. 25–28.

[2] N. Kharlov, V. Borovikov, V. Litvak, A. Pogonin, V. Melnikov, "Energy survey of non-sinusoidal operating states of multiconductor power transmission lines," *Electrichestvo (Electricity),* 2011, no.12, pp. 12-15.

[3] N. Kharlov, V. Borovikov, "Results of a survey of operating states of distribution electrical networks of Siberia and southern Russia," in *Proc. Energy-21: Sustainable Development & Smart Management,* Irkutsk, Russia, 2015, pp. 183–188.

[4] J. Zhu, E. Bećirović, J. Milanović, "The Effect of Network Modelling on Harmonic Propagation Studies in Power Electronics Rich Transmission Networks," in *Proc. APSCOM*, Hong Kong, China, 2018, pp. 1–6.

[5] G. J. Wakileh, *Power Systems Harmonics.* Berlin Heidelberg, Germany: Springer Verlag, 2001, p. 221.

[6] A. Novitskiy, S. Schlegel, D. Westermann, "Measurements and Analysis of Supraharmonic Influences in a MV/LV Network Containing Renewable Energy Sources," in *Proc. PQ & SEEM*, Kärdla, Estonia, 2019, pp. 1–6.

[7] SIRIUS® *Technical Reference Manual*, DEWESoft GmbH, Kumberg, Austria, 2015.

[8] Electromagnetic compatibility (EMC) – Part 4-7: Testing and measurement techniques – General guide on harmonics and interharmonics measurements and instrumentation, for power supply systems and equipment connected thereto, IEC 61000-4-7, 2009.

[9] Electromagnetic compatibility (EMC) – Part 4-30: Testing and measurement techniques – Power quality measurement methods, IEC 61000-4-30, 2015.

[10] C. Rüster, F. Haussel, T. Hühn, N. El Sayed, "VEREDELE-FACDS Field Trial: Wide Area Power Quality Assessment with IOT Sensors and Cloud-Based Analytics," in *Proc. ETG Congress*, Bonn, Germany, 2017, pp. 1–5.

[11] A. Novitskiy, S. Schlegel, D. Westermann, "Analysis of Supraharmonic Propagation in a MV Electrical Network," in *Proc. EPE*, Brno, Czech Republic, 2018, pp. 1–6.

[12] A. Novitskiy, P. Tikhonov, T. Jiang, S. Schlegel, T. Hühn, N. El Sayed, C. Rüster, D. Westermann. "Influence of Renewable Energy Sources on Supraharmonic Distortion in Modern MV/LV Distribution Networks," in *Proc. PQM*, Moscow, Russia, 2018, pp. 142–147.

[13] Instrument Transformers - The use of instrument transformers for power quality measurement, IEC/TR 61869-103, 2012.

[14] K. Kunde, H. Däumling, R. Huth, H.-W. Schlierf, J. Schmid, "Frequency Response of Instrument Transformers in the kHz range," *etz*, v. 6, pp. 1-4, 2012.

[15] M. Redfern, S. Terry, F. Robinson, Z. Bo. "A Laboratory Investigation into the use of MV Current Transformers for Transient Based Protection," in *Proc. IPST*, New Orleans, LA, USA, 2003, pp. 1–6.

[16] Electromagnetic compatibility (EMC) — Part 2-12: Environment — Compatibility levels for low-frequency conducted disturbances and signaling in public medium-voltage power supply systems. IEC 61000-2-12, 2003.

[17] Electromagnetic compatibility (EMC) — Part 2-2: Environment — Compatibility levels for low-frequency conducted disturbances and signaling in public low-voltage power supply systems, IEC 61000-2-2, 2018.

[18] Technical Requirements for the connection and operation of customer installations to the medium voltage network (TAR medium voltage), VDE-AR-N-4110. 2018.

[19] Electric cables – Calculation of the current rating – Part 1-1: Current rating equations (100 % load factor) and calculation of losses – General. Ed. 2.1, IEC 60287-1-1, 2014.

[20] Conductors of insulated cables. Ed. 3.0, IEC 60228, 2004.

[21] Y. Du and J. Burnett, "Experimental Investigation into Harmonic Impedance of Low-Voltage Cables," *IEE Proceedings - Generation, Transmission and Distribution*, vol. 147, issue 6, pp. 322-328, Dec. 2000.

[22] J. Palmer, R. Degeneff, T. McKernan, T. Halleran, "Pipe-Type Cable Ampacities in the Presence of Harmonics," *IEEE Transactions on Power Delivery*, vol. 8, No. 4, pp. 1689–1695, Oct. 1993.

[23] W. Frelin, L. Berthet, Y. Brument, M. Petit, G. Perujo, J. Vannier. "Thermal Behavior of LV Cables in Presence of Harmonic Currents," in *Proc, ISEF*, Arras, France, 2009, pp. 1–8.

[24] S. Dubitsky, G. Greshnyakov, N. Korovkin. "Refinement of Underground Power Cable Ampacity by Multiphysics FEA Simulation," *Int. Journal of Energy*, vol. 9, pp. 12-19, 2015.

[25] Electric Cables—Calculations for Current Ratings—Finite Element Method, IEC/TR 62095, 2003.

[26] D. Meeker, "Finite Element Method Magnetics, User's Manual," Version. 4.2, May 2020.

Alexander Novitskiy received his Ph.D. degree in electrical engineering from St. Petersburg State Polytechnic University in 1993. In 1994–1995, he worked as a Researcher at Tianjin University of Technology, China. Since 1996, he has been a Researcher at Ilmenau University of Technology, Germany. In 2006, he received his Dr.-Ing. habil. (D.Sc.) degree from that University. Since 2007, he has been a Senior Scientist in the Power Systems Group, Department of Electrical Engineering and Information Technology. His research interests include power quality, electromagnetic compatibility and interferences, simulation and analysis of steady states and transients in electric power systems..

Steffen Schlegel received his Ph.D. degree in electrical engineering from Ilmenau University of Technology, Ilmenau, Germany, in 2015. He is Chief Engineer and Head of the research team “Vertical System Operation” at Power Systems Group. A special focus of his research is on system integration of transmission and distribution grid operation, new power system operation methodologies with an active interface between distribution and transmission grid operators.

Dirk Westermann received the Diploma in electrical engineering and the Ph.D. degree from the University of Dortmund, Dortmund, Germany, in 1992 and 1997, respectively. In 1997, he joined the ABB Switzerland Ltd., where he held several positions in R&D and Technology Management. He became a Full Professor of power systems at Ilmenau University of Technology in 2005. Since 2018, he has been the Director of the Thuringian Energy Research Institute.
His research interests include design, control and operation of power systems. He is an IEEE Senior Member, an active member of CIGRE and IEC working groups.

Frequency Stability of the European Interconnected Power System Under Grid Splitting in Market Zones

Carmelo Mosca[1,*], Ettore Bompard[1], Gianfranco Chicco[1], João Moreira[2], Vincent Sermanson[2], Dante Powell[2]

[1] Dipartimento Energia "Galileo Ferraris", Politecnico di Torino, Torino, Italy
[2] Drafting Team Planning Standards, ENTSO-E, Bruxelles, Belgium

***Abstract* — This paper proposes a graph theory-based approach to define the possible separation of the market zones in large power systems. The market zone partitioning is used to assess the frequency stability based on a set of parameters, including the inertia, the running capacity of the separated areas, and the power exchanged on the interconnection lines. A system split indicator is finally used to rank the worst split lines. The methodology has been tested on real scenarios of the interconnected Continental Europe power system.**

***Index Terms*: frequency stability, grid separation, market zones, power system inertia, system split.**

I. Introduction

The energy policy framework adopted by the European Union to facilitate the transition from fossil fuels towards cleaner renewable energy sources (RES) is drastically changing the European interconnected power system [1]. Grid reinforcement, investment and new policies are needed to allocate a high level of RES, to reduce market electricity prices, and to increase the security of supply in future scenarios with a low number of conventional generating units, bringing to high capacity exchange between the national power systems. At the same time, RES are typically interconnected to the power system through power electronic devices, decoupling the generator from the grid without contributing to the overall system inertia [2]. Furthermore, the power electronic devices cannot provide inherently support to the grid, in terms of ancillary services for frequency and voltage stability, jeopardizing the system stability [3]. In this context, ensuring power system stability requires a coherent set of actions and mitigation solutions at the Transmission System Operator (TSO) level, across neighbors, or at synchronous area level, depending on different stability phenomena. Frequency stability requires a synchronous area perspective, and the frequency containment process is specified by the European Commission Guidelines [4]. These Guidelines are designed according to the reference incident of 3 GW for the Continental Europe (CE) synchronous area. Several solutions have been investigated to support frequency stability in the case of low inertia, ranging from physical components (as energy storage systems or synchronous compensators [5]) or market modifications, as well as the addition of inertia constraints in the unit commitment phase [6]. Other studies have been conducted to determine the critical power imbalances and maximum admissible rate of frequency change showing that for the CE synchronous system, the reference incident does not imply particular concerns, at least for the overall frequency stability [7]. However, the past system splits outlined the possibility of imbalance higher than the reference incident and, especially, in smaller regions. In the case of multiple line outages, cascading line failures can separate synchronously interconnected transmission grid into two or more asynchronous areas. In these cases, the frequency stability of the system is endangered, given the increasing power exchange between various regions resulting in larger power imbalances, and the decreasing system inertia leading to higher frequency gradients [8].

The bulk transmission system can be represented as a graph, with physical nodes and branches. Starting from this representation, simplifications have been proposed to reduce the complexity of large-scale systems [9]. High-level major nodes may be formed, where each node contains a subsystem whose internal connections do not limit power exchanges [10]. From another point of view, major nodes may be formed by using clustering algorithms [11] to represent bidding zones in the prospect of zonal electricity markets [12]. These high-level major nodes are then connected to design simpler graph structures.

Currently, there are a few studies on the definition of a methodology for the identification of system splits. Some

[*] Corresponding author.
E-mail: carmelo.mosca@polito.it

http://dx.doi.org/10.38028/esr.2020.04.0005
Received October 16, 2020. Revised November 11, 2020.
Accepted December 03, 2020. Available online February 01, 2021.

studies were aimed at determining the splitting boundary to damp system oscillations post-fault. A method for searching those splitting boundaries is presented in [13] to minimize the load-generation imbalance in each island. Spectral partitioning is used in [14] to determine the weak links based on topologic considerations for a static system. An approach to the systematic identification of critical system split topologies is described in [15], with the definition of relevant initial contingencies corroborated by time-domain simulations to determine the actual cascading line failure leading to a system split. The identification of a cutset for a large-scale power system is presented in [9] for the application to controlled islanding aimed at preventing the effects of cascading outages.

In this paper, the identification of system split is based on the consideration of the market exchanges between the European market zones in the context of future scenarios developed in the Ten-Year Network Development Plan (TYNDP) by ENTSO-E. A graph theory approach is used to calculate all the possible system splits into two asynchronous areas and their inertia is used to calculate the frequency performance of the system in terms of the Rate of Change of Frequency (ROCOF). The worst split lines are ranked using a system split indicator. The obtained results can be used by the TSOs to take eventual mitigating actions, in terms of grid reinforcement, regulations, or new protection schemes. This is a novel view on the existing approaches.

The outline of this paper is as follows: Section II gives a brief overview of the frequency regulation schemes adopted in Europe, the process of the system development in the framework of the TYNDP, and an overview of past system split in the world. Section III considers the implemented methodology to identify possible system splits and describes the process and the inertia calculation method. In Section IV, the methodology is applied in future scenarios of the European interconnected power system. The last section contains the conclusions.

II. European Frequency Dynamics and Planning

A. Frequency dynamics in power systems

Frequency variations occur in power systems due to mismatches between active power generation and demand. After such mismatch, the energy stored in the rotating masses of the synchronous generating units instantaneously provides balance actions through the inertial response, resulting in a change in rotor speed and the system frequency. Inertia is essential for the first instantaneous balance between generation and demand, even if it is not enough to restore the system frequency, power units capable of varying their power output according to the frequency changes are required, giving the primary frequency regulation. If a power imbalance occurs, each generator in the power system follows a different oscillatory motion around the center of inertia. Nevertheless, all individual machines can be aggregated into a single unit, whose mechanical behavior is governed by a single swing equation to represent the response of all generators:

$$\frac{df}{dt} = \frac{f_0}{2H_{sys}S_{tot}}\left(\Delta P_m - \Delta P_L + D\cdot\Delta f\right), \quad (1)$$

where ΔP_m is the mechanical power produced by the regulating resources in the grid; f_0 is the nominal frequency, H_{sys} is the aggregated inertia of the system; S_{tot} is the total rated power of the generators, and D represents the load damping coefficient due to the load frequency dependency.

In a synchronous zone, the power-demand variations are addressed by the Load Frequency Control (LFC) scheme. This scheme comprises, in a temporal sequence, the Frequency Containment Process (FCP, primary) automatically activated to stabilize the frequency deviation using the Frequency Containment Reserve (FCR, secondary); the Frequency Restoration Process (FRC) automatically and manually activated in the area where the imbalance occurs to return the frequency to its nominal value using the Frequency Restoration Reserve (FRR); and the Replacement Reserve Process (RRP, tertiary) manually activated to replace the activated FRR using the Replacement Reserve (RR). The LFC has its characteristics and qualities for each synchronous zone. ENTSO-E grid is composed of 8 synchronous zones: Continental Europe, Baltic, Nordic, British, Irish, Sardinia-Corsica, Cyprus, and Crete. Each synchronous area is presented in Fig. 1 with the belonging countries. In this paper, the focus is on the CE synchronous zone.

B. Ten Year Network Development Plan (TYNDP)

The TYNDP is published by ENTSO-E every two years to present how the grid is going to develop in the next 10 to 20 years and how the grid development can effectively contribute to achieving different and sometimes competing goals set by the European Energy Transition [16]. The main role of the TYNDP is to identify where investment in the electricity system would help deliver the Energy Union and benefit all Europeans. This has been done in two stages: (I) starting with a theoretical overview of the optimal set-up allowing for the decarbonization of the EU power system at the lowest cost (system needs analysis), and (II) a call for transmission and storage projects (under different stages of development) across Europe and complemented by an analysis of their performance under the different scenarios. Scenarios describe possible European energy futures up to 2050 but are not forecasts: they set out a range of possible futures used to test foreseen electricity and gas infrastructure needs and projects. The TYNDP starts with the development of scenarios or visions of the future European power system (e.g., in 2030 and 2040). Scenarios are a prerequisite for any study analyzing the future of the European energy system, and they are developed by ENTSO-E and its gas counterpart ENTSO-G. Each scenario's impacts on energy markets and

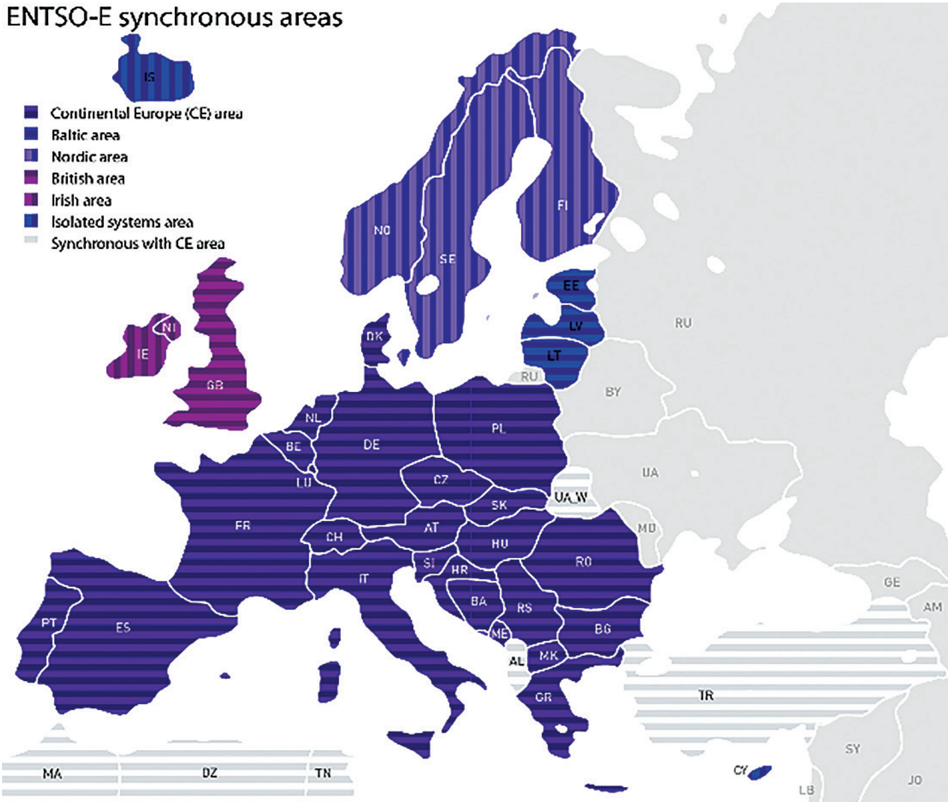

Fig. 1. ENTSO-E synchronous areas.

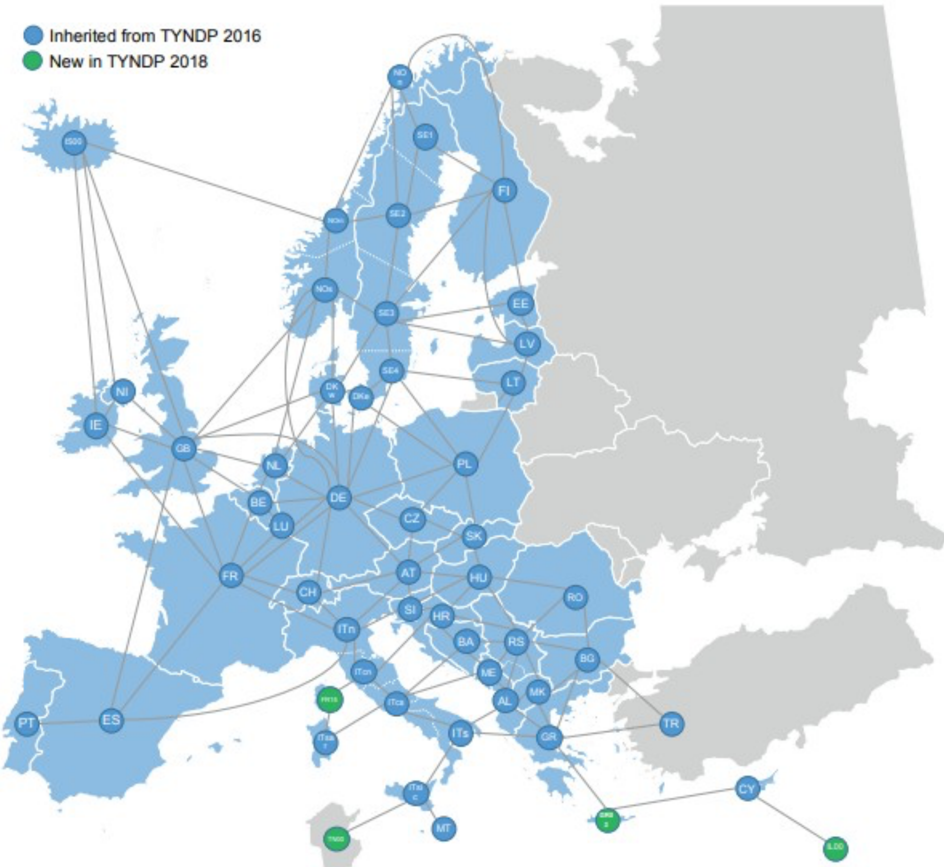

Fig. 2. Market zones from the TYNDP18.

networks are analyzed with the help of tailored modeling tools for the identification of system needs (IoSN) and to understand which parts of the network infrastructure are working well, and where it needs to be stronger [17]. For each scenario, the system needs are identified using market and network simulations. The market simulation outputs represent the input for the IoSN network simulation, to analyze possible bottlenecks and identify projects which would benefit the system in a feasible and cost-efficient manner. Market simulations are performed using different market zones and the ones used for the TYNDP 2018 are shown in Fig. 2. The European bulk power system is divided into different interconnected market zones, which are characterized by interchanged transfer capacities.

The ENTSO-E has agreed common definitions for these exchanges: Net Transfer Capacity (NTC), Available Transfer Capacity (ATC), Transmission Reliability Margin (TRM), and Already Allocated Capacity (AAC) [18]. NTC and ATC are an important basis for the market to anticipate and plan cross-border transactions and for the TSOs to manage the electricity exchanges. NTC calculations require that TSOs perform extensive studies of load flows in the interconnected European transmission system. The NTC is interpreted as the expected maximum volume of power that can be exchanged through the interface between two systems, which does not lead to violation of network constraints in either system, respecting some technical uncertainties on future network conditions. Future market simulation tools use the future NTC as a constraint to calculate the AAC for each hour of the year. In this work, the AAC is used as the possible imbalance that could follow a system split. TSOs need to systematically assess the long-term changes in various operational parameters such as inertia and short-circuit current levels, operational requirements such as flexibility, and availability of ancillary services such as reactive power support, frequency response, and contribution to short-circuit current [19].

TYNDP recently started exploring real-time system operation needs (voltage and frequency control) in response to new challenges expected to grow in the future because of the changing energy generation mix and increasingly responsive energy demand [20], [21]. Focusing on the frequency stability, small synchronous areas would see rapid and large frequency excursions following a normal generation loss, large synchronous areas would not see the same size of frequency excursions unless a significant disturbance occurs such as a system split.

C. Overview of major system split events

The separation of the European synchronously interconnected power system into two or more asynchronous areas represents one of the major concerns for the system stability. This section discusses the state-of-the-art of system split concepts and presents a brief overview of the past system splits, which occurred throughout the world.

In a system split event, the synchronous area splits into separate islands. The exports and imports between these islands before the system split event turn into power imbalances for the separate islands after the split. The larger the export or import of the island before the split, the greater the imbalance after the split and, therefore, the greater the need for large and quick adjustment for generation and demand. Not only the resulting imbalances are difficult to predict but also the resulting equivalent system inertia will differ from island to island. Based on scheduled grid expansion measures for future grid development scenarios, corresponding market simulations, and dynamic system studies, the ENTSO-E proposes a maximum admissible power imbalance of 40% per region within CE and a maximum admissible frequency gradient of 2 Hz/s. This generalized approach aims at covering any system split scenario without conducting a detailed analysis of the potential split topologies [7]. However, under some conditions, it is reasonable to consider the existence of large initial ROCOFs exceeding 2 Hz/s. A system split is more prone to occur across congested transit corridors and thus interrupting these transits. As transits are increasing in magnitude, distance, and volatility, the power imbalance following a system split event is likely to increase. This would consequently lead to larger, longer, and quicker frequency excursions in subsequently formed islands. The increased imbalance must be compensated by fast frequency response including fast control reserves or frequency-related defense measures, for example, Limited-Frequency-Sensitive-Mode Over-frequency (LFSMO) or Low-Frequency Demand Disconnection (LFDD). According to the system defense operation guidelines, a system split will result in an emergency state because of out-of-range contingency. TSOs will not act preventively to mitigate the impact of out of range contingency but will react by activating their defense plan. Defense plans are designed to help during those severe disturbances but cannot stabilize all system split scenarios with extreme imbalances. Potentially needed restoration plans will employ adequate resources to stabilize the islands and later to re-synchronize the system.

Various blackouts occurred in different parts of the world [22], among which the major system disturbances in CE that occurred on September 28th, 2003, with the Italian system separation [23], and on November 4th, 2006 [8]. After the major disturbances in 2003 and 2006, the third serious event in the CE system was a blackout in Turkey on March 31st, 2015 [24]. All these events had similar characteristics such as high corridor loading, under-frequency load shedding, and non-conforming power plant behavior with respect to abnormal frequency deviations. Two major blackouts occurred in Brazil on November 10th, 2009, and on February 4th, 2011, involving, respectively, the disconnection of a HV transmission line and a HV substation. In both cases, cascading failures following the main events led first to regions islanding and later to the system collapse [25]. On July 30th, 2012, the Indian power system suffered a severe disturbance, which led to a blackout initiated by overloading of an inter-regional tie line and followed by cascading failures and separation of the interconnected regions [26]. On July 12, 2004, the south part of the Hellenic Interconnected Transmission System (including Athens) was split from the rest of the system and collapsed, which was initiated by the opening of a north-south HV transmission line [27].

III. System Split Methodology

A. Inertia calculation from market studies

Before introducing a system split identification methodology, it is necessary to describe the procedure for the inertia calculations. Generally, the power system planning process requests data from all the TSOs for different studies. Different future scenarios are considered, which include installed capacities, demand, and cross-border capacities. For each scenario, a market simulation is performed, the market modeling outputs are given with an hourly granularity and show the hourly dispatch for each unit's type and for the countries in the interconnected areas. The requested data for frequency studies are the typical values of inertia $H_{g,i}$ provided by TSOs per fuel type g and the nominal capacity $P_{gn,i}$ of the generator i for all the N synchronous plants in the country. This information is organized into subcategories based on technology type, from which the average inertia constant H_g and the reference average capacity P_{gn} for each type of synchronous units are established per country:

$$H_g = \frac{\sum_{i=1}^{N} H_{g,i} P_{gn,i}}{\sum_{i=1}^{n} P_{gn,i}}, \tag{2}$$

$$P_{gn} = \frac{\sum_{i=1}^{N} P_{gn,i}}{N}. \tag{3}$$

The market modeling simulation gives the total generated power in [MW] for each hour h and fuel type per country $P_g(h)$. The number of units n running for each technology can be estimated by using the reference average capacity of a unit:

$$n_g\left(h\right) = \frac{P_g\left(h\right)}{P_{gn} \cdot l_g}, \tag{4}$$

where l_g is the loading factor per country and for the generator technology type g. The loading factor is the ratio between the generated energy in a year, divided by the energy the plant would have produced when generating at maximum power. Generally, high loading factors characterize nuclear and conventional power plants, while lower values characterize RES. The number of units is rounded up to have an integer value and to be precautionary. In this way, it is possible to calculate the inertia for one specific hour h in a specific zone z using the number of dispatched units multiplied by the average capacity and the inertia constant of the unit type:

$$H_z\left(h\right) = \frac{E_{k,z}}{P_{tot,z}} = \frac{\sum_{g=1}^{G} H_{g,z} P_{gn,z} n_{g,z}}{\sum_{g=1}^{G} P_{gn,z}}, \tag{5}$$

where $E_{k,z}$ is the kinetic energy and $P_{tot,z}$ the total running capacity of the zone z at hour h.

The estimated inertia is calculated based on the online generator's capacity, neglecting the contribution from the demand, and RES is considered not contributing to the inertia.

The initial ROCOF and the magnitude of the frequency deviation depend on the imbalance between generation and demand compared to the total kinetic energy and the frequency dependency of the load, based on the swing equation (1). A set of zones constitutes a subsystem of the interconnected power network. The ROCOF df / dt can be computed by subsystem s and by hour h:

$$\left.\frac{df\left(h\right)}{dt}\right|_s = \frac{f_0 \, \Delta P\left(h\right)}{2 E_{k,s}}, \tag{6}$$

where E_k is the kinetic energy of the subsystem, f_0 is the nominal frequency, and ΔP_h is an imbalance that can occur in the subsystem at hour h.

We focus only on ROCOF as it describes the immediate and instantaneous response of the system. What happens next depends on the load sensitivity to frequency, the generators' primary control time response, the primary reserve, the generating units protection design and settings, the defense plan design and settings.

To rank the split subsystems, the ROCOF values are normalized using the maximum absolute ROCOF value $\left|\left.\frac{df\left(h\right)}{dt}\right|_s\right|_{\max}$. The maximum absolute ROCOF is selected as the maximum obtained from the computation in one scenario or in all for comparison reasons. Therefore, the system split indicator SSI used to rank the split lines is defined as:

$$SSI = \frac{\left.\frac{df\left(h\right)}{dt}\right|_s}{\left|\left.\frac{df\left(h\right)}{dt}\right|_s\right|_{\max}}. \tag{7}$$

The SSI indicator is positive in case of over-frequency and negative in the case of under-frequency phenomena.

B. Methodology and process description

The system split methodology focuses on identifying and characterizing the consequences of the theoretical system splits in large interconnected power systems, with reference to the planning phase, where all the electrical characteristics are not fully known. The starting point is

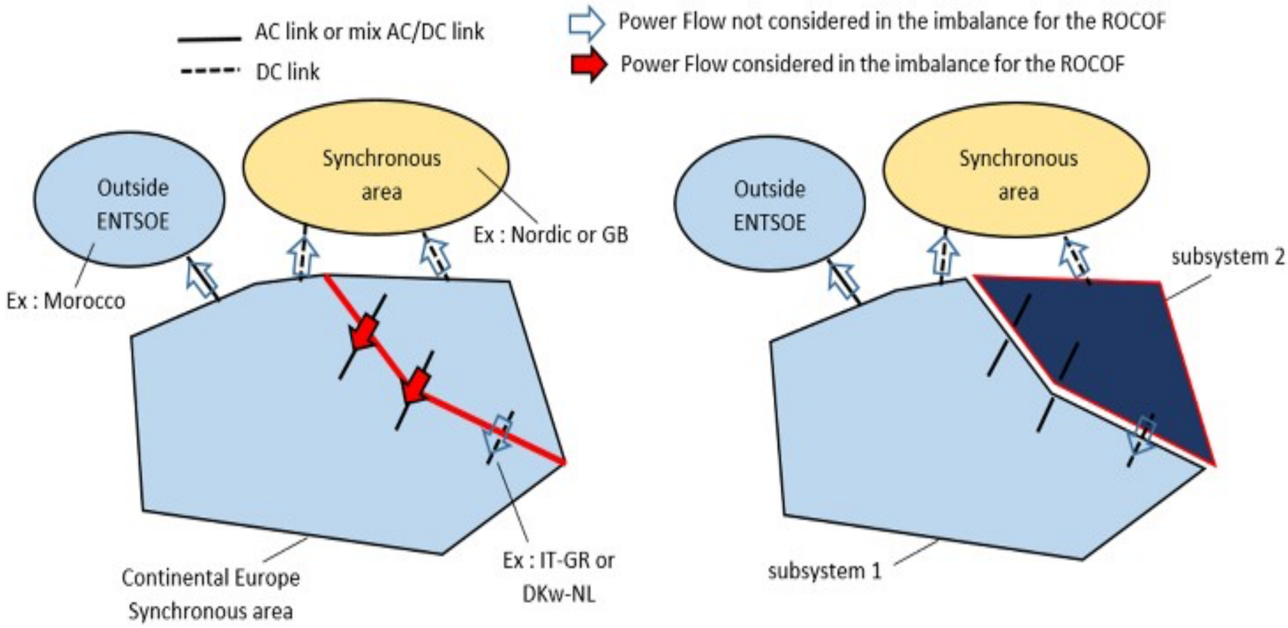

Fig. 3. Details of the considered power flows for the imbalance evaluation.

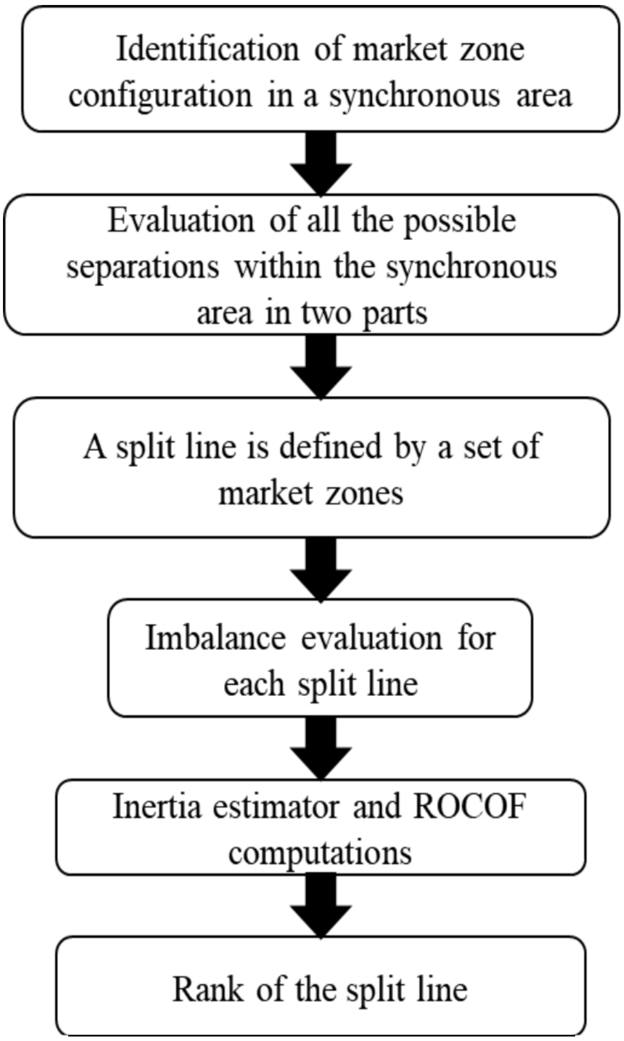

Fig. 4. Split identification methodology.

the definition of the market zones, i.e., the areas within which market participants can exchange energy without capacity allocation. If the number of market zones is very large, it can be possible to wisely aggregate them for implementation reasons. Having all the market zones, it is possible to evaluate their possible separation in two or more parts. The splitting cuts are searched recursively, from each node, extending with neighboring nodes connected through AC links or AC+DC links and ensuring the cut creates only connected sets. HVDC links within a synchronous area are ignored in the computation of splitting cuts. It is assumed that the HVDC link would remain in service after the split, which is confirmed from other past major blackouts [23]. The split line is defined by a set of market zones, and the power imbalance is evaluated through each split line. Knowing the imbalance and the sets of market zones, it is possible to evaluate the inertia and running capacity in each set and calculate the frequency performance indicators.

The imbalance of an area is the sum of the AAC flows going out of the area towards the rest of the synchronous area (except if the link is purely HVDC). When two split areas within a synchronous area are connected via a purely DC link, the flows are ignored in the imbalance: it is as if the HVDC were replaced by two loads. When there is an AC link with a node outside the synchronous area, it is ignored in the imbalance: it is as if the link were replaced by two loads (Fig. 3).

The rank of the split line is made using the *SSI*, defined in (7). The overall process is depicted in Fig. 4.

IV. Case Study

The proposed methodology has been applied to the CE synchronous area in 2030 and 2040 horizons, coming from the TYNDP 2018, which comprises 26 countries. The

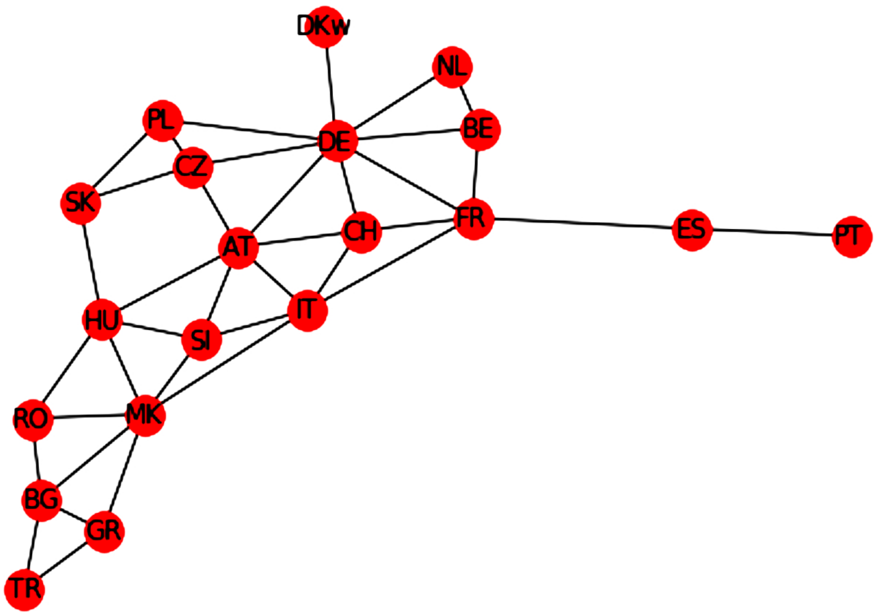

Fig. 5. Graph of the considered market zones in CE.

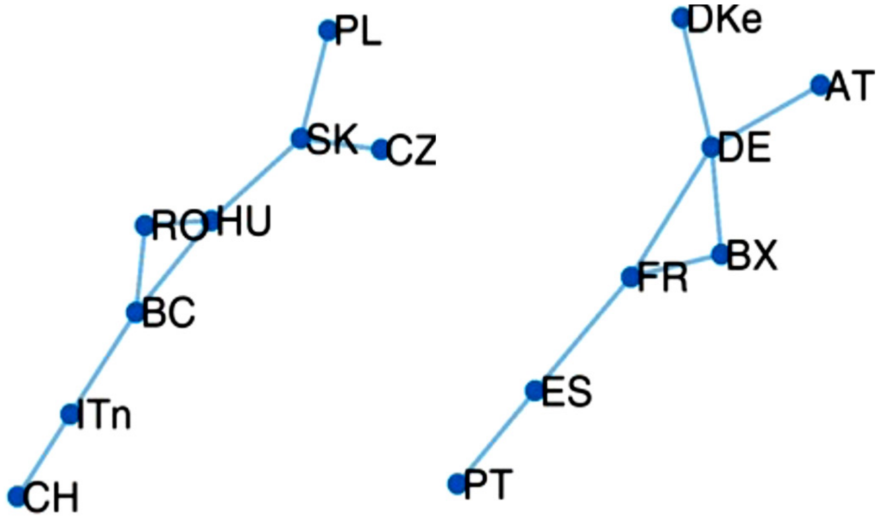

Fig. 6. Split asynchronous areas.

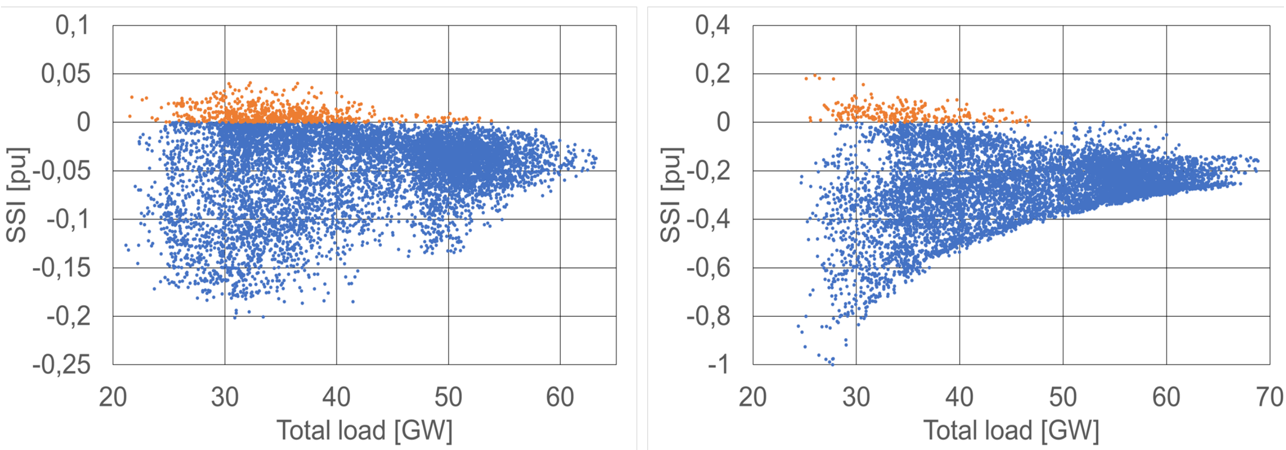

a. b.

Fig. 7. SSI values vs total load for all hours for the Italian subsystem separated from CE (a. ST 2030, b. GCA 2040).

Table 1. Merged Market Zones for Computational Reasons

Node	Synchronous Area	Market zones
BE	CE	['BE', 'LUb‘,'LUg',]
DE	CE	['DE', 'LUv', 'LUg']
FR	CE	['FR', 'LUf']
IT	CE	['IT', 'ITcn', 'ITCO', 'ITcs', 'ITN', 'ITS', 'ITsar', 'ITsic', 'MT']
MK	CE	['AL', 'BA', 'HR', 'ME', 'MK', 'RS']

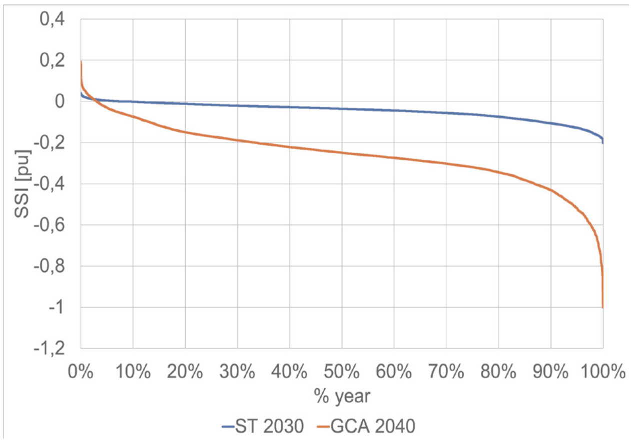

Fig. 8. SSI duration curve for all hours for the Italian subsystem separated from CE (ST 2030, GCA 2040).

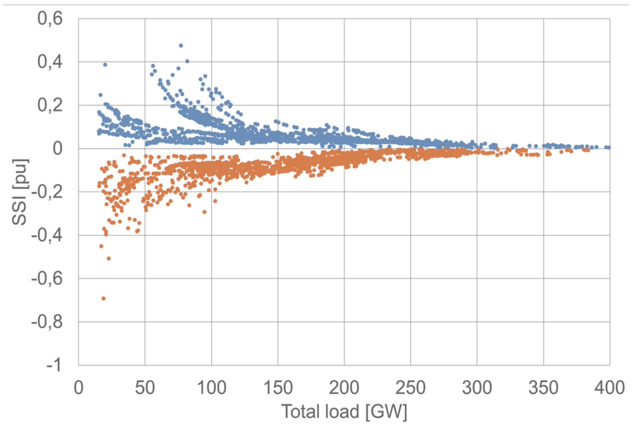

a. ST 2030

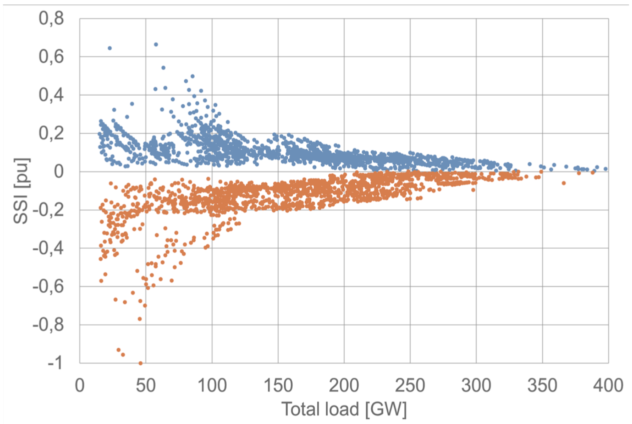

b. GCA 2040

Fig. 9. SSI values for subsystems with a total load higher than 15 GW with respect to the total load.

considered scenarios are Sustainable Transition (ST) 2030 simulated by Plexos and Global Climate Action (GCA) 2040 and simulated by PROMED, both for the climatic year 2007 [28].

The market model considers the 32 market zones reduced to 20 nodes for computational reasons. They are shown in Fig. 5 using the graph framework.

Table 1 indicates the merged market zones. Smaller market zones have been aggregated (Balkan countries), small structural antennas have been aggregated to bigger nodes (Luxembourg), and the Italian market zones are in a unique one.

All the theoretical bisections are found using the process described in Section II. Considering 20 market zones, 730 valid partitions of CE are obtained. An example of two split areas is given in Fig. 6. For each split line, the imbalance has been calculated by summing the AAC flows.

The inertia studies are performed on eleven types of units: • Nuclear • Lignite • Coal • Gas • Oil • Hydro • Wind • Solar • Other Renewable • Battery • Bio. These unit types are further divided into 44 sub-units based on technology type. Each subcategory has its parameters for inertia constant and average capacity. The inertia study is a post process of the market simulation output, which is then combined with the inertia parameters by fuel type collected and provided by the TSOs.

The values of the *SSI* have been calculated for all the possible subsystems and for each hour of the year. First, the case for only one subsystem is presented (the Italian area separated from CE), followed by the values for all subsystems, filtered by the area size.

All the computed *SSI* values for Italy separated from CE are plotted in Fig. 7 with respect to the subsystem total load. Separated situations are identified for over-frequency and under-frequency using different colors (orange for over-frequency and blue for under-frequency). To compare the two scenarios, the *SSI* values for the Italian subsystem separated from the rest of Europe are referred to the maximum absolute ROCOF in both the ST 2030 and GCA 2040. In the ST 2030 scenario, the worst under-frequency situation is at hour 1680 ($SSI = -0.20$) with an imbalance around 13 GW and a total load around 31 GW. The worst over-frequency situation is at hour 8555 with $SSI = 0.04$, due to an imbalance around 7 GW and a total load around 32 GW. In the GCA 2040 scenario, the worst under-frequency situation is at hour 2670 ($SSI = -1$), with an imbalance around 14 GW and a total load around 28 GW.

Table 2. Ranking of worst ten split lines

	ST 2030		GCA 2040	
	Under-frequency			
	Split line	***SSI* [pu]**	**Split line**	***SSI* [pu]**
1	AT_CH_SI	-0.69	AT_IT	-1
2	BE_NL	-0.51	CH_IT	-0.96
3	AT_HU	-0.45	IT_SI	-0.93
4	AT_CH_HU	-0.40	AT_IT_SI	-0.77
5	AT_CZ	-0.38	AT_CH_IT	-0.70
6	AT_CH_IT	-0.38	CH_IT_SI	-0.68
7	AT_IT	-0.38	GR_IT_MK	-0.68
8	AT_HU_SI	-0.37	BE_NL	-0.67
9	CH_IT	-0.37	IT_MK	-0.63
10	AT_CH_IT_SI	-0.34	AT_CH_IT_SI	-0.61
	Over-frequency			
1	DE_DKw	0.48	DE_DKw	0.66
2	DE_DKw_NL	0.40	BE_NL	0.64
3	BE_NL	0.39	CH_DE_DKw	0.54
4	AT_DE_DKw	0.38	DE_DKw_NL	0.50
5	CH_DE_DKw	0.37	AT_DE_DKw	0.47
6	AT_DE_DKw_SI	0.36	CZ_DE_DKw	0.44
7	CZ_DE_DKw	0.34	BE_DE_DKw_NL	0.43
8	BE_DE_DKw_NL	0.34	AT_DE_DKw_SI	0.43
9	CH_DE_DKw_NL	0.33	CH_DE_DKw_NL	0.42
10	AT_DE_DKw_NL	0.32	AT_CH_DE_DKw	0.39

The worst over-frequency situation is at hour 8571 with *SSI* = 0.19, due to an imbalance around 8 GW and a total load around 26 GW. As seen in Fig. 7, there is a slight trend towards higher values of ROCOF with low load situations.

The results are plotted in Fig. 8 as duration curves for all the hours of the year for the Italian subsystem separated from the rest of Europe, for two scenarios − ST 2030 and GCA 2040. As Italy imports for most hours of the year, the worst situation is for under-frequency phenomena, with negative *SSI* values for 8472 and 7986 hours, respectively, in the ST 2030 and GCA 2040.

The situation is increasingly worsening moving towards 2040. The maximum absolute value of ROCOF is for the scenario GCA 2040 in under-frequency. The worst under-frequency *SSI* for ST 2030 is − 0.2, around 20% of the worst *SSI* for the GCA 2040. The worst over-frequency *SSI* is 0.04 for ST 2030 and 0.19 for GCA 2040.

All the cases with a subsystem load higher than 15 GW are filtered out. 15 GW is considered here as suitable to identify large power system areas possibly affected by dangerous splits. Fig. 9 shows the values of the *SSI* for the two analyzed scenarios plotted with respect to the total subsystem load. The *SSI* is calculated using the maximum absolute ROCOF for all considered subsystems and scenarios.

In ST 2030, 2864 points are found, while in GCA 2040 - 2863 points, with 593 splits and 730 splits. The worst under-frequency case is the separation of Austria-Switzerland-Slovenia at hour 358, with an *SSI* of − 0.69, due to an imbalance around 11 GW and a total load of 18.6 GW in the scenario ST 2030, while the separation of Austria-Italy appears at hour 7, with an *SSI* of −1 Hz/s, due to an imbalance around 20 GW and a total load of 46 GW in the scenario GCA 2040. The worst over-frequency case is the separation of Germany-Denmark at hour 4258, with an *SSI* of 0.47 Hz/(GWs), due to an imbalance around 24 GW and a total load of 77 GW in the scenario ST 2030. In the scenario GCA 2040, the worst over-frequency case is the same separation of Germany-Denmark at hour 4530, with a system split indicator of 0.66, due to an imbalance around 26 GW and a total load around 58 GW. Table 2 indicates the ranking of the worst ten split lines for the cases of under- and over-frequency per scenario.

V. Conclusion

This paper has presented and assessed a methodology to identify large-scale power system splits into subsystems and evaluated their frequency stability. The system is considered to be composed of market zones, and all the possible separations in two synchronous areas are found using a graph approach. A set of parameters considering the inertia, the running capacity of the separated areas, and the imbalances among them, are used to evaluate the ROCOF and the system split indicator from the output of market simulations at different planning horizon and timeframes. The methodology has been tested on the simulations coming from the TYNDP 2018 scenarios of ENTSO-E. The results suggest interesting findings on the identification of possible dangerous split lines to monitor already in the planning phase. They also show that the ROCOF values above 2 Hz/s could be verified across the spectrum of system split cases and in subsystem areas with load size larger than 20 GW. The trend from the analyzed scenarios ST 2030 to GCA 2040 indicates that the situation might worsen due to the increasing penetration of power electronics generation not contributing to the total system inertia. It is important then to further look at sustainable mid-term and long-term mitigation measures for reduced inertia and possible splits to guarantee the frequency stability of the power system in terms of grid reinforcement, regulations, or protection schemes. The identification of possible splits depends on several factors as the aftermath of cascading outages, including the failure or misbehavior of protections and depending on the power transfers. These aspects will be a focus of future developments of this work, together with further indicators to rank the split lines (for example, considering the probabilities of separation), and the analysis of the worst situations in detailed dynamic simulations.

Acknowledgment

The authors gratefully acknowledge the contributions and work of all the members of the Drafting Team Planning Standards at ENTSO-E.

References

[1] European Commission. Clean Energy for all Europeans, 2019.

[2] J. Fang, H. Li, Y. Tang, F. Blaabjerg, "On the Inertia of Future More-Electronics Power Systems," *IEEE Journal of Emerging and Selected Topics in Power Electronics*, vol. 7, no. 4, pp. 2130-2146, Dec. 2019.

[3] F. Conte, S. Massucco, M. Paolone, G.P. Schiapparelli, F. Silvestro, Y. Zuo, "Frequency stability assessment of modern power systems: Models definition and parameters identification," *Sust. Energy, Grids and Networks*, vol. 23, 2020, art. 100384.

[4] European Commission. Commission Regulation (EU) 2017/1485 - Establishing a guideline on electricity transmission system operation, 2017.

[5] C. Mosca, F. Arrigo, A. Mazza, E. Bompard, E. Carpaneto, G. Chicco, P. Cuccia, "Mitigation of frequency stability issues in low inertia power systems using synchronous compensators and battery energy storage systems." *IET Generation, Transmission & Distribution*, vol. *13,* no. 17, pp. 3951-3959, Jul. 2019.

[6] C. Mosca, E. Bompard, G. Chicco, B. Aluisio, M. Migliori, C. Vergine, P. Cuccia, "Technical and Economic Impact of the Inertia Constraints on Power Plant Unit Commitment," *IEEE Open Access Journal of Power and Energy*, vol. 7, pp. 441-452, Oct. 2020.

[7] ENTSO-E. Frequency Stability Evaluation Criteria for the Synchronous Zone of Continental Europe, 2016.

[8] UCTE. Final Report System Disturbance on 4th November 2006, 2007.

[9] G. Xu, V. Vittal, "Slow Coherency Based Cutset Determination Algorithm for Large Power Systems," *IEEE Trans. Power Syst*., vol. 25, no. 2, pp. 877-884, May 2010.

[10] N.I. Voropai, "Generalized Technology of Hierarchical Modeling of Complex Energy Systems," *Energy Systems Research*, vol. 2, no. 4, pp. 22-25, 2019.

[11] G. Chicco, P. Colella, A. Griffone, A. Russo, Y. Zhang, E.M. Carlini, M, Caprabianca, F. Quaglia, L. Luzi, G. Nuzzo, "Overview of the Clustering Algorithms for the Formation of the Bidding Zones," *2019 54th International Universities Power Engineering Conference (UPEC)*, Bucharest, Romania, Sep. 2019.

[12] T. Brouhard, M. Hennebel, M. Petit, C. Gisbert, "Bidding Zones of the European Power System: Benefits of a Multi-Dimensional Approach to the Evaluation of Possible Delineations," *2020 17th International Conf. on the European Energy Market (EEM)*, 2020.

[13] C.G. Wang, B.H. Zhang, Z.G. Hao, J. Shu, P. Li, Z.Q. Bo, "A Novel Real-Time Searching Method for Power System Splitting Boundary," *IEEE Trans. Power Syst.*, vol. 25, no. 4, pp. 1902-1909, Nov. 2010.

[14] B. Rozel, R. Caire, N. Hadjsaid, J. Rognon, C. Tranchita, "Complex network theory and graph partitioning: Application to large interconnected networks," *2009 IEEE Bucharest PowerTech*, Bucharest, 2009, pp. 1-6.

[15] C. Cieslak, J. Massmann, C.O. Their, A. Schnettler, "Identification of System Split Topologies in Transmission Grids," in *2018 53rd Intern. Univ. Power Engin. Conf. (UPEC),* Sep. 2018, pp. 1-6.

[16] ENTSO-E. TYNDP 2018 Executive Summary, 2018.

[17] ENTSO-E. TYNDP 2018 Identification of the system needs methodology, 2019.

[18] ENTSO-E. Definitions of Transfer Capacities in liberalized Electricity Markets, 2001.

[19] ENTSO-E. Methodology: Frequency Stability Studies, 2019.

[20] ENTSO-E. European Power System 2040 Completing the map, 2019.

[21] ENTSO-E. TYNDP 2020 System dynamic and operational challenges, 2020.

[22] G. Andersson, P. Donalek, R. Farmer, N. Hatziargyriou, I. Kamwa, P. Kundur, N. Martins, J. Paserba, P. Pourbeik, J. Sanchez-Gasca, R. Schulz, A. Stankovic, C. Taylor, V. Vittal, "Causes of the 2003 major grid blackouts in North America and Europe, and recommended means to improve system dynamic performance," *IEEE Trans. Power Syst*., vol. 20, no. 4, 2005.

[23] UCTE. Final Report of the Investigation Committee on the 28 September 2003 Blackout in Italy, 2004.

[24] ENTSO-E. Report on blackout in Turkey on 31st March 2015, 2015.

[25] A. Martins et al., "Lessons learned in restoration from recent blackout incidents in Brazilian power system," in Proc. CIGRE Paris Conf., Paris, France, 2012, pp. 1–9.

[26] V. Rampurkar P. Pentayya, H. A.Mangalvedekar, and F. Kazi, "Cascading failure analysis for Indian power grid," *IEEE Trans. Smart Grid*, vol. 7, no. 4, pp. 1951–1960, Jul. 2016.

[27] C.D. Vournas, V.C., Nikolaidis, A.A. Tassoulis, "Postmortem analysis and data validation in the wake of the 2004 Athens blackout," *IEEE Trans. Power Syst*., vol. 21, no. 3, pp. 1331-1339, Aug. 2006.

[28] ENTSO-E. TYNDP 2018 Scenario Report, 2018.

Carmelo Mosca received the M.Sc. degree in electrical engineering (with honors) from Politecnico di Torino (POLITO), Turin, Italy. He is currently pursuing the Ph.D. in Electrical, Electronics, and Communication Engineering from POLITO. His research interests include power system operation and planning, power system dynamics, data analytics, and renewable energy integration.

Ettore Bompard received the Ph.D. in electrical engineering from Politecnico di Torino, Turin, Italy. He is presently Professor of Power Systems at the Department of Energy of Politecnico di Torino and scientific director of the Energy Security Transition Lab at the Energy Center, Torino. His research interests include electricity markets analysis and simulation, smart grids design and modeling, power system vulnerability assessment and security management, energy security, science-based support to policy decision making, and data analytics applications to power systems.

Gianfranco Chicco received the Ph.D. degree in Electrotechnics Engineering from Politecnico di Torino (POLITO), Turin, Italy. He is a Full Professor of Electrical Energy Systems at POLITO. His research interests include power system and distribution system analysis and optimization, multi-energy system optimization and planning, electrical load management, data analytics, and artificial intelligence applications to energy systems.

João Moreira graduated in Electrical and Computer Engineering, Energy Systems from Instituto Superior Técnico da Universidade Técnica de Lisboa, Lisbon, Portugal. He is a senior engineer in the Planning Area at REN (National Energy Networks). His background experience includes power system dynamics analysis, planning and grid development, the grid user technical requirements, and TSO cooperation work under ENTSO-E scope.

Vincent Sermanson graduated from the French Ecole Supérieure d'Electricité (Power Systems Department) in 1996. He worked for two years at the University of Liège, Belgium, and for one year at EPRI, Palo Alto, USA. After being in charge of dynamic simulation tools and studies in EDF then RTE, he is now a senior planning study engineer and system dynamics expert at RTE.

Dante Powell received the M.Sc. degree in energy systems and thermal processes from Cranfield University, Cranfield, UK. He is currently a long-term planning senior specialist at ENTSO-E and principal market modeler for the ENTSOs' scenarios. His research interests include power system planning and analysis, scenario building, energy transformation, and infrastructure development.

Future Directions for Power System Interconnection from Korea's Perspective

Jae Young Yoon*, Sunghwan Song

Korean Electrotechnology Research Institute, Uiwang, Kyunggido, Republic of Korea

***Abstract* — The power system interconnection between Northeast Asian countries has been discussed since 2000 but has not been realized to date due to various obstacles. This paper specifies the expected future energy policy, long-term energy supply plan, and necessity of power interconnection from the Korean viewpoint, including the climate change agreement. There are very many interconnection scenarios presented by various institutes in NEA countries now. These studies contain the overall preliminary feasibility results but do not consider the environmental effects, energy security, and market reforms. Do these existing studies show how we could interconnect specific countries? This paper discusses the trading potentials for green energy utilization between countries and some obstacles to be removed to promote the energy interconnection projects from technical, economic, marketable, and energy security standpoints. Especially, energy security in terms of politics, as well as vulnerability characteristics of renewable energy, could cause the interconnected system blackouts. These could be a serious obstacle to realization and continuous stable operation of these interconnection projects. Finally, this paper will specify the future directions and possible scenarios for power system interconnection by integrating these issues comprehensively from Korea's perspective.**

***Index Terms*: power system, interconnection, Northeast Asia, energy policy, international energy cooperation.**

* Corresponding author.
E-mail: ysa1624@keri.re.kr

http://dx.doi.org/10.38028/esr.2020.04.0006
Received September 18, 2020. Revised September 29, 2020.
Accepted October 11, 2020. Available online February 01, 2021.

I. Introduction

This paper deals with the future directions and potentials of power system interconnection between NEA countries from Korea's perspective. These will include the prospects for the Korean power industry, CO_2 emission reduction target, and existing power interconnection scenarios for the promotion of power system interconnection. Many institutes have published the power system interconnection scenarios since 2000, and these scenarios contain the overall preliminary feasibility results. These existing studies show which methodology could be used to interconnect this complex total system for a specific country. This paper discusses the trading potentials for green energy utilization and some obstacles to be overcome to promote energy interconnection projects in Korea. Especially, energy security in terms of politics, as well as vulnerability characteristics of renewable energy itself, could cause the interconnected power system blackouts. These could be a serious barrier to the promotion, realization, and continuous stable operation of these interconnection projects. This paper will specify the future directions and possible scenarios for power system interconnection by integrating these issues from Korea's perspective.

II. Future plan on power supply

This section deals with a plan on the power industry and the potentials of power system interconnection on the Korean side. It focuses on the overview of the power industry, energy supply plan, and energy policy, including the CO_2 reduction scheme in Korea.

A. Power Supply Plan in Korea

According to the 8th power supply and demand plan [1], the total power target demand is expected to reach 589.5 TW·h in 2030, and the annual increase rate will be about 1.0%. The target peak load will be expected to reach 100.5 GW in 2030, and the annual increase rate will be 1.3%. This means that the annual growth rate of power consumption will be expected to be saturated in the near

Table 1. Target power demand (unit: tw·h/gw)

Year	Consumer Demand (TW·h)	Peak Load (GW)	
		Summer	Winter
2020	540.1	88.8	90.3
2021	548.9	90.4	92.1
2022	556.1	91.5	93.3
2023	561.7	92.6	94.5
2024	566.2	93.5	95.7
2025	569.8	94.4	96.7
2026	572.8	95.1	97.6
2027	575.2	95.8	98.4
2028	577.0	96.4	99.1
2029	578.5	97.0	99.8
2030	589.5	97.5	100.5
2031	580.4	98.0	101.1
Annual Increase Rate	1.0%	0.9%	1.3%

[Target Demand (kW·h)] = [Base Demand (BAU)] –
[Demand Management] + [Others (EV)])

Table 2. Confirmed installed capacity in Korea (as of 2030)

Subjects	Nuclear	Coal	Renewable	LNG	Others	Sum
Effective cap. (GW)	20.4	38.9	8.8	44.3	6.0	118.3
Rated cap. (GW)	20.4	39.9	58.5	44.3	6.1	169.2

Table 3. RES capacity by type in Korea (as of 2030)

Subjects	PV	Wind	Hydro	Others	Sum
Rated Capacity (GW)	33.53	17.674	2.105	5.152	58.461
Peak contribution (%)	15.6%	1.9%	28.1%	-	15.4%
Effective Capacity (GW)	5.231	0.336	0.591	2.614	8.772

future. This target demand means the base demand under BAU (Business As Usual) scenario minus the quantity for demand response management plus other affecting factors such as electric cars, and others. The 9th basic power demand and supply national plan will be published soon later within this year, and this forecast may be somewhat different from the above-mentioned values.

Regarding the peak demand periods, currently, we have the double peak demand annually, both summer daytime (early August) and winter midnight (early January) peaks. But, we expect this trend to change to single peak demand (summer daytime peak). This will be described in detail in the next 9th basic electric demand-supply plan.

It is expected that the total rated installed capacity will reach 169.2 GW, and the renewable energy capacity will be 58.5 GW in 2030. However, Korea has no sufficient primary energy resources and imports almost 95% of its primary energy resources. Currently, the Korean power market is undergoing restructuring and experiencing internal turmoil stemming from difficulty acquiring power plant sites and dealing with environmental issues. We have complex issues that involve international cooperation (power system interconnection), power industry restructuring (market reform), CO_2 reduction plan, and public acceptance issues related to the construction and operation of power system facilities. To overcome these difficulties, the Korean government is planning an energy policy to expand the renewable energy supply and develop cooperation with neighboring countries. These are the key factors to promote the power system interconnection.

Therefore, the Korean government has the renewable energy extension plan, the so-called 3020 and 4030 policy. The 3020 policy means a renewable generation share will be increased by 20% of total generation until 2030. Also, this 3020 policy was changed by the 4030 policy, which increases the RES supply target to 35-40% within 2040. According to these policies, the Korean government has a plan to abolish nuclear and coal-fired generations for the protection of air quality and reduction of CO_2 emission. The renewable energy supply will significantly expand to 35-40% of the total generation (kW·h) by 2040. But, the nuclear and coal energy portion will decrease rapidly. This plan contains the baseline demand and the target demand. The baseline demand means the electricity demand under a scenario, in which the current technology development, consumption trend, and energy policy will be continuously maintained.

The installed effective generation capacity will reach 118.3 GW in 2030. We can see that the renewable energy sources will increase very rapidly from 11.3 GW in 2017 to 58.5 GW in 2030. These 58.5 GW of renewable energy resources include 33.5 GW of solar sources and 17.7 GW

Table 4. Renewable energy share by year in Korea

	2022	2026	2030	2031
Generation Amounts (TW·h)	58.3 (9.6%)	89.5 (14.4%)	125.8 (20.0%)	126.0 (19.9%)
Capacity (GW)	23.3 (16.4%)	38.8 (25.4%)	58.5 (33.7%)	58.6 (33.6%)

Table 5. CO2 emission target before NDC submission

Subject	CO_2 Target	Remarks
Total	574.3 Mtons (608.4-34.1)	Including 34.1 Mtons for additional reduction potential of transition sector
Total (2030)	536.0 Mtons (574.3-38.3)	38.3 Mtons reduction by importing or forest resources absorption
Transition sector target	192.7 Mtons (333.2-140.5)	Prospective amounts equal to 333.2 Mtons, Reduction quantity of 140.5 Mtons (42.2%)

of wind sources. These two types of sources account for 88% of total renewable capacity. The gas generation plants also increase from 37.4 GW in 2017 to 44.3 GW in 2030. However, the nuclear power plants will decrease from 22.5 GW in 2017 to 20.4 GW in 2030. Even though the renewable capacity will increase to 58.5 GW based on total rated capacity, the effective rating is only 8.8 GW considering the practical capacity factor of RES [2].

As already mentioned, the renewable generation share by year is described and will reach 20% of the total power generation in 2030.

B. CO_2 Reduction Plan in Korea

According to the 8th base power demand and supply plan, the power generation sector accounts for one-third of CO_2 emission, around 34% or more, and is the key factor for the national CO_2 reduction plan under the Paris agreement. The average emission quantity per unit generation (kW·h) is around 0.459 tCO_2/MW·h now, but, in the future, this value will go down gradually because of the increase in renewable energy resources. The total CO_2 emission target is 536 Mtons, including the additional reduction potential of the transition sector and reduction in imports in 2030. This is a 37% reduction target for the existing BAU scenario and a 22.3% lower value than in 2015. The transition sector target accounts for 192.7 Mtons in total national emission quantity, and, as a result, the reduction amount for the transition sector is 140.5 million tons (42.2% of the transition sector original emission quantity equal to 333.2 million tons). In addition to this transition sector target, we will have the additional reduction potential of 34.1 Mtons through the renewable energy transition (6.4% of total CO_2 emission target of 536 Mtons). The final emission target will be confirmed before the submission of NDC in 2020. Therefore, this target could change. The CO_2 market is now operating, and the trading charge of CO_2 is changed from time to time. But, according to the IEA base projection for CO_2 emission, CO_2 cost is estimated at \$10-30/tCO_2e. This CO_2 cost could be a promotion factor for the power system interconnection in NEA

III. Expected Scenarios on Power System Interconnection

A. Importing Capability of Korea

As mentioned above, the peak demand of Korea in 2030 will be expected to reach 100.5 GW. Given energy security from a general standpoint, the maximum interconnection

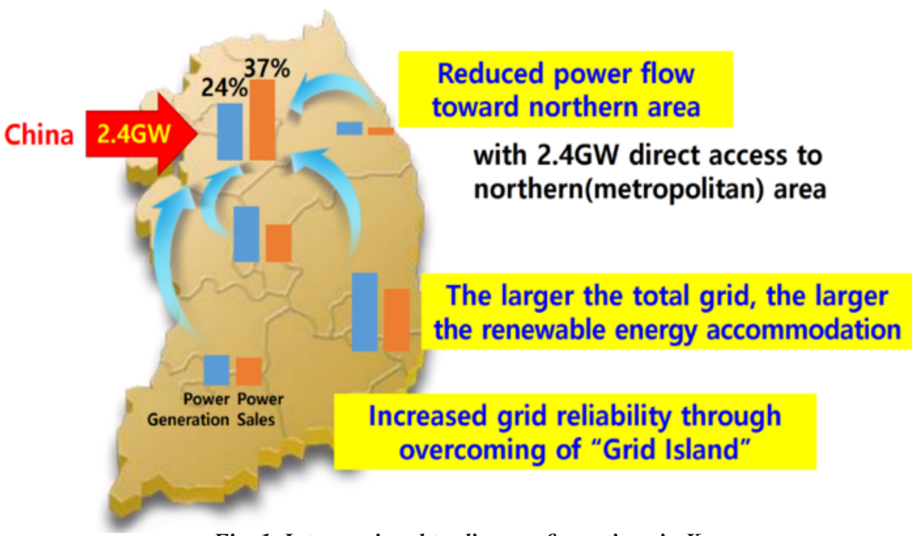

Fig. 1. Intra-regional trading configurations in Korea.

Fig. 2. Concept Diagram on multilateral PSI in NEA [4].

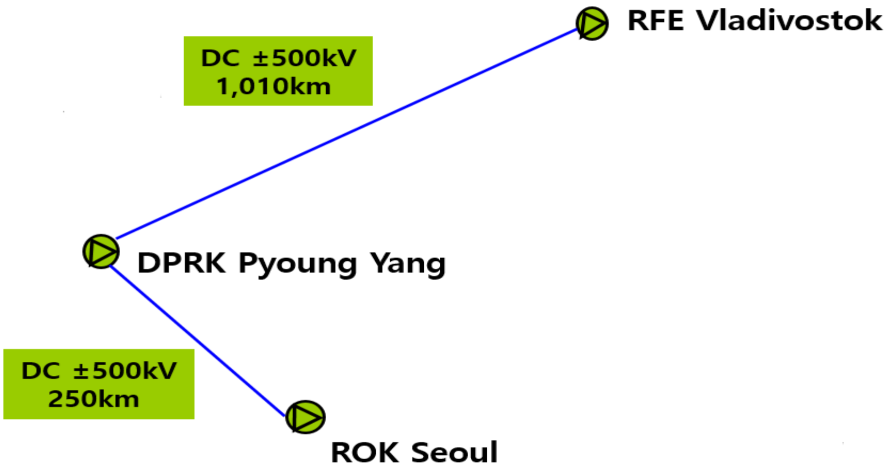

Fig. 3. A scenario of interconnection between Korea and Russia through DPRK [5].

capacity is less than 5% of the peak demand. Therefore, the maximum importing capability of Korea from all countries is supposed to be less than 5 GW in 2030. In general, the blackouts in the power network have a huge social, economic and political impact. If the power resources are diversified, the total supply cost increases, but power supply reliability improves. This is because even if a failure occurs in one power source, the remaining power sources operate normally. The same concept also applies to power system interconnection between countries. For importing countries, if they have only one import transmission line, it is very dangerous from an energy security perspective. This means the maximum interconnection capacity from one country, one point to Korea, must be limited to as much as or lower than 3 GW.

In addition to the power system interconnection promotion, our Korean power system has some transmission restrictions from the eastern and southern generation sites to the northern load center nearby the Seoul metropolitan area. If we have the interconnector with neighboring countries, these transmission restrictions can be mitigated. We could also solve the CO_2 reduction and the serious dust (PM2.5, PM10) problems if we import renewable energy.

Regarding the interconnection project, we have common issues in terms of system interconnection and market integration. These can be divided into specific categories, technical, economic, and market integration issues. These issues could be the obstacles to be overcome for power trading in NEA.

[Technical] Transmission planning & operation

- Conclude an agreement for planning, construction, and operation of cross-border interconnected power system.
- Harmonize the interconnected system reliability standards.

Avoid the vulnerability by importing the renewable energy.

[Economic/Environmental]

- Pricing and Trading Method: Fixed or Negotiated in steady-state and emergency conditions.
- Creation of Greenmarket (Power and CO_2 trading).

[Market Integration]

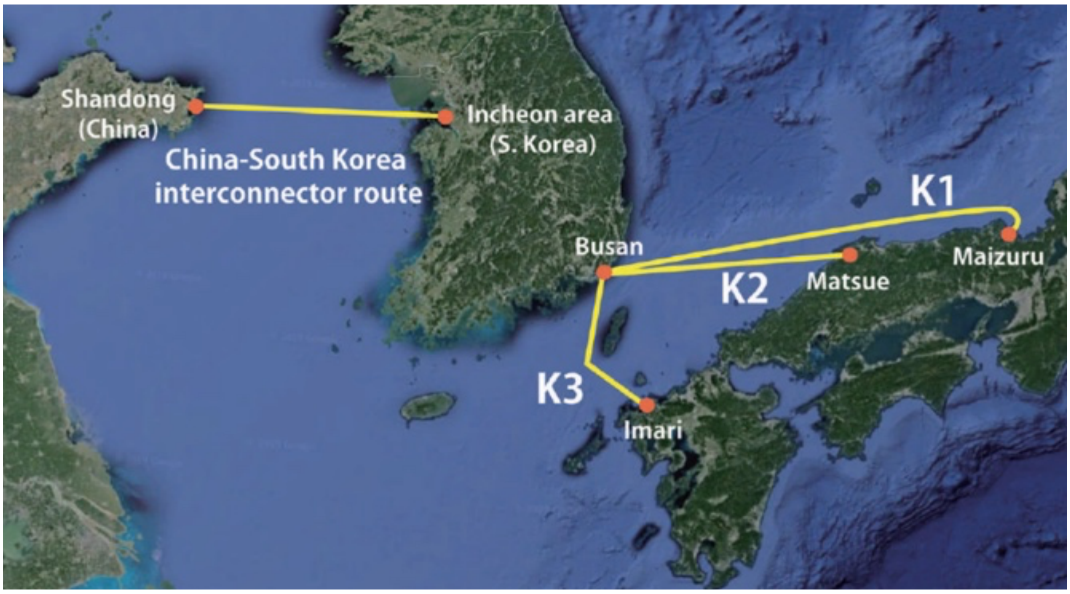

Fig. 4. Scenario of interconnection between Korea, China, and Japan

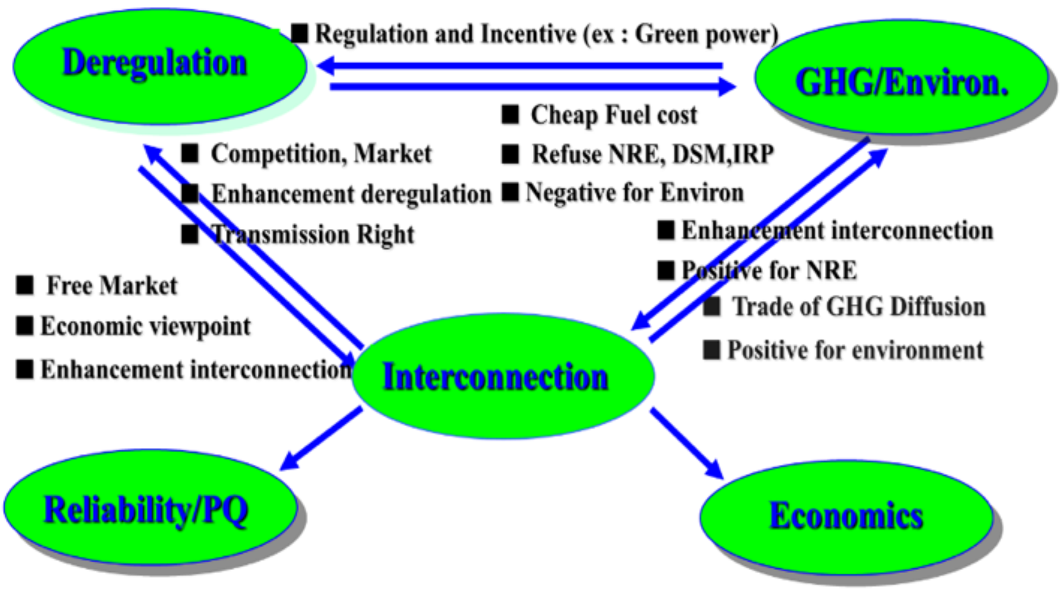

Fig. 5. PSI and other related issues.

- Integrated power market creation & Correlation with energy market deregulation and other issues.
- Institutional consideration: Need for a change in power market legislation of each country.

[Financing, Political and Energy Security]

- Investment financing and cost recovery method.
- Countermeasures for energy security in a political sense.

B. Interconnection Scenarios

Korea has power system interconnection plans with neighboring countries, including China, Russia, and Japan. Many scenarios on power system interconnection between Korea and neighboring countries (Russia, China, Japan, and Mongolia) have been studied since 2000. Many institutes have published various reports on the potential, possibility, and preliminary feasibility study results. They included various contents for the realization of power system interconnection with corresponding countries and pointed out some issues to be solved on a bilateral or multilateral basis [3]. However, all of these study results are outdated, and, hence, they should be revised in the near future.

NEA-CBT reports since 2000 (Multilateral PSI)

- NEAREST (KERI and ESI 2003)
- Asian Super Grid (JREF 2011)
- GOBITEC (ECS 2014)
- Northeast Asia Supergrid (KEPCO, KEEI with Skoltech, 2014)
- GRENATEC (HRENATEC 2010)
- Asia Pacific Power Grid (Japan Policy Council 2011)

Bilateral PSI Scenarios

- Korea-China, Korea-Japan, Korea-Russia, Korea-DPRK in Korea perspectives
- China-Russia, Russia-Japan …

The above reports have a somewhat similar or different concept and contents from a technical, economic, and marketable viewpoint with each other. Among these studies, the study for GOBITEC, which focuses on the renewable energy development in GOBI desert and interconnection with importing countries, is the best alternative for cross-border green power trading. This GOBITEC produced power could be transmitted to neighboring countries like Russia, China, Korea, and Japan. In addition to GOBITEC, we would utilize the Russian hydro potential, and this will be a good candidate for the power system interconnection. Relying on this concept, we could consider the overall power system interconnection concept around NEA countries. This will be the whole power system interconnection scenarios based on a multilateral economic and political agreement. However, now, the bilateral power system interconnection concept is more popular and well-developed than multilateral trading.

Regarding the bilateral interconnection, at first, power system interconnection between Korea and Russia through DPRK has been studied and discussed at a private and governmental level since 2000. The feasibility study was also performed jointly by Korean and Russian institutes, which established some interconnection scenarios. But, owing to the DPRK territory, transit and complicated political situations, this plan is still in progress. Secondly, the interconnection plan between Korea and China is now under consideration between KEPCO (Korea Electric Power Corporation) and SGCC (State Grid Corporation of China). This interconnection plan has a capacity of 23 GW and annual power trading of around 20 TW·h. This interconnection plan will be implemented by a submarine cable, and the converter station will be located at nearby Weihai (China) and Incheon (Korea). Also, power system interconnection between Korea and Japan is now under processing, but this is only a private level discussion and faces some barriers. Softbank, as a private company, is only interested in this interconnection plan. We may expect this interconnection plan to take a somewhat longer time than other projects because of quite complex problems.

IV. Future directions

The final goal of power system interconnection and market integration is to enhance technical reliability, economic efficiency, and regional peaceful relations. This impact induces the generation mix change and an increase in the renewable energy supply. Cross-border interconnector usually diversifies, harmonizes and optimizes the total generation mix because it maximizes renewable energy resources. CDM (Clean Development Mechanism) project could be applied to new developed renewable resources. Generally, power system interconnection may impact other power industry issues. It is strongly related to the energy industry deregulation, and a generation mix change due to environmental issues. All of these aspects have some interrelated positive or negative factors. We believe the power system interconnection will give us the net additional positive effects.

From Korea's viewpoint, we have some complex energy issues that involve international power cooperation with NEA countries, including DPRK, and national CO_2 reduction problem under the Paris agreement. To solve these problems, the Korean government is planning an energy policy to expand the renewable energy supply and power system interconnection with neighboring countries. Therefore, the Korean government expects to import eco-friendly energy related to the CO_2 reduction plan and expand the renewable energy, so-called 3020 and 4030 policies. These are the major factors to promote the power system interconnection from Korea's viewpoint.

From a geopolitical standpoint, Korean Peninsula is the central area of Northeast Asia's power system interconnection. South Korea is also planning a power system interconnection with neighboring countries. However, there are various political, economic, and technological obstacles, and we will try to overcome them in the future. We all think that this grand project will be a physical power network and a regional peaceful corridor. Therefore, we may expect this project will be realized within the near future through the multilateral political and business agreements despite the significant obstacles it faces.

References

[1] MOIST, “8th Power Supply and Demand Plan," 2017

[2] Korean government “3RD renewable energy plan," 2018

[3] J. YOON, "Power System Interconnection in NEA," KERI, 2014.

[4] “Power system interconnection in Korea's perspectives," KERI, 2017

[5] “Feasible power exchange model Between the ROK, the DPRK, and Russia," IEEE GM, 2011

Academic SVs and photos were not submitted with the manuscript

Problem of Excess Electricity and Capacity due to the Commissioning of the Astravets Nuclear Power Plant

B.I. Nigmatulin*, M.G. Saltanov

Institute of Energy Problems, Moscow, Russia

Abstract **— The paper presents a review and analysis of sales and marketing opportunities for the electricity generated by the Astravets Nuclear Power Plant (NPP) in terms of sales destinations (domestic market, export to Europe and Russia). The study comprehensively scrutinizes the issues of competitiveness of the electricity generated by the Astravets NPP and parameters of its production cost, price, and repayment of investment. We address the economic, technological, and political risks of electricity sales, along with the standpoints of the leadership of the industry and those of academic and public organizations. A range of possible scenarios for the development of the situation is analyzed.**

Index Terms: **nuclear power plant, Astravets NPP, Russia, Belarus, electricity market, investment project, excess electricity.**

I. Introduction

1. Speaking of the Astravets Nuclear Power Plant

The Astravets Nuclear Power Plant is the first nuclear power plant in Belarus, it is of the AES-2006 type. It comprises two VVER-1000 nuclear reactors. It is located at the northwestern border of Belarus in the agro-town of Vornyany, 18 kilometers from the town of Astravets in the Hrodna region, 40 km from the Lithuanian capital Vilnius.

The actual starting up of the first NPP reactor took place in August 2020. The official starting up of the first rector of the Astravets NPP took place on November 7, 2020. The main partner of Belarus in the NPP construction project is the Russian company Atomstroyexport.

* Corresponding author.
E-mail: maxisal@mail.ru

http://dx.doi.org/10.38028/esr.2020.04.0007
Received October 17, 2020. Revised November 09, 2020.
Accepted November 23, 2020. Available online February 01, 2021.

2. Speaking of money

Under an agreement on cooperation in the construction of nuclear power plants, signed in 2011, Russia has committed to providing Belarus with a $10 billion loan. The “ASE Group” is to become the general designer and contractor. The loan from Russia amounts to 90% of the NPP construction cost, while the remaining 10% is to be provided by Belarus. The loan repayment was to begin six months after the NPP commissioning and was to be made in equal installments every six months in USA dollars until 2035. Half of the used loan part was to be charged 5.23% per annum, and the other half was to be charged at a floating LIBOR rate (about 1% or less) + 1.83% per annum. Annual payments on this loan from 2021 to 2035 were estimated at $1 billion. In 2020, the governments of Belarus and Russia signed a protocol on amendments to the agreement on state export loan for the NPP construction by the Belorussian side, dated November 25, 2011. [1] The protocol provides for a two-year extension, compared to the current conditions, of the loan availability period, grace period, and, accordingly, the loan term. Under this document, the loan interest rate decreases to 3.3% per annum and changes from floating to fixed.

3. Speaking of sales

When deciding to build the Astravets NPP, the authorities estimated the demand for electricity in Belarus by 2020 at 47 kWh [2]. There were plans to commission the first reactor of Astravets NPP in 2019 and the second one - in 2020. Now, the deadline has been pushed back by at least one year.

By this time, Belarus had failed to increase its economic potential to ensure demand for additional energy after the NPP commissioning.

In 2019, the electricity output of the existing plants was 39.755 billion kWh. Two reactors of the Astravets NPP will generate ~18 billion kWh of electricity.

The question naturally arises: what to do with the "extra" electricity after the nuclear power plant is launched?

This issue is currently the most important for the two power systems of the two countries. There is a great deal of discussion, myths, and speeches on the subject. All the

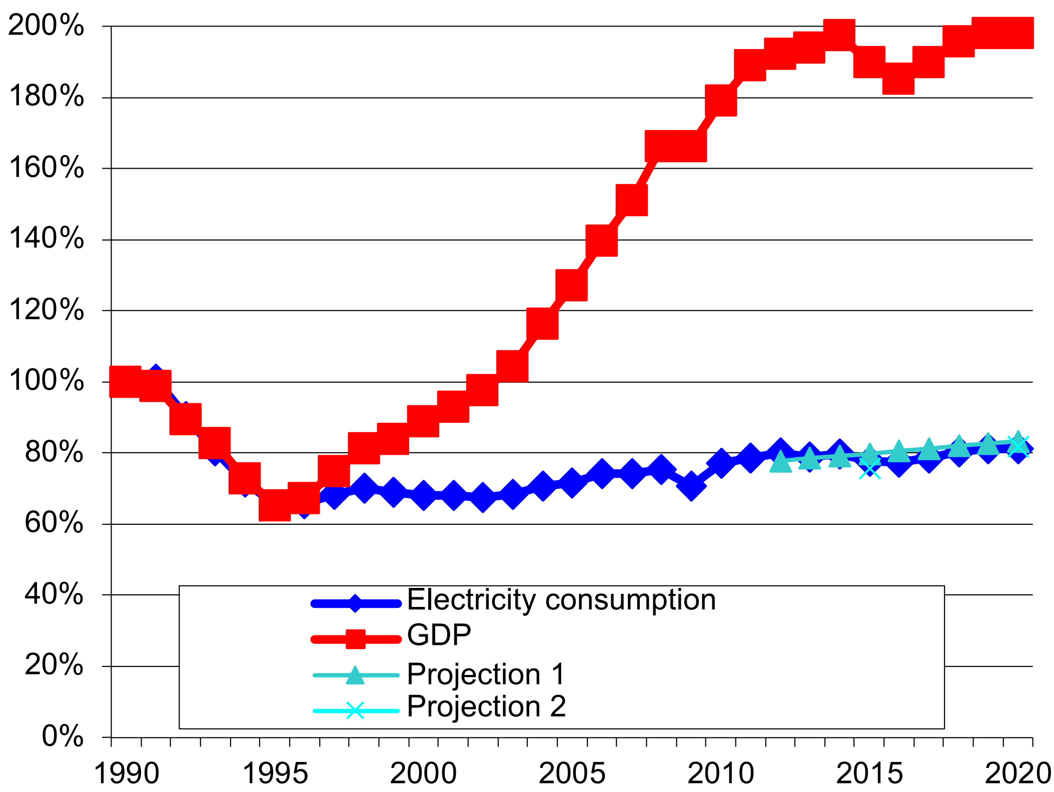

Fig. 1. Historical data and the projection made by B.I. Nigmatulin in 2012 for economic and energy industry performance indicators of the year 2020 .

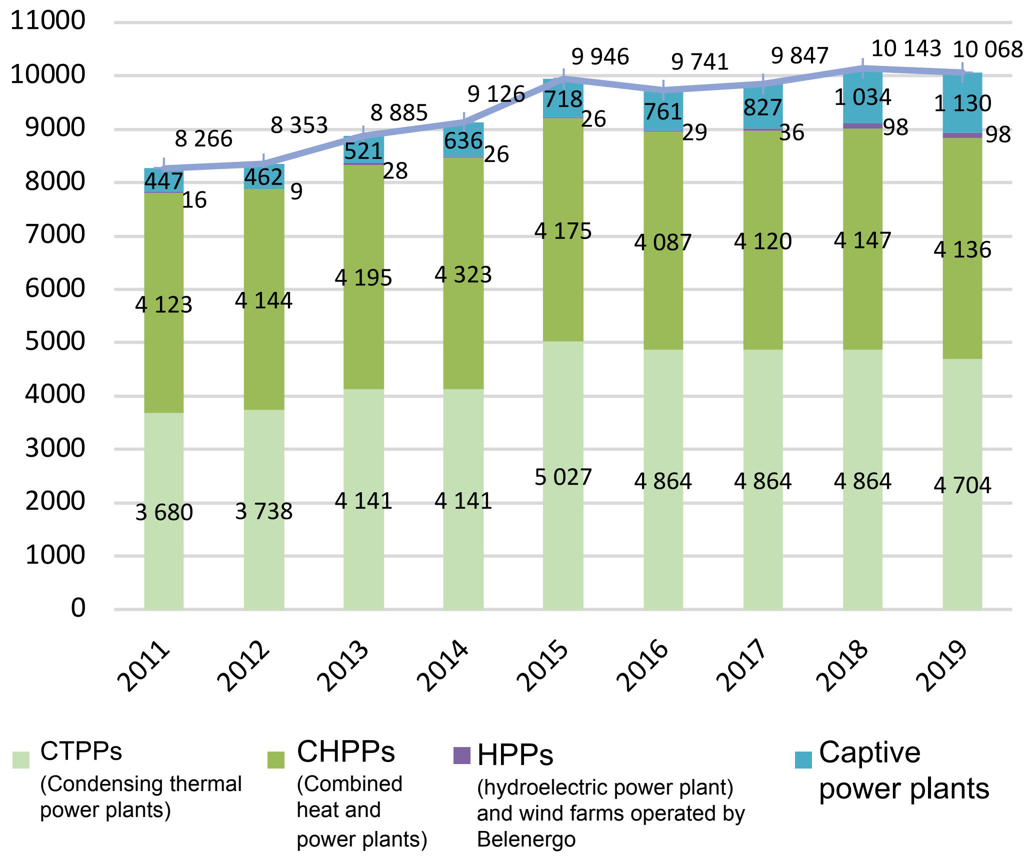

Fig. 2. The mix of installed capacity of generating sources in the power system as of January 1, MW.

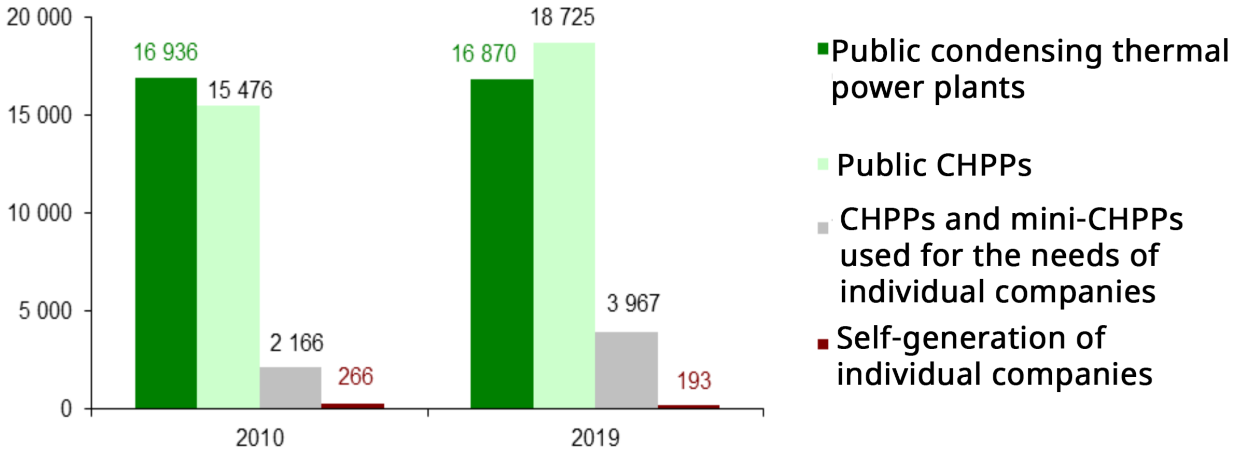

Fig.3. Electricity generation by power producer category. (million kWh) [5].

standpoints cover a broad spectrum ranging from those claiming that "the Astravets NPP is completely redundant and will prove a heavy burden on the budgets of countries and consumers" to "All electricity will be sold for the benefit of Russia and Belarus, even if we build another Astravets NPP."

II. Belarus does not need the Astravets NPP for domestic consumption

1. Belarus' GDP growth potential does not need the Astravets NPP.

The potential for GDP growth and economic growth in Belarus does not need electricity produced by the Astravets NPP. B.I. Nigmatulin showed this back in 2012 based on the correlations of economic and energy development, primarily on an analysis of the elasticity coefficient of electricity consumption in terms of GDP [3].

The installed capacity of Belarus' power system as of January 1, 2019, was 10.068 GW [41], including 4,704 MW of electric power capacity of 3 condensing thermal power plants (CTPPs), 3,856 MW of 14 CHPPs of a capacity over 50 MW, and others.

Today, Belarus exports electricity and buys virtually none of it, even without launching the nuclear power plant.

As of now, power generators are hydroelectric and thermal power plants. Belarus needs 33 to 36 billion kWh of electricity per year, which is fully covered by the capacity of power plants now without the NPP. The two NPP reactors will produce about 18 billion kilowatt-hours of power. This is ~50% of Belarus' needs, but these needs are already fully covered without the NPP.

Thus, after the NPP launch, there will be a 50% surplus of power unless other hydroelectric and thermal power plants cease operating.

Calculations by the Republican Unitary Enterprise “BelTEI" [4] (a leading research center of the State Production Association “Belenergo”) show a projection of the demand for electricity in the Republic for 2035 under three scenarios: the reference case, reduced demand case, and increased demand case of 40.7 billion kWh/year, 39.6 billion kWh/year, and 40.8 billion kWh/year, respectively.

The minimum load of the Belarusian power system is ~5-6 GW. With only two reactors of the Astravets NPP (2,400 MW) and the Lukoml SDPP [State-owned District Power Plant, which is a condensing thermal power plant] (2,890 MW) in operation, it will already be exceeded, and the capacity of the remaining 40 TPPs in Belarus remains unclaimed.

Accordingly, it is necessary to shut down the CTPPs and CHPPs, which is not always an option due to the need for CTPPs to operate in a regulated mode, cogeneration modes, social consequences of shutting down, and others. Alternatively, one should limit their total generation, which markedly reduces their profitability and increases the price.

For example, the Lukoml SDPP operates as a load following plant and the fluctuations in the daily power amount to 1,100 MW [6]. The installed capacity is 2,890 MW. Consequently, the SDPP 1,100/2,890 MW = 40% of its capacity subject to adjustments, and 1,789.5 MW is the baseload that must be transferred to the NPP. It is assumed that with the commissioning of the Astravets nuclear power plant, only the 300 MW power unit, and CCGT-427 unit will continue operating at the Lukoml SDPP [7]. The Lukoml SDPP will be practically shut down.

Pavel Drozd, Director-General of the State Production Association “Belenergo” said that all CHPPs included in the Association would operate exclusively in the cogeneration mode, which provides mainly heat to consumers [8].

The installed capacity utilization factor (ICUF) of CHPPs and CTPPs, in this case, will be just disastrous, with a disastrous production cost per kWh and Gcal [6]. Even if we take no account of depreciation costs at

CTPPs and CHPPs, the decrease in operating costs is not proportional to the output but slower. Accordingly, the effect of reducing the fuel component (uranium vs. gas) is much lower than planned when directly comparing the fuel costs of TPPs and the NPP.

If gas prices are drastically reduced (compared to the expected gas price according to a trend of rising gas prices at the start of construction), the effect is even lower.

Thus, although the Sectoral Program for the Development of the Electric Power Industry (approved by the Decree of the Ministry of Energy of the Republic of Belarus No. 31 of September 4, 2019), does note that the standard service life of a significant part of the generating source equipment will expire by 2020 (which requires their replacement, modernization, or reasonable terms of extension of operation), The total capacity of such equipment is 4,235.7 MW, including that of the Lukoml SDPP - 2,455 MW, Beloozersk (Berezovskaya) SDPP - 330 MW, Novopolotsk CHPP - 270 MW, Minsk CHPP-3 - 220 MW, Mozyr CHPP - 205 MW, Bobruis CHPP-2 - 180 MW, Hrodna CHPP-2 - 180 MW, Svetlogorsk CHPP - 155 MW, Mogilevsk CHPP-2 - 150 MW, and 90.7 MW by other CHPPs. The scope of decommissioning of electricity-generating capacities at TPPs will be determined after the NPP reaches its design capacity and successfully integrates into the balance of the power system, the practice suggests that such intentions to replace almost half of the power system capacity, having encountered with infrastructure, economic, social (Lukoml SDPP alone employs more than 1,600 people) and circuit and operating mode issues with respect to regulation and introduction of district heating remain unrealized, and the plants are modernized and extend their service life.

2. Attempts to create an additional consumer for the Astravets NPP power prove ineffective so far

Originally, the Astravets NPP construction project did not involve finding a market for all its output. The search for potential consumers among business entities began in 2016. At that time, consumption was estimated at 1.6 billion kWh per year (~9% of generation). Per Decree No. 582 of the Council of Ministers of the Republic of Belarus of October 6, 2020 [11], the number of potential projects increased from 148 to 178 over the year, and the projection for electricity consumption was increased by 100 million kWh, from 2.7 to 2.8 billion kWh. Overall, the demand is ensured for 1,191.6 MW of commissioned capacity and 2.8 billion kWh of the Astravets NPP output. This is half of the total capacity of the system of the two VVER-1200 reactors and 15.6% of the output.

In 4 years, 6.7% of demand for the Astravets NPP power was ensured. The contribution of the last year was merely 0.5%.

However, whether even this demand is real depends on the economic situation, which determines the conditions and opportunities of consumers themselves. For example, the Belneftekhim concern's projects are the most energy-intensive (construction of a complex for hydrocracking of heavy oil residues, a nitrogen complex, etc.), but their efficiency depends on the state of the market for its products, i.e., petroleum products, fertilizers, and others.

3. Speaking of electrode boilers

The heating value of natural gas is 8-10 Gcal/1000 m^3 [12]. At \$127 per 1,000 m^3, the cost of a gigacalorie would be \$13-16/Gcal. 1 Gcal corresponds to 1163 kWh. Accordingly, to achieve comparable efficiency of electrode boilers, 1 kWh should cost 1.1-1.4 cents. The expected price of the Astravets NPP electricity is 10-13 cents, which is an order of magnitude higher. Hence, the same applies to the marginal difference in the efficiency of heat generation methods. In electrode boilers, when using electricity from the Astravets NPP, it is an order of magnitude less than in conventional natural gas-fired boiler houses.

Electrode boilers in Belarus are planned to be commissioned for a capacity of 916 MW (eventually up to 1,116 MW). Commissioning of equipment with a total capacity of 760 MW is envisaged at power plants, including Beloozersk (Berezovskaya) and Lukoml SDPP, CHPPs, and mini-CHPPs. Another 156 MW will be put into operation at boiler houses [13].

In this context, even based on the Astravets NPP electricity price of 10 cents/kWh, the cost of a gigacalorie will be at least \$116. Retail tariffs for heat, for example, supplied by the republican unitary enterprise “Minskenergo” to legal entities and sole proprietorships, which have been effective since January 1, 2020, are 86-142 Gcal (104 BLR / Gcal, on average), given the 2.1085 USD / BLR exchange rate, [14] or about 50 USD per Gcal, which is more than two times lower than that which can be produced in electrode boilers powered by the Astravets NPP electricity.

Total heat consumption in 2019 was 55 (32.9+22.1) million Gcal. It would take 64 billion kWh of electricity to generate heat with electrode boilers. Thus, the entire Astravets NPP excess can be utilized by electrode boilers. At 100% load of electrode boilers (24 hours a day, 365 days a year), their electricity consumption will be 1,160*8,760=10.2 billion kWh or 8.8 million Gcal.

In this case, at least US\$ 60-65 million will be lost for every million gigacalories.

4. Uranium instead of gas - what's the point?

Assuming the 2020 gas price for Belarus of ~127 \$/1,000 m^3 [15], given the consumption of ~241 goe/kWh [16], the gas price in the price of electricity is 0.127 \$/m^3: (1,140 goe/m^3) * 241 goe/kWh=0.027 \$/kWh.

Accordingly, the gross amount resulting from saving natural gas to generate 18 billion kWh is \$486 million per year. At the same time, the loan payments (even under the new, relaxed conditions of 3.3% per year) are ~\$700

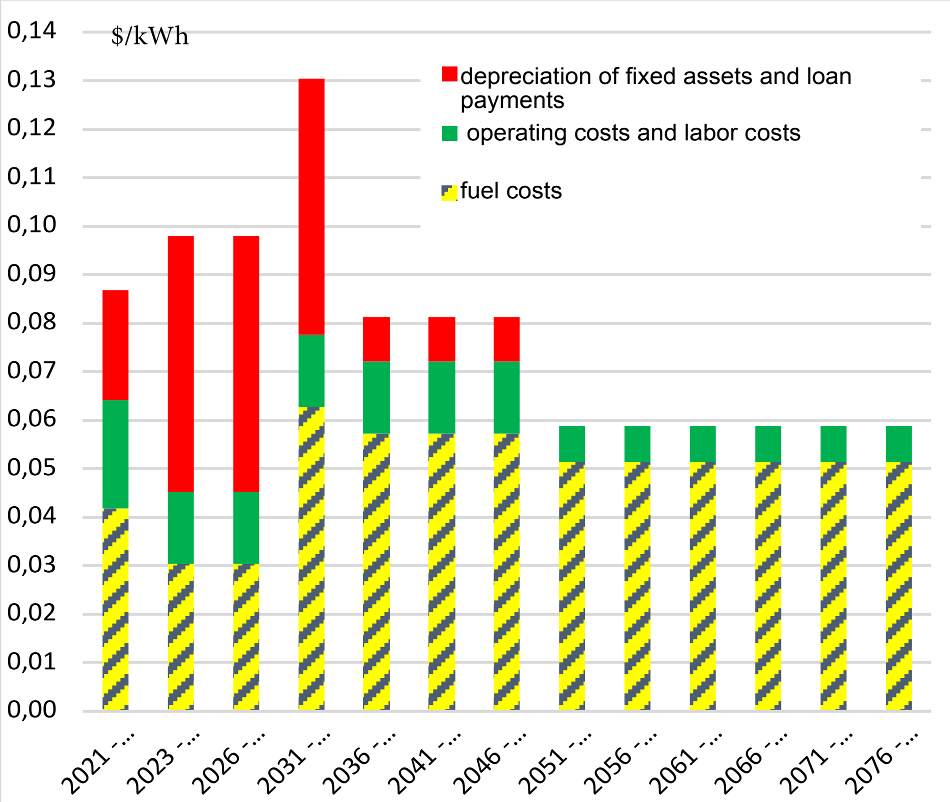

Fig. 4. Components of the cost of electricity generated by the Astravets NPP (aggregated).

million per year [17]. The amount corresponds to the size of the used loan part of US$ 9-10 billion. Other estimates, based on varying amounts of the loan used, are US$ 500-760 million a year, which is also more than the above value.

That is more than $200 million higher than the savings.

However, for the power system and power plants, the price of gas is higher than the price of supply at the state border. For legal entities consuming more than 600 million m^3 of gas per year, the gas price is 333.14 Belarusian rubles per 1,000 m^3, or ~$158/1,000 m^3 (Given the exchange rate of the Belarusian ruble to the USA dollar of 2.1085:1) [18]. Accordingly, the fuel component is $0.033/kWh, with total savings of $600 million per year, which is $100 million less than the loan payments.

The above calculations were based on gross savings, i.e., assuming that nuclear fuel costs nothing. However, its price is ~0.019 $/kWh [19].

The key motivation behind the construction of the Astravets NPP was the economic effect to be generated by the difference between the prices of nuclear fuel and gas. This difference, given the same sales prices, can yield an additional cash flow to return the capital investment. This effect amounts to 0.027-0.019=0.008 $/kWh. At 18 billion kWh per year, this is $144 million per year. Thus, the payback period of the $10 billion loan principal is 70 years, and given the interest (3.3% per year) of $330 million per year, this means that the loan principal will never be repaid.

III. Is it possible to sell the Astravets NPP electric power to repay the loan? The electricity generated by the Astravets NPP is more expensive than that from thermal power plants in Belarus. It is more expensive than electricity in Europe and more expensive than electricity in Russia

1. Price calculations for 2018

The 2018 BelTEI calculations [20] show that the price of electricity generated by the nuclear power plant will be even higher than the price of electricity generated by gas-fired thermal power plants. As projected to 2035, the cost of electricity from different types of generating sources, taking into account the increase in fuel prices and the network component, at the start will be:

- 12.57 cents/kWh at gas-fired TPPs; (Hereinafter a cent means US$ cent. At a gas price of $152/toe, or $133/1,000$m^3$)

- 14.33 cents/kWh at the nuclear power plant.

According to BelTEI's aggregated calculations, the planned cost of electricity output of the Astravets NPP, given the current prices of nuclear fuel and the loan component, is estimated at 10.2 cents/kWh, including the fuel component of 1.9 cents/kWh.

Given the terms of the loan for 2018 and the fact that the loan was for 25 years (from 2010 to 2035, repayment of the loan starts with the launch of the NPP in equal installments over 30 months), the loan component is preserved until 2035. On July 14, in Moscow, the

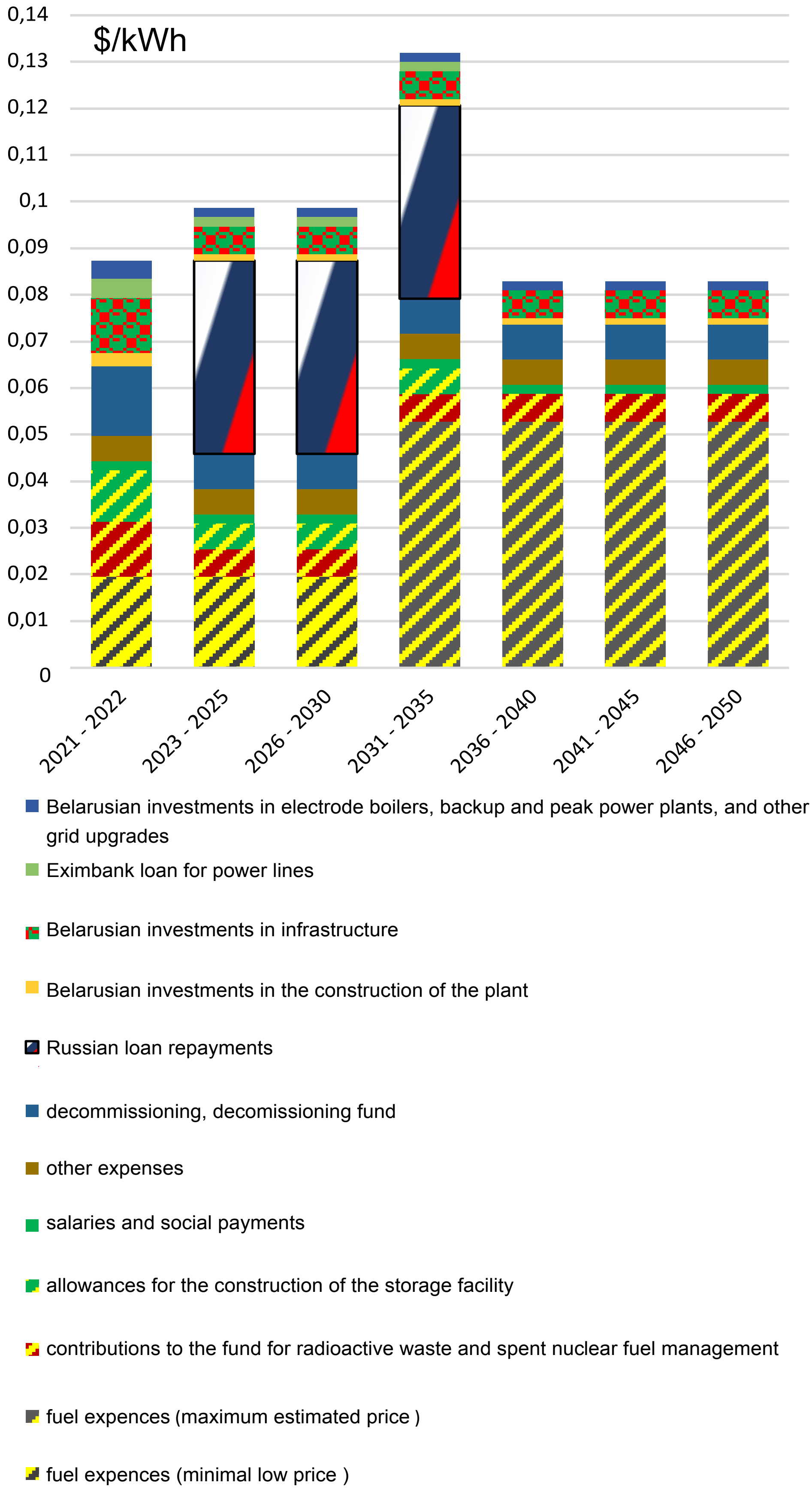

Fig. 5. Components of the cost price of electricity generated by the Astravets NPP (in detail).

governments of Belarus and Russia signed a protocol on amendments to the agreement on the state export loan for the construction of nuclear power plants by the Belarusian side, dated November 25, 2011. The interest rate on the loan was reduced to 3.3% per annum, with the rate changed from floating to fixed. With a projected 2.7-fold increase in nuclear fuel prices, the fuel component would increase to 5.13 and the total cost of production to 13.43 cents/kWh. In the total cost of electricity supplied to consumers, the network component is 0.9 cents/kWh, and then, with the network component factored in, the total cost at the NPP would be 13.43+0.9 = 14.33 cents/kWh.

2. Price calculations for 2020

The updated alternative calculations [21] assume that loan terms changed in mid-2020.

The fuel component for the fuel purchase is assumed to be 1.9 cents per 1 kWh, and in general, considering the costs of fuel management and disposal (the calculation of the electricity cost factors in the need to form a budget for spent nuclear fuel management over 30 years and a budget for the construction of storage facility over 15 years.), the fuel component reaches values of 3.0-5.7 cents per 1 kWh.

Operating costs cover labor costs, operating costs proper, and additional costs of 1.5-2.2 cents, including plant decommissioning costs in the cost price of electricity generated by the Astravets NPP. With a 30-year decommissioning fund, the cost of decommissioning the nuclear power plant in the cost price of electricity would be 0.75 cents (0.37 cents with a 60-year fund and 1.5 cents with a 15-year fund.

Capital costs in the cost price of electricity generated by the Astravets NPP, including payments under the loan agreement between Russia and Belarus, the capital components of the cost of infrastructure around the plant, the modernization of the power grid in the cost of electricity generated by the Astravets NPP, etc., are estimated to be 4-4.6 cents until 2050. However, it should be noted that the calculations are not based on the $10 billion loan, as outlined in the Agreement, but on $6.4 billion [22]. Thus, the actual loan exposure can be much higher.

It is worth noting that it is difficult to calculate the exact amount of the loan debt without accurate information about the cost of the plant and the dates of transferring portions of the loan funds, which is not publicly available today. With the likely underestimation of the cost of the plant, the cost of the loan component increases by 0.4 to 0.6 cents per each underestimated US$ billion.

3. The domestic market in Belarus.

As a whole, from 2023 to 2035 (after the launch of both reactors) the calculations as anchored to a single point (on buses) as well show that the cost price of the Astravets NPP electricity may range from 9.9 to 13.2 cents per 1 kWh, depending on fuel prices in the first years of operation of the plant. The cost price of electricity will be 9.7 - 10.7 cents on average for the period.

This exceeds the cost price of current gas-fired power generation by 2.5-3.5 times or is comparable to it under the most unfavorable gas prices.

Hence, according to calculations by Belarusian experts, the cost price of electricity in the entire Belarusian energy system will increase 1.8 times, to 7.26 cents per kWh, after the launch of both reactors. [23]

Notably, based on the 2020 tariff decisions in Belarus [24], the price for the end consumer averages 13 cents/kWh for business entities (77%), 9 cents/kWh for households (23%), and 11 cents per 1 kWh on average in the country [25], [26], [27].

This price already includes distribution and marketing expenses. Based on these estimates, the Astravets NPP is unprofitable when selling electricity in the domestic market, provided their share in the price for the end consumer is more than 17%. In Germany, this share is over 20%, while in Russia it reaches 50%.

4. Comparison of the price offered by the Astravets NPP with prices in the foreign market (Europe, Russia)

Is it possible to repay the loan by selling the Astravets NPP electricity in the foreign market?

According to the above calculations, the capital costs (assuming 100% sales and the ~83% ICUF) in 2023-2035, taking into account the Russian loan, are ~5.3 cents/kWh, of which the Russian loan is ~3.7-4.1 cents/kWh.

The electricity cost, excluding capital costs, can be attributed to operating costs that include fuel component. Thus, in 2023-2035, the Astravets NPP electricity priced based on operating costs, excluding capital costs (that ensure repayment of loans) and setting up of a decommissioning fund, is ~3.9 cents per kWh.

Cash flow for return on investment can only come from the difference between the sales price and the operating cost of electricity production if such a difference exists at all.

In this case:

- in the European market (the NordPool exchange), with which both the Baltics and Belarus trade, in 2019, the day-ahead market price for the Baltics was 45.86-46.28 euro/MWh [28], or ~5.1-5.2 cents per kWh. At the same time, the price is much lower during the night hours that are relevant for the NPP.
- in the Russian electricity market, in the interconnected power system of Center [29], the day-ahead weighted average index of equilibrium price for selling electricity in the market is 1.284 rubles/kW, for buying - 1.229 rubles/kWh (November 2019 - November 2020). In terms of the US$ exchange rate used in the interstate trade, this would be 1,771.85 cents per kWh.

Thus, the difference (the "margin") that could be spent to reimburse capital costs, including the repayment of the Russian loan, will be no more than 5.1-3.9=1.2 cents per kWh when sold in the European market. Given this margin, the corresponding annual flow of funds would not exceed

$ 0.2 billion, which is less than the interest payments on the loan alone (!). According to calculations by Belarusian experts, payments on the Russian loan alone under the new terms (3.3% per annum) are ~ $ 0.7 billion a year, of which 0.49 billion is the principal of the loan, and 0.21 billion is the interest thereon.

However, even with no interest factored in, the volume of the "margin" in the case of sales in the European market corresponds to the term of repayment of the load principal of US$ 10 billion of over 50 years. This is provided that all electricity is sold to Europe.

Planning sales of the Astravets NPP electricity in the Russian electricity market (in the "day-ahead" segment) should take into account that its price (1.77-1.85 cents per kWh) is even lower than the fuel component in the total price of the Astravets NPP electricity, which is 1.9 cents per kWh. Thus, it is impossible to repay the loan by selling the Astravets NPP electricity in the Russian electricity market.

This is impossible, among other things, because there is no possibility to sell capacity, which is a source of income for Russian power plants (and the main one for NPPs).

5. Comparison of the Astravets NPP price with the demand price in the Russian market

Even if we assume that an appropriate mechanism for selling the Astravets NPP power to the Russian market at full cost has been found, it should be evaluated in terms of the end consumer, for example, comparing it to the single-rate tariff in a relevant region of Russia, in particular, in the Smolensk region.

Let us take a typical consumer of 15-500 MWh per month [30] as an example (Mini-market with a gas station. Round-the-clock cycle plant, etc.). In July 2020, the single-rate tariff for them (at the point of consumption) factored in electricity and capacity from the last resort supplier, the JSC “Atomenergosbyt,” and was 2.6-3 rubles/kW. That is, the price in the Russian market was 3.94.2 cents/kWh at an exchange rate of 70.4 rubles/US$. This price (the ultimate consumer one!) is 1.75 times lower than the average cost of electricity in the Belarusian power system of 7.26 cents per kWh [31] and corresponds (see above) to the operating costs of the Astravets NPP of 3.9 cents/kWh, disregarding the recovery of the funds invested in it. The case in question, however, even does not consider the costs of transmitting electricity from the Astravets NPP to the Russian consumer.

Thus, recovery of investment in the Astravets NPP due to the difference in prices (not only for electricity but for the energy supply in general) in Russia and Belarus is also impossible.

6. Comparison of the "worth" of electricity in Belarus and its neighbors in terms of purchasing power parity and energy-GDP ratio

Unfortunately, pricing in the energy industry in a non-market environment is highly distorted, and calculation in terms of PPP, which adequately captures the place of the energy industry in the economy, is not accepted in the energy industry of Belarus. This is well-justified and reasonable because, in the absence of the market, pricing is based on the cost of production, which, in turn, is based on the cost of gas. And this fuel component is tied to the US$ exchange rate.

If pricing were initiated from the side of demand, which is determined by purchasing power, we would have to evaluate and compare the product competitiveness in terms of purchasing power parity. Accordingly, it is necessary to assess and compare the electricity price in Belarus, Russia, and, for example, the Baltic States.

At the same time, comparing the value of Belarusian and Russian electricity for the consumer expressed through the purchasing power parity, we should consider the proportions of the PPP US$ value and its exchange rate value in both countries. In 2019, it was $0.4/$PPP in Russia, $0.33/$PPP in Belarus, and $0.51/$PPP in Lithuania. Accordingly, the Belarusian electricity introduced into the economy would have cost the consumer 11/0.33 = 33.3 cents PPP/kWh, and the Russian electricity would have cost 4.2/0.4 = 10.5 cents PPP/kWh, i.e., more than three times cheaper.

The same ratio holds when comparing Belarus and Lithuania.

This means that it is three times less profitable for Belarus' neighbors to buy electricity from it than to buy their own.

In 2019, consumption in Belarus was 33.185 billion kWh (Figure 3). The average price for the consumer (see above) is 11 cents per kWh (according to the exchange rate). The nominal GDP of Belarus was (based on the World Bank data) US$ 63.08 billion. Accordingly, the share of payment for electricity by the economy and population in the GDP was 5.9%. For comparison, in the United States this figure is 2.1%, in Europe - 3.5%, and in Russia - 4.1%. With the commissioning of the Astravets NPP, the disparity will increase.

At the same time, the physical energy-GDP ratios in Russia and Belarus are almost the same - 0.22 and 0.18 kWh/$PPP, respectively. In Belarus, it is slightly lower. Despite this, however, the energy burden on the economy is heavier.

7. Summary

All of the above is a fraction of all the possible uses of the Astravets NPP. However, they all indicate that its power is prohibitively expensive and excessive for the country and its neighbors, and its generation, hence, is unprofitable without expanding the market given the specifics of the nuclear power plant. Electricity prices are uncompetitive without special preferences on the part of the government.

However, even the above-mentioned prices for the Astravets NPP electricity were based on its full planned load (the NPP's installed capacity utilization factor is 81-83%). Meanwhile, this load depends on how much electricity can be sold in the market, and is it possible to sell it?

IV. Is it possible to sell the Astravets NPP electricity at all

1. Export to the West?

"Currently, we have many offers and several contracts to export electricity. By the end of 2019, we expect to more than double electricity exports as compared to the last year. I think that with the commissioning of the nuclear power plant, our export potential will increase both technically and economically," said Deputy Head of the Ministry of Energy of Belarus M. Mikhadiuk in his interview to the state agency BELTA on September 18, 2019 [32]. According to him, contracts for exporting Belarusian electricity are signed not only for 2019 but also for the years ahead. "Using the inter-system tie-lines we have with Lithuania, Ukraine, Poland, and Russia, it is possible to export electricity. If there are promising contracts, these ties can be expanded. Therefore, the export will not be zeroed out. I think it will only increase," Mikhadyuk stated.

At the same time, Energy Minister V. Karankevich [33] said: "Last year (2019), power generation in the country as a whole increased by 5% compared to 2018. This was made possible by a significant, more than a two-fold increase in power export. The export of electricity amounted to 2.4 billion kWh." Lithuania was the principal buyer, with 1.5 billion kWh [34].

However, these figures mean that under the production of 39.8 billion kWh per year (see Fig. 3), export was 2.4/39.8=6%, and, accordingly, domestic consumption decreased by ~1%.

Thus, with the already existing excess of electricity exported to the foreign market, possible cessation of export and commissioning of the Astravets NPP make the Belarusian energy system as redundant as possible, consequently, the least efficient possible.

1.1. The European Union and the Baltic states

On August 12, 2020, the European Commissioner for Environmental Protection stated that the Baltic States must take the necessary measures to ensure that electricity generated by the Belarusian nuclear power plant (the Astravets NPP) located near the Lithuanian border and 50 km from Vilnius will not enter the EU energy system. The Seimas (Parliament) of Lithuania declared the Astravets NPP a threat to the national security of the country and in 2017 legislatively banned the purchase and transit of the electricity generated by the NPP through its power grids. The Baltic States confirmed the ban on imports of electricity from the Astravets NPP. At a meeting of the Latvian government on August 25, 2020, the ministers agreed to stop the electricity trade with Belarus if Minsk launches the Astravets NPP [35]. The Baltic States adopted legislative measures to impose the embargo through their elaboration down to specific techniques and technologies [36].

In 2025, the BRELL "energy ring" will cease to operate and the inter-system ties with the Baltic will be severed.

1.2. Ukraine

Following Lithuania [37], Ukraine also refused electricity from Belarus [38]. The country also meets its demand with the domestic generation. Kyiv officials say that they see no point in import but want to export electricity. Just like the Baltic States, Ukraine is in the process of synchronization with ENTSO-E. The synchronization is planned to be completed even earlier - in 2023. After that, Belarus will have an option to export, even to the EU, but it will have to build an HVDC link with Ukraine, which will cost several hundred million euros. The Ukrainian grid operator Ukrenergo told DW that they are not currently negotiating with the Belarusian side on the HVDC link. "The company does not plan to implement such a project, at least not until the Ukrainian and European power systems are synchronized," he said. In addition to subjective reasons, we should consider the exclusion of Crimea with its demand from the Ukrainian energy system (up to 1 GW).

1.3. Poland

Poland is also not counted as a possible importer. "Based on a brief review of the policies of neighboring states, the conclusion is that there is no guaranteed possibility of exporting electricity. Given the uncertainty of the electricity export/import issues, to ensure energy security, the development of the electric power industry of the Republic of Belarus should be planned omitting the above factor," says the Sectoral Program for the Development of the Electric Power Industry (amended by Decree No. 31 of the Ministry of Energy of the Republic of Belarus of September 4, 2019). Technologically, it also makes no sense because the tie-lines with Poland are weak, and the operation of the power systems is not synchronized.

At the same time, Poland's stance on electricity import from Belarus has been much tougher: "Absolutely no" since 2017 [39]. All the more so because in October 2020, the Polish government passed a decree to update its nuclear power program. The changes involve the construction of two nuclear power plants with six nuclear reactors in total with an overall capacity of 69 GW. Nuclear power plants are to be constructed at six-year intervals [40].

The Belorussian Concept for Developing Power Generation Facilities and Power Grids to 2030 also takes this into account [41] - "the economic prerequisites alone do not guarantee the possibility of exporting electricity to Poland, since due to the negative attitude of the European Union to the construction of the Astravets NPP, the Union politically guides Poland towards ruling out the possibility of importing electricity from the Belarusian power system."

1.4. Summary

Thus, given the price, political situation, and development plans of countries and power systems, such export destinations as Ukraine, the Baltic States, Poland, and the European Union seem to be absolutely unattainable.

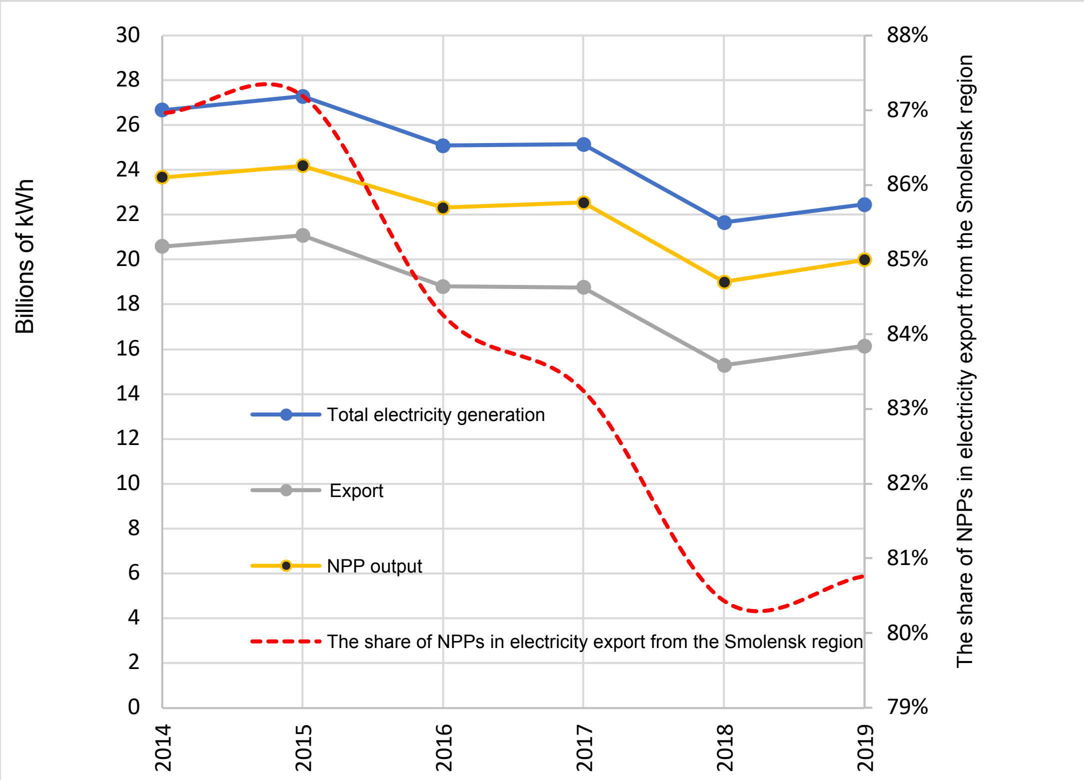

Fig.6. Electricity generation and export in the Smolensk region.

2. Export to Russia?

The energy balance of central and western Russia could change dramatically with the introduction of the Astravets NPP. Its capacity is excessive for Belarus, sales to the West are impossible due to, among other reasons, the elimination of the BRELL "energy ring;" the decisions made by the Baltic States, Poland, and Ukraine; and the lack of demand in Europe. Practically, the only way out is to export to Russia in the direction of the Interconnected power system of Center (the Smolensk region). At the same time, Belarusian electricity can take its place in the Russian power market only at the expense of the Russian electricity generation.

The power system of the Smolensk region, as well as the power system of Belarus, are redundant. The installed capacity of power plants exceeds the combined maximum load by a factor of four. The electric power is transmitted to the power systems of Bryansk, Kaluga, Ryazan, and Tver regions. The power balance of the power system is shown in Table 1. As seen, power output from the Smolensk power system has been decreasing almost continuously since 2014. Accordingly, with its domestic power demand (maximum load <1 GW), any import from Belarus will be excessive for the Smolensk region; and also for the Tver, Kaluga, Bryansk, and Ryazan regions (for which the Smolensk region may serve as a transit region and where the power flow from the Smolensk power system drops or at least does not increase); and for the Moscow region, where it does not exist.

Table1. Smolensk power system power balance for 2014-2018 [42]

As it follows from the chart (Fig.6):

a. the power export from the Smolensk region is generally declining,
b. the share of exported nuclear power (baseline mode) is declining ahead of schedule,
c. the output of Smolensk NPP is decreasing,
d. the Smolensk NPP is increasingly focused on covering the demand of the region itself, which is small in the first place.

Thus, the electric power of Astravets NPP is not needed in Russia, FOR THE TIME BEING.

This is confirmed in the official documents of the strategic development of the power system of Belarus: [43] "Planning the development of the electric power industry of the Republic of Belarus to 2020 should take into account that, given the lower fuel price for thermal power plants in the Russian Federation, the availability of nuclear power plants in the European Russia, as well as the excess capacity, Russian electricity under market conditions until 2020 will be more competitive compared to the electricity generated in the power system of Belarus, which rules out the possibility of exporting electric power on market terms from the Republic of Belarus to the Russian Federation in the near future.

Thus, with the existing energy market model, the absence of the capacity market segment in the Union's CEM, and non-transparent schemes of paying back the

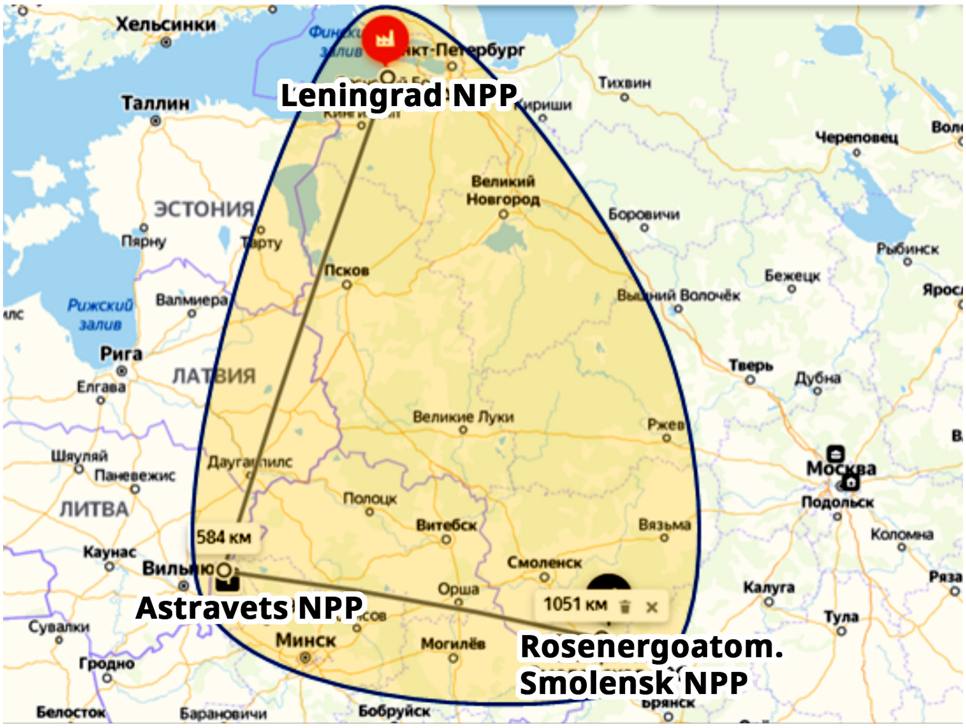

Fig. 7. Configuration of the nuclear power node: IPSs of Center, Northwest, and Belarus.

capital invested in the Astravets NPP, there are political risks of implementing mechanisms of non-market pricing for its electricity (For example, a reduction in the rate and an increase in the tenor of the loan for the Astravets NPP construction reduces the investment component in the price of electricity in the absence of a capacity market in Belarus and the common electric power market (CEPM) of the EAEU (the Union)), leading to greater competitiveness of the Astravets NPP electricity in the Russian electricity market (the WECM of the Russian Federation), its overstocking, and massive driving out of the Russian generation from the market.

Furthermore, the absence of a consumer, primarily with respect to the baseload part, leads to double risks, first of all, for the Smolensk NPP.

2.1. Additional risks for Russia

The problems are aggravated not only by an extremely controversial approach to the plant economics but also by a completely unexpected and full-fledged development of this approach.

In particular, on November 06, 2020, the President of Belarus A.G. Lukashenko stated that the country needs a second nuclear power plant not to depend on oil and gas supplies. "...There will be enough electricity. Our pathetic protesters lament that there's no way to use it but, listen, how come there's no way to use the electricity? We need to build one more such plant to get rid of the dependence on hydrocarbons. This plant is a stroke of luck, a gift," Lukashenko said. [44]

The absence of financial resources in Belarus for construction (it is financed by Russia), on the one hand, and limited sales and, hence, recovery of investment in the Astravets NPP, on the other hand, can make phase two of the Astravets NPP (as well as the project of the existing NPP) a huge and irrecoverable burden on the budget of the Russian Federation.

Moreover, as a "perk", it will be accompanied by the Russian electricity market collapse in the case of uncontrolled subsidization of the investment component of the price.

And, here is "the cherry on top", the Baltic States have already blocked (since November 1, 2020) Russian electricity import to Europe [45], [46] to guarantee the blockade of the Astravets NPP electricity sales to Europe and the Baltic States through Russia as per the substitution arrangement. With the technical inability to "mark" electricity and separate power flow from Belarus, the only solution is to stop the power flows altogether. Similar mechanisms (a ban on import of Russian and Ukrainian nuclear power) were used by the European Union (Eurelectric) to prevent the unification and parallel operation of the EU and CIS power systems in 2002-2007.

2.2. The Astravets NPP instead of the Smolensk and Leningrad NPPs

The situation could change radically if, instead of extending the service life (as it already was in 2012), units 1, 2, 3 of RBMK-1000 at the Smolensk NPP, located 475 km from the Astravets NPP, would be decommissioned in 2027, 2030 and 2035, respectively. That is 3,000 MW. In case of abandoning additional construction of the second reactor of the Astravets NPP, the capacity of nuclear power plants (Smolensk NPP + Astravets NPP) will be reduced by 600 GW. Otherwise, with the construction of the second reactor of the Astravets NPP, the region will have an additional 1,800 GW of power. The region will be completely dependent on the operation of the Astravets NPP. This, however, raises the questions such as what to do with Desnogorsk with its 27,000 inhabitants, the city where the nuclear power plant maintenance personnel resides? How to regulate? What will it cost to develop the grids?

At the same time, in this region, it is planned by 2025 to decommission four RBMK-1000 units of the Leningrad NPP, which is 600 kilometers from the Astravets NPP. This could lead to a shortage to be met by both the Russian market and the Astravets NPP. The Leningrad NPP, however, has already built next-generation 3+ power units with VVER-1200 reactors to replace the RBMK-1000.

Therefore, when considering the replacement of the decommissioned capacity at the Smolensk and Leningrad NPPs, assuming that they have not been resolved yet, it should be noted that this is not the case. They have already been resolved in Russia. The relevant documents have already been signed at the government and industry levels.

In June 2020, Rosatom decided [47] to arrange work and appoint those responsible for investment projects to build two units at the Leningrad NPP-2 and two units at the Smolensk NPP-2. Previously, they were included in the General Scheme for Allocation of Electric Power Facilities to 2035 [48], approved by the Russian government.

For the new Leningrad NPP units, the VVER-1200 design was adopted, similar to the first stage of construction of the Leningrad NPP-2. The Smolensk NPP will adopt the VVER-TOI design, similar to the one being built at the Kursk NPP-2. New power units of Smolensk NPP-2 with VVER-TOI reactors of a total capacity of 2,510 megawatts will be built 6 kilometers from the operating nuclear units of the plant. By the end of 2020, it is planned to develop and approve a roadmap for the investment project "Smolensk NPP-2 Nuclear Units 1,2" and open financing for implementation of measures under the roadmap.

Therefore, even if all three RBMK1000 units at the Smolensk NPP are removed from operation, a possible reduction in the capacity of the load center will not exceed 500 MW.

2.3. Risk years for the Russian and Belarusian energy sector: 2021-2027

Thus, if we do not take into account the scenario of replacing Russian nuclear capacity with Belarusian capacity (possibly jointly owned and operated by Russian and Belarusian companies), in 2021-2027, the Russian and Belarusian energy industries will compete with each other because of the physical availability of excess capacities and unregulated generation.

This situation will lead to:

- the need to subsidize the Astravets NPP in Belarus, both in terms of paying back the investment and in terms of the cost of creating additional regulated sales,
- the additional burden on consumers, state budgets, and the budgets of energy companies,
- the market risks in Russia in terms of overcapacity and non-market competition, non-transparent pricing, and reduced profitability.

2.4. Risks of market mechanisms

There is no capacity market in Belarus. The producer enters the market with a single price, which can factor in both the amount of electricity and capacity volume.

In the Russian market (the Wholesale Electricity and Capacity Market of the Russian Federation, WECM), Russian producers receive payment for capacity within the framework of the capacity market segment: capacity supply agreements (CSA) and competitive capacity outtakes (CCO).

The absence of a capacity market in Belarus and the mismatch between the Belarusian and Russian markets in this segment of the electricity market will lead to the fact that the compensation of the investment component in the cost of electricity generation (which was taken to the capacity market in Russia and financed accordingly), when the Belarusian entity operates in the Russian wholesale electricity market, will prove impossible, as well as it will prove impossible for the Astravets NPP as a nuclear power plant to operate in the WECM of the Russian Federation [49].

From 2025, Belarus, Russia, and other EAEU member states will trade in electricity through the EAEU common electricity market (CEM of the Union). The only commodity to be traded there will be electricity, the price of which may also factor in capacity. In this case, the trade will not take place from the producer to consumer, but at interstate cutsets.

The Astravets NPP, even if owned by Russia, enters the "day-ahead" market of the Russian WECM through the Union's CEM with the full price, including the investment component, while the Russian NPPs do so only with the price for electricity without the capacity charge factored in.

At the same time, the entry of the Astravets NPP into the domestic market and the Union's CEM with different electricity prices could formally lead to discrimination against the consumer. This introduces corresponding risks of non-compliance with the antitrust legislation of the EAEU. On the one hand, Belarusian consumers should enjoy equal rights with Russian consumers, consumers should be in equal conditions, and, on the other hand, external consumers will not be able to pay for the Astravets NPP capacity.

For nuclear power plants, the capacity charge is the main component of the price. The Astravets NPP will not be able to enter the Union's CEM with the full price that would factor in, through this charge, paying back the investment (according to expert estimates, $50/

MWh [50] is for paying back the investment and $35/MW is operating and fuel costs; the total is $85/MWh). In Russia, nuclear power plants enter the market with a price-acceptance bid, which may be zero as well, and the main payment is received in the CSA segment, which is not part of the mechanisms of the common market of the EAEU since capacity trading is not available in all countries of the Union, in Belarus, in particular.

For example, if the Astravets NPP enters the Russian market only with an electricity price, all investments become the liability of the Belarusian consumer, and they indirectly subsidize the Russian ones, who pay for the capacity of their NPPs through the internal mechanisms of the Russian WECM and do not pay for the Astravets NPP capacity. If the Astravets NPP enters the Russian market at the full price anyway, its energy is not competitive, since the Astravets NPP does not participate in the CSA of the Russian Federation and will not be able to recover investment costs, having formed, as a generator, the corresponding deductions under the RF CSA. This means that its price in the market has to be higher than in Russia by the value of these costs.

It is also worth taking into account that the Russian rules of the WECM, which ensure the first-priority loading of NPPs in the Russian market [51] (e.g., the Leningrad NPP, Smolensk NPP), do not apply to the entities of electricity markets of other states. In this sense, the Astravets NPP is at a disadvantage in the market if compared to the similar capacity of nuclear power plants, which can be used as a result of the extension of the operating life of the Smolensk NPP and Leningrad NPP.

V. Conclusion. What to do?

If we do not consider the shutdown of the first reactor and the construction of the second reactor at the Astravets NPP, the range of theoretically possible options for solving the sales problem is not broad. In particular, it includes such possible and impossible options as:

Selling all Astravets NPP electricity in the domestic market. This entails the shutting down of half of the thermal power plants in Belarus and the reorientation of the consumer to replace them with the Astravets NPP with the corresponding costs, which are compensated either by an increase in tariffs or from the country's budget. The energy industry will become unprofitable, its burden on the GDP, which is already 3 times higher than that in the USA, 1.7 times higher than in Europe, and 1.4 times higher than in Russia, may increase by at least 20-25%, due to these costs and the loan exposure.

Export. Since export to Europe is unlikely, export means the export to Russia, which involves:

either the complete unification of the electricity and capacity markets or rather, the unconditional and complete implementation of the Russian model in Belarus. Given the decisions adopted by the EAEU member states in 2015-2020, this is impossible.

or granting the Astravets NPP rights, obligations, and preferential advantages equivalent to those of Russian NPPs. Specifically (while the project may be implemented according to the BOO [Build - Own - Operate] model, similar to the Akkuyu NPP in Turkey), the plant should operate in an islanded and extraterritorial mode in terms of dispatch control with the System Operator of the Unified Power System (SO UPS) serving as the basis (the practice of coordination of planning of the Russian and Belarusian power systems can contribute to this). In this case, an appropriate legal regime should be ensured, with cardinal adjustments to the legal framework of Russia and Belarus, allowing for the participation of the Astravets NPP in the capacity market in the WECM of the Russian Federation. In this case, for Rosatom, the Astravets NPP could be a more or less full-fledged replacement for the Smolensk NPP units being decommissioned (in the absence of new construction activities) or the use of a particular structure of contracts for supply to the Russian market through "one window," which makes it possible to bring the supply of two products traded in the Russian market (electricity and capacity) to a single product of the common market of the Union, that is electricity. However, this approach, proposed by Russia and considered in 2016-2018, was rejected by the rest of the EAEU member states. Nevertheless, the possibility of applying the relevant contractual structure is not ruled out, although highly problematic.

It should also be taken into account that if the Smolensk NPP is replaced by the Astravets NPP, even if left with its single reactor (traditionally, the NPP has an even number of reactors), the social issues of Desnogorsk will have to be solved.

All of these scenarios entail a revision of the Master Plan for the Development of the UPS to 2035 and Rosatom's decisions on the construction of two VVER-TOI units at the site of the Smolensk NPP.

At the same time, all of these options suggest setting a price, which is more acceptable to the consumer than the existing ones in the Russian market. This problem can be tackled by radically changing the terms of loan repayment, including the alteration of its indemnification forms to Russia, the relaxation of loan conditions (as has already happened) down to complete writing off the loan or the transfer of the loan exposure from the electricity price to the state budget. Even this, however, does not exclude, and, actually, aggravates the consequences for the Russian electricity market with the emergence of a new (and, under these conditions, competitive) producer against the background of its surplus power.

Thus, the only transparent and consistent way out of this situation is to find an additional consumer for the Astravets NPP electricity and capacity.

References

[1] Decree of the Government of the Russian Federation of 19.06.2020 N 1640-r "On Signing of the Protocol on Amendments to the Agreement between the Government of the Russian Federation and the Government of the Republic of Belarus on Granting State Export Credits to the Government of the Republic of Belarus for the Construction of a Nuclear Power Plant within the Territory of the Republic of Belarus of 25 November 2011". (in Russian)

[2] https://primepress.by/news/kompanii/eksport_elektroenergii_posle_zapuska_belaes_tseny_net_dogovorennosti_est-13540/

[3] Development of the electric power industry in Russia and Belarus: the price of fancies. B.I. Nigmatulin

Chairman of the Expert Council of the Community of Russian Consumers of Electricity. Institute of Energy Research, Moscow, Russia. Talk at the XIV Minsk International Forum on Heat and Mass Transfer. September 13, 2012. (in Russian)

[4] Review of the electricity and heat sector in the Republic of Belarus EEP/CQS/17/01, THE REPUBLICAN UNITARY ENTERPRISE BELTEI) Minsk, 2018 p.81 (in Russian)

[5] https://www.belstat.gov.by/ofitsialnaya-statistika/realny-sector-ekonomiki/energeticheskaya-statistika/graficheskii-material-grafiki-diagrammy/proizvodstvo-elektricheskoi-energii-po-kategoriyam-energoproizvoditelei/

[6] https://aftershock.news/?q=node/901741

[7] https://www.sb.by/articles/vlastelin-koltsa0901.html

[8] https://minenergo.gov.by/kak-belajes-gotovitsja-k-integracii-v-jenergosistemu/

[9] https://aftershock.news/?q=node/901741

[10] Sectoral program for the development of the electric power industry as amended by Resolution No. 31 of the Ministry of Energy of the Republic of Belarus of September 4, 2019 (in Russian)

[11] https://pravo.by/document/?guid=12551&p0=C22000582&p1=1&p5=0

[12] GOST 22667-82 (ST SEV 3359-81) (in Russian)

[13] https://www.belta.by/economics/view/elektrokotly-moschnostjju-916-mvt-dlja-integratsii-belaes-v-energosistemu-budut-vvedeny-do-kontsa-goda-399760-2020/

[14] https://minenergo.gov.by/deyatelnost/ceni_tarifi/

[15] https://www.interfax.ru/business/690139

[16] https://www.energo.by/content/deyatelnost-obedineniya/osnovnye-pokazateli/

[17] https://ecohome-ngo.by/wp-content/uploads/2020/07/Ekodom-otsenka-sebestoimosti-elektroenergii-BelAES-2020-07-29.pdf

[18] Natural gas prices for legal entities and sole proprietorships in the Republic of Belarus (per the Decree No.8 of the Ministry of Antimonopoly Regulation and Trade of January 30, 2020) (in Russian.)

[19] Review of the Electric and Heat Power Sector / The Republican Unitary Enterprise BELTEI Minsk, 2018. 295. https://drive.google.com/file/d/1SMgNFW2belqb_IS_dXt45PKS7oEhFcUj/view?usp=sharing p.124 (in Russian)

[20] Review of the Electric and Heat Power Sector in the Republic of Belarus EEP/CQS/17/01, The Republican Unitary Enterprise BELTEI), Minsk, 2018 p.126 (in Russian)

[21] https://ecohome-ngo.by/wp-content/uploads/2020/07/Ekodom-otsenka-sebestoimosti-elektroenergii-BelAES-2020-07-29.pdf

[22] https://www.interfax.ru/business/681439

[23] https://ecohome-ngo.by/otsenka-sebestoimosti-proizvodstva-elektroenergii-na-ostrovetskoj-aes-i-eyo-vliyanie-na-energeticheskij-kompleks/

[24] Electricity tariffs for legal entities and sole proprietorships. Registered: Ministry of Antimonopoly Regulation and Trade of the Republic of Belarus. Order No.21 of January 31, 2020 (in Russian)

[25] https://www.energosbyt.by/tariffs.php

[26] https://www.energo.by/content/deyatelnost-obedineniya/sbytovaya-deyatelnost/rynok-elektricheskoy-i-teplovoy-energii/

[27] https://minenergo.gov.by/wp-content/uploads/jelektro-1.pdf

[28] https://www.nordpoolgroup.com/Market-data1/Dayahead/Area-Prices/ALL1/Yearly/?view=table

[29] https://www.atsenergo.ru/results/rsv/oes

[30] https://time2save.ru/calculaters/kalulator-cenovih-kategoriy

[31] https://ecohome-ngo.by/otsenka-sebestoimosti-proizvodstva-elektroenergii-na-ostrovetskoj-aes-i-eyo-vliyanie-na-energeticheskij-kompleks/

[32] https://primepress.by/news/kompanii/eksport_elektroenergii_posle_zapuska_belaes_tseny_net_dogovorennosti_est-13540/

[33] https://minenergo.gov.by/belarus-v-2019-godu-uvelichila-jeksport-jelektrojenergii-bolee-chem-v-dva-raza/

[34] https://www.belstat.gov.by/ofitsialnaya-statistika/realny-sector-ekonomiki/energeticheskaya-statistika/statisticheskie-izdaniya/index_17875/

[35] https://sputnik.by/politics/20200926/1045761769/Strany-Baltii-reshili-kak-blokirovat-elektroenergiyu-s-BelEAS.html

[36] http://tap.mk.gov.lv/lv/mk/tap/?pid=40493750&mode=mk&date=2020-11-03

[37] http://tap.mk.gov.lv/lv/mk/tap/?pid=40493750&mode=mk&date=2020-11-03

[38] https://www.belnovosti.by/ekonomika/vsled-za-litvoy-ukraina-otkazalas-ot-elektroenergii-iz-belarusi

[39] https://tass.ru/ekonomika/4846204

[40] https://tass.ru/ekonomika/9757867

[41] The strategic concept of the development of electricity

generating capacities and power grids to 2030. Decree of the Ministry of Energy of the Republic of Belarus No. 7 of February 25, 2020. (in Russian)

[42] https://rek.admin-smolensk.ru

[43] Sectoral program for the development of the electric power industry for 2016 - 2020, approved by Decree No.8 of the Ministry of Energy of the Republic of Belarus of March 31, 2016 (as amended by Decree No.31 of the Ministry of Energy of the Republic of Belarus of September 4, 2019) (in Russian)

[44] https://www.belta.by/president/view/lukashenko-minsk-nado-postepenno-perevodit-na-elektrotransport-414380-2020/

[45] https://lt.sputniknews.ru/economy/20201106/13621500/Litva-budet-blokirovat-elektroenergiyu-iz-Belorussii-do-vykhoda-iz-BRELL.html

[46] https://naviny.media/new/20201104/1604480526-kabmin-latvii-utverdil-otkaz-ot-importa-iz-rossii-elektroenergii-s

[47] https://rosatom.ru/journalist/news/v-rossii-budut-postroeny-chetyre-novykh-energobloka-aes/

[48] http://static.government.ru/media/files/zzvuuhfq2f3OJIK8AzKVsXrGIbW8ENGp.pdf

[49] Para. 4.10, 119, etc. of The Rules of the Wholesale Electricity and Capacity Market of the Russian Federation - PP RF No.1172 of December 27, 2010 (in Russian)

[50] https://ecohome-ngo.by/wp-content/uploads/2020/07/Ekodom-otsenka-sebestoimosti-elektroenergii-BelAES-2020-07-29.pdf

[51] Para. 87.1 of The Rules of the Wholesale Electricity and Capacity Market of the Russian Federation - PP RF No.1172 of December 27, 2010 (in Russian)

Bulat Nigmatulin
Dr. habil. in Engineering, Full Professor at the National Research University Moscow Power Engineering Institute.
Graduated from the Faculty of Power Engineering of the Bauman Moscow State Technical University (1967) and the Faculty of Mechanics and Mathematics of the Lomonosov Moscow State University (1969). He defended his doctoral thesis in 1971 and his habilitation thesis in 1983.
Deputy Minister of the Russian Federation for Atomic Energy (1998-2002).
He currently serves as Director-General at the Institute of Energy Research and Advisor to the Vice President for Marketing and Business Development at the JSC “Rusatom Overseas” of the Rosatom State Nuclear Energy Corporation.

Maxim Saltanov Graduated from Moscow Power Engineering Institute in 1986. Qualification: Thermal Physics Engineer. Nuclear and thermal power plants. Honored Power Engineer of the CIS. Currently is an expert at the Institute of Energy Problems.

Summary of the International Scientific Conference “Energy-21: Sustainable Development And Smart Management” September 7-11, 2020 Irkutsk, Russia

N.I. Voropai*, V.A. Stennikov

Co-chairmen of Program Commitee of the conference
Melentiev Energy Systems Institute of Siberian Branch of Russian Academy of Sciences, Irkutsk, Russia

The International Scientific Conference “energy-21: sustainable development and smart management” was held in Irkutsk, Russia, on September 7-11, 2020. The Conference was organized by the Melentiev Energy Systems Institute SB RAS with the financial support of the Russian Foundation for Basic Research (RFBR) and with the participation of the Global Energy Interconnection Development and Cooperation Organization (GEIDCO), the Forum of Gas Exporting Countries, and the Global Energy Association.

Over 170 attendees from 18 foreign and 69 Russian organizations from 8 countries (Russia, Qatar, China, Japan, Republic of Korea, Vietnam, Mongolia, Germany, Azerbaijan, and Uzbekistan) took part in the event. The participants presented more than 130 papers.

The Sessions of the Conference focused on the following main areas:

1. Transforming smart energy systems
2. Advanced energy technologies: environmentally friendly and resource-saving energy, renewable energy sources.
3. Eastern vector of Russia's energy strategy: current state, look into the future.
   a. World energy markets and international cooperation.
   b. Development of the economy, the energy sector (and energy industries) of the Russian Federation and its eastern regions.
   c. Local power supply systems in the East of the Russian Federation.
4. Interstate power interconnections, global power interconnection.
5. Reliability of fuel and energy supply to consumers, energy security.
6. Power quality.

More information is available on the Conference website: http://isem.irk.ru/energy21

Having discussed the reports and papers on the development, functioning, and transformation of the energy sector, the Conference states the following:

The ongoing global technological transformation of energy systems is both a challenge and a window of great opportunities for Russia that must be used to ensure the efficiency, availability, and environmental friendliness of energy supply systems. Innovative equipment and technologies, including their smartization, radically change the properties of energy systems, which increases the level of their efficiency, controllability, stability, survivability, and at the same time creates new problems in the functioning of these systems due to changes in their properties. The technological transformation of the energy sector brings about new challenges in managing and controlling the operation and expansion of energy systems, which requires in-depth fundamental studies with the scientific community playing a major role in their organization and implementation.

Electric power integration is one of the dominant global trends, providing significant systems effects to its participants. The Russian electric power system is one of the largest in Eurasia and the world. It acts as an essential participant in such integration and interacts with the energy systems of neighboring countries. One of the serious problems is the electric power reintegration in the post-Soviet space, in particular, the reintegration of Russia, Central Asia, and the Caucasus with joint access to the electricity markets of the Middle East, Asia Minor, and South Asia. The process of establishing an interstate power interconnection in Northeast Asia is becoming increasingly more practically realizable, in which Russia, based on the

http://dx.doi.org/10.38028/esr.2020.04.0008

regions of Siberia and the Far East, can also become a noticeable player while receiving economic benefits.

A big socio-economic problem of Siberia and the Russian Far East is a low level of income, which cannot compensate for the harsh natural and climatic living conditions for the population, and leads to its decline in these regions.

The policy of science and technology development of Russia, including its eastern regions, should provide for mechanisms to integrate into the chain of added values not only of exports of energy resources but also of the expansion of energy systems providing appropriate conditions for the population and the growth of production of goods and services, based on innovative and environmentally sound technologies.

The comprehensive and priority development of Siberia and the Far East's territories is recorded in some of the strategic state documents: Presidential Address to the Federal Assembly, 2020; Energy Security Doctrine of the Russian Federation (approved by the Decree of the President of the Russian Federation of May 13, 2019, No. 216); Energy strategy of the Russian Federation until 2035 (approved by the Order of the Government of the Russian Federation dated June 9, 2020, No. 1526-r). Conversion to gas in East Siberia and the Far East is one of the prime objectives for developing national energy and economy and addressing social problems in these regions.

The main problems in local power supply systems, which are commonplace in the East of the Russian Federation, are associated with the underdevelopment of the transport infrastructure and the unsatisfactory state of energy sources, which leads to high values of energy tariffs and budget subsidies allocated to compensate for the lost revenues of energy producers.

The environmental problems of the territories of special nature management (for example, the Central Ecological Zone of the Baikal Natural Territory) are caused by the high share of coal in the fuel balance, the predominance of low-efficiency small-capacity boiler houses, the lack of equipment for cleaning exhaust gases and high heat losses in the heat supply systems of consumers.

Under the current conditions of the operation and expansion of energy systems, their reliability and energy security issues have become of particular relevance. This is due to a lack of investment in the industry, high wear and tear of production assets, significant depletion of existing oil and gas fields, the need to develop new, much more expensive oil and gas fields in the harsh climatic conditions of the Arctic zone, and low prices for hydrocarbons in world markets. The excessive amount of old emergency prone generating capacities remains an unresolved issue, which negatively affects both the reliability of the power supply and the price of electricity. In the practice of managing the expansion of power systems, the energy security requirements are still not taken into account. The issues of a comprehensive approach to management and interrelated development of energy industries within the national energy sector, as well as the improvement in the quality of training of qualified personnel for the energy sector, remain highly topical. The lack of domestic efficient generating equipment and the use of foreign generating equipment in the domestic power industry often leads to problems with the power supply to large power regions, in particular, due to the incompatibility of settings for the operating parameters of foreign equipment and the specified disturbances of domestic power systems.

Based on the delivered presentations, exchange of views, and conclusions of discussion, the Conference recommends the following:

Given the considerable socio-economic importance of the energy issues under consideration and the attained high theoretical and practical level of their study, the recommendations formulated for the executive branch authorities are as follows:

1. It is necessary to immediately start to implement, on a permanent basis, the objectives set in the Federal Law "On Strategic Planning in the Russian Federation" of 28.06.2014 N 172), which regulates the relations arising between participants in strategic planning in the process of goal-setting; forecasting; planning and programming of socio-economic development of the Russian Federation, the subjects of the Russian Federation and municipalities, economic sectors and areas of state and municipal governance; ensuring national security of the Russian Federation; as well as monitoring and controlling the implementation of strategic planning policy documents.
2. To meet the objectives at the federal, regional, and municipal levels, as stipulated by the Federal Law "On Strategic Planning," strategic directions for the expansion of energy systems at the corresponding level shall be established and regularly updated. The methodological basis for achieving such objectives is the theory and methods of the systems analysis of energy development, while the scientific tools should be based on domestic technologies and ensure the completeness and integrity of the information base to perform the functions of strategic planning, development, and updating of energy policy, and monitoring of the implementation of strategic and policy decisions in the management of energy development at each level of the hierarchy of governmental authorities in the Russian Federation. It is necessary to develop mechanisms to translate systems efficient solutions for energy development from the upper levels of government to the level of individual energy companies owned by different entities.
3. Planning the development of Russia's energy industries should place emphasis on ensuring the reliability of fuel and energy supplies to consumers, given the most important requirements of energy security

of Russia under various energy sector operating conditions. Elaborating the issues of the development of the energy industries of the Russian Federation, one should employ the expertise in integrated research and systems analysis as gained in specialized scientific organizations, particularly in the Russian Academy of Sciences (including the Melentiev Energy Systems Institute, SB RAS)

4. Currently, Russia has completed a complex and time-consuming (years-long) stage of work on the formation of a large number of policy documents defining the strategic development of the economy and energy in the East of the country to 2030-2035, taking into account the energy cooperation of Russia with the countries of the Asia-Pacific Region (APR). The stage of 2036 to 2050 is conceptually significant. This is the stage of innovative development of the Russian energy sector characterized by a transition to fundamentally different technological capabilities of highly-efficient use of conventional energy resources and new energy sources, as well as by the emergence of the prosumer.
5. The prime objective should be to develop a scientifically-based strategy (roadmap) for long-term (to the year 2050) innovative development of the energy sector of the country and its eastern regions in the context of the objective inevitability of the paradigm shift in energy cooperation between Russia and the APR countries: the transition from energy trade to innovative and technological cooperation. Such a strategy can be developed only relying on the close cooperation of teams of research and design institutes, companies, banks, and others, with the active support on the part of the Government of the Russian Federation and regional authorities.
6. To promote the conversion of Siberia and the Russian Far East to gas, it is necessary to coordinate the activities of executive branch authorities of federal subjects of Russia and domestic business; define the powers and obligations of the parties; develop relevant regional conversion-to-gas programs; design public-private partnership schemes to ensure reliable funding of the construction of main and regional transport pipeline infrastructure. It is also essential to provide regulatory documents and other enactments on social guarantees for the citizens in terms of compensation for the costs they incurred when switching to gas.
7. It is necessary to actively conduct comprehensive research into energy (electric power, oil energy, gas energy) integration of Russia within the existing and emerging interstate energy interconnections in Eurasia, including those in the former Soviet Union, in Northeast Asia, and other areas, with the participation of Russian and foreign organizations.
8. There is an urgent need to formulate a comprehensive program for the development of local energy in Russia's East, including the Arctic regions and areas of new development, with a focus on maximizing the efficiency and reliability of energy supply through diversification of energy production, including the transition to alternative energy sources (liquefied natural gas, crude oil, and coal from local fields), small-capacity nuclear power plants, and renewable energy sources.
9. Implementation of a project to build small- and medium-capacity nuclear power plants will make it possible to reduce greenhouse gas emissions while developing domestic energy technologies that have a powerful multiplier effect and high export potential. The presence of the IAEA-supervised small nuclear power system facilities with high integral safety in the Eastern and Arctic regions will serve as a basis for solving the social, economic, environmental, and geostrategic development problems of Russia.
10. At present, the only feasible way to make heat generation in the Central Ecological Zone of the Baikal Natural Territory more environmentally sound is to use electricity for heating purposes. The implementation of this direction requires a revision of the list of activities prohibited within the zone; development and approvement of special tariff solutions aimed at compensating revenue shortfalls of heat and electricity producers, as well as a substantial modernization of the electric grid infrastructure.
11. As part of the work to determine the regulatory reserve of generating capacity, one should justify the regulatory values of the probabilistic criterion for the adequacy of the Unified Power System of Russia and off-grid power systems and ensure its adoption in the practice of managing the expansion of the Unified Power System of Russia and off-grid power systems.
12. It is necessary to initiate comprehensive research works on the systems analysis of the reliability issues of fuel and energy supply to consumers under various operating conditions of the energy sector and energy systems in the future up to the year 2035, taking into account the interrelated operation of energy industries within the energy sector of the country with a scientific justification of the relevant measures.
13. It is necessary to establish the directions for systematic improvement in the education system to train highly qualified personnel for the domestic power industry.
14. Based on the results, the Conference decided to send this document to the leading Russian publications in the field of energy, relevant ministries and agencies of the Russian Federation, energy companies of the Russian Federation, the administrations of the eastern regions of Russia, and foreign and international organizations.